INFORMATION TO USERS

This manuscript has been reproduced from the microfilm master. UMI films the text directly from the original or copy submitted. Thus, some thesis and dissertation copies are in typewriter face, while others may be from any type of computer printer.

The quality of this reproduction is dependent upon the quality of the copy submitted. Broken or indistinct print, colored or poor quality illustrations and photographs, print bleedthrough, substandard margins, and improper alignment can adversely affect reproduction.

In the unlikely event that the author did not send UMI a complete manuscript and there are missing pages, these will be noted. Also, if unauthorized copyright material had to be removed, a note will indicate the deletion.

Oversize materials (e.g., maps, drawings, charts) are reproduced by sectioning the original, beginning at the upper left-hand corner and continuing from left to right in equal sections with small overlaps. Each original is also photographed in one exposure and is included in reduced form at the back of the book.

Photographs included in the original manuscript have been reproduced xerographically in this copy. Higher quality 6" x 9" black and white photographic prints are available for any photographs or illustrations appearing in this copy for an additional charge. Contact UMI directly to order.

UMI

A Bell & Howell Information Company
300 North Zeeb Road, Ann Arbor MI 48106-1346 USA
313/761-4700 800/521-0600

Université d'Ottawa · University of Ottawa

The Copolymerization of Butyl Acrylate / Methyl Methacrylate at Elevated Temperatures

Malik Hakim

A thesis submitted to the School of Graduate Studies and Research in partial fulfillment of the requirements for the degree of

M.A.Sc. in Chemical Engineering

Department of Chemical Engineering
University of Ottawa

Abstract

High temperature multi-component polymerizations have prompted a great deal of interest on the part of the paints, coatings and adhesives industry. Due to this interest, a study of the kinetics of bulk and solution butyl acrylate / methyl methacrylate (BA/MMA) copolymerization was performed over a wide range of temperatures.

Reactivity ratios for the bulk and solution (in toluene) BA/MMA copolymer system were estimated for reaction temperatures of 60°C to 140°C and exhibited a weak temperature dependence. These parameters increased with increasing temperature which signaled a tendency of both monomers to homopolymerize. The bulk reactivity ratios were comparable to those estimated in the solution experiments and were used to successfully predict copolymer composition up to high conversions of monomer to polymer for various reaction conditions.

Conversion profiles followed a typical s-shaped diffusion-controlled polymerization curve. The rate of polymerization increased with increasing temperature. Composition drift was determined to be significant at 40 to 50 wt% conversion for high and low temperatures. The use of solvent altered the conversion profiles by delaying the onset of the gel effect. However, the solvent did not affect composition and molecular weight profiles. All data obtained concurred with classical kinetic trends.

Depropagation, which often plays a role at higher temperatures, was not observed for the BA/MMA copolymer system. A study of other copolymer systems that were prone to higher rates of depropagation was also performed in order to ascertain whether model discrimination could be carried out using composition data.

Résumé

La polymérisation de plusieurs composants en haute température ont mérité une grande attention de la part de l'industrie des peintures, des revêtements et des adhésifs. À la lumière de cet intérêt, nous avons élaboré une étude sur la cinétique de la polymérisation grossière et de la polymérisation en solution du composé acrylate de butyle / méthacrylate de méthyle à plusieurs températures.

Les rapports de réactivité pour ce copolymère en présence de toluène, pour la polymérisation grossière et en solution, ont été estimées pour des températures de réaction de 60°C et de 140°C, ce qui démontre une faible variation des rapports de réactivité avec la température. Ce paramètre augmente avec la température ce qui tend les monomères à se polymériser de façon singulière. Les rapports de réactivité pour la polymérisation grossière sont comparables à ceux obtenus avec les expériences de polymérisation en solution. Les rapports de réactivité prédisent avec succès la composition du copolymère à de grandes conversions, et ce, pour plusieurs conditions de réaction.

Le profil de conversion est fidèle à la courbe en S typique d'une polymérisation contrôlé par diffusion. Le taux de polymérisation augmente avec la température. L'accentuation de la composition semble être prédominante à une conversion autour de 40% à 50% pour les basses et hautes températures. L'utilisation du solvant altère le profil de la conversion en retardant l'effet de gel. Cependant, le solvant n'affecte pas le profil de composition et de masse moléculaire du composé. Toutes les données obtenus sont représentatives de la cinétique classique pour notre composé.

La dépropagation, qui généralement joue un rôle à des températures élevées, n'a pas été observé pour le système acrylate de butyle / méthacrylate de méthyle. Dans le même sens, une étude pour d'autres copolymères, qui ont un taux élevé de dépropagation, a été réalisé afin de vérifier si notre modèle n'offre aucune discrimination quant à l'utilisation des données de compositions.

Acknowledgments

There have been many important people that have supported me through out my academic career. I recall the time that my father, Zoher Hakim, taught me the multiplication tables. At the age of eight, I remember walking up and down the stairs, every Saturday, reciting the tables in their entirety. By the time I was eleven years old, I was learning algebra, solving two equations with two unknowns. Mom (Malakie Bkaily Hakim) was no push over either. Every day she would make certain that my homework was done. With that, my first acknowledgement goes out to them. Thank you both for your diligence and firm commitment to my future. I will never forget it.

All through out my masters study, my supervisor, Marc Dubé, guided me almost every step of the way. Thank you Marc for the weekly meetings, constant progress reports, your patience and dedication to my studies. You gave me the space to find my own way and established the learning structure I needed to fulfill my objectives.

As I grew up, my friends and I developed an intellectual community our own. The world was our oyster. Anything and everything was up for discussion. I remember strolling through High Park (in Toronto) with big Mischa, pondering the existence of god. Some mornings we strolled into that park to go to school and never came out until the end of the day. Thank you Fadi, Lila, big Mischa, James, Sylvie, Julie, Ruby, Charles and Steve. You all make it worth while.

Thank you Esther for all of your support through my last years of study. You helped take care of our son at time when my studies became intense.

My last dedication is to my little Mischa. For everything I am and all that I will become, I would give all away for you in a second. Thank you for being in my life.

Nomenclature and Molecular Formulas

A_p	Propagation collision frequency factors
A_d	Depropagation collision frequency factors
A_{ij}	Arrhenius frequency factor
C_M	Chain transfer to monomer constant
C_S	Chain transfer to chain transfer agent constant
C_i	Chain transfer to initiator constant
E_{ij}	Energy of activation
E_p	Propagation energy of activation
E_d	Depropagation energy of activation
F_i , $\overline{F_i}$	Instantaneous mole fraction of copolymer composition
f_{it}	Mole fraction of monomer in reaction medium after polymerization for certain period of time
f_i	Mole fraction of monomer feed
f_{int}	Initiator efficiency
[I]	Initiator concentration
k_p	Propagation rate constant
k_t	Termination rate constant
k_{tc}	Termination by combination rate constant
k_{td}	Termination by disproportionation combination rate constant
k_{tp}	Primary radical termination rate constant
k_{tr}	Total chain transfer rate constant
$k_{tr,M}$	Chain transfer to monomer rate constant
$k_{tr,S}$	Chain transfer to chain transfer agent rate constant
$k_{tr,I}$	Chain transfer to initiator rate constant
k_{ii}	Homopropagation rate constant
k_{ij}	Cross-propagation rate constant
$k_{\overline{ii}}$	Homopropagation rate constant
$k_{\overline{ij}}$	Homopropagation rate constant
$k_{t\,SD}$	Segmental diffusion termination rate constant
$k_{t\,\overline{SD}}$	Reverse of segmental diffusion termination rate constant
$k_{t\,\overline{TD}}$	Reverse of translational diffusion termination rate constant
$k_{t\,TD}$	Translational diffusion termination rate constant
$k_{t\,CR}$	Chemical reaction termination rate constant
$k_{t\,\overline{CR}}$	Chemical reaction termination rate constant
M_n	Number-average molecular weight
M_w	Weight-average molecular weight

M_z	Z-average molecular weight of a molecular weight distribution
M_{z+1}	Z-average molecular weight of a molecular weight distribution
$[M\cdot]$	Polymer free-radical concentration
$[M_i]$	Monomer feed concentration
$[M_t]$	Monomer concentration in reaction medium after polymerization for a certain period of time.
MWD	Molecular weight distribution
r_{ij}	Copolymer reactivity ratio
R_p	Rate of propagation
R_i	Rate of initiation
R_t	Rate of termination
R_{tr}	Rate of chain transfer
R	Ideal Gas Constant
[S]	Chain transfer agent concentration
T	Temperature
ν	Kinetic chain length
x , X	Weight percent conversion of monomer to polymer

Butyl Acrylate

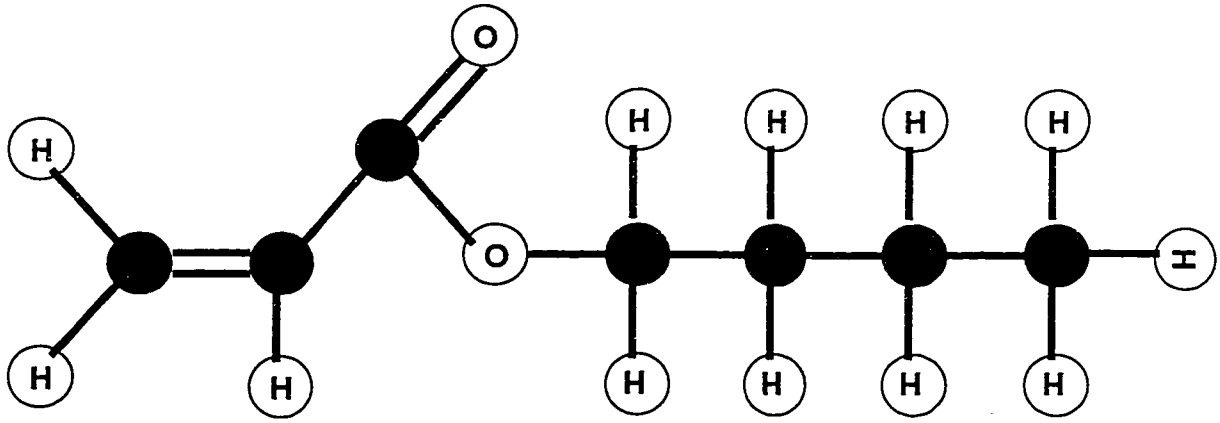

Methyl Methacrylate

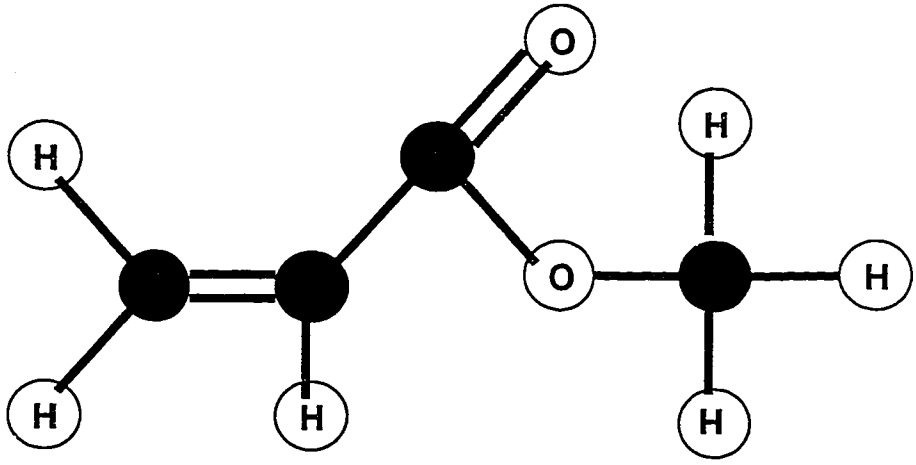

Table of Contents

Appendices

CHAPTER 1

Introduction

Polymers are extended chains of unit molecules. They are very important in the manufacture of rubber, resins and a variety of other synthetic products. A polymer may be comprised of one or more different types of unit molecules. A copolymer is made up of two different unit molecules. In this study these molecules are butyl acrylate and methyl methacrylate. The manufacture of copolymers are very popular due to the blended properties obtained by using more than one type of unit molecule. In this case butyl acrylate (with its low glass transition temperature) will lend flexibility to the product while methyl methacrylate (with its high glass transition temperature) will lend mechanical strength to the final polymer.

The wide range of polymer products that may be manufactured with specific properties and high degrees of quality control are the basic reasons why the study of copolymer systems has been popular. The copolymers discussed in this study were produced via free-radical polymerization reactions that involve the addition of one or more molecular units (termed monomers) to a growing radical chain in order to form long (sometimes branched) chained molecules.

The temperature effects on the kinetics of copolymerization was an important consideration of this study. Most industrial scale polymerizations are run at relatively low temperatures (20 to 80 °C). This fact is reflected through the academic and industrial researchers' emphasis on low temperature homo- and copolymerization reactions.

Recently, there has been mounting interest in running the reactions at high temperatures (80 to 140 °C). This is due to the following advantages of operating at elevated temperatures:

- Increases in the rate of reaction and a resultant decrease in the time to reach a desired conversion.
- Reduction in the initial initiator and chain transfer agent concentrations resulting in cost savings and decreased impurities in the reaction medium.
- Decrease in viscosity related problems involving the storage and transportation of the final polymer product.
- Decrease in residual monomer concentrations in the final polymer product (an important environmental concern).
- Increase in the overall efficiency of the polymerization process.

However, there are some disadvantages inherent to the operation of polymerization reactions at high temperatures:

- Special safety considerations are required to run reactions at high temperature conditions.
- The high temperature conditions may increase the rates of depropagation (reverse polymerization) which may affect the kinetics of the system.
- Unwanted side reactions not present at low temperatures may dominate the polymerization.

These factors need to be considered when working at these conditions.

Copolymerization reactions may be run in bulk (i.e. only monomers and initiators) or in solution (i.e. with an added solvent such as toluene). The advantage of the use of solvents is to decrease viscosity related problems at higher conversions. This also enhances heat transfer to and from the reaction mixture. To this date, there were very few studies performed on the effect of solvents on the kinetics of high temperature polymerization. For this reason, one of the major objectives of this study was to document the effects of varying amounts of solvent on the copolymerization kinetics of the system.

The prospect of high productivity and reduced operating costs is the basis for utilizing this approach in this thesis. To date, very little work has been done in this field and this work is expected to launch more extensive studies in high temperature multi-component polymerizations with the future goal of implementing industrial-scale high temperature processes. In attempting to assist the manufacture of polymer products at high temperature conditions, effective process control needs to be applied to the system. This requires an intrinsic understanding of the process at these conditions. This knowledge can be gained through a systematic and detailed study of the system. The final form of the study is an experimentally validated mechanistic model of the system that may be incorporated into a control scheme and also used to predict polymer characteristics (i.e. compositions) at certain conditions, thus reducing the need of costly experimentation.

The bulk homopolymerization of methyl methacrylate has been well studied in the literature whereas that of butyl acrylate has received substantially less attention. This is due to the tendency of butyl acrylate to form branched polymers that are generally difficult to work with. To this date, little work has been done on the copolymerization of butyl acrylate (BA) and methyl methacrylate (MMA) in bulk and in solution with toluene.

The aforementioned considerations will be explored in greater detail in Chapter 4. These considerations form the basis for the objectives of this study. The first goal is the study of high temperature kinetics of the BA/MMA copolymer system. The second objective is to study the effects of solvent on the kinetics of the system. These main

goals form the basis for future development of experimentally validated models that may help explain the underlying mechanisms in copolymer reaction systems.

1.1 Thesis Outline

In order to fulfill the thesis objectives, a few secondary goals must be met. These are outlined at the beginning of every chapter. This list provides an overview of the major emphasis of each chapter in order to describe the systematic approach used to satisfy the main purposes for this work :

- Chapter 2 **Literature Survey**

  This chapter highlights some of the work performed on butyl acrylate and methyl methacrylate homo- and copolymer systems. Emphasis is placed on what paths of study would be important to further the investigation into these systems.

- Chapter 3 **Free Radical Polymerization Reaction Kinetics**

  This chapter highlights the theoretical basis of free-radical polymerization kinetics. Emphasis is placed on the reaction mechanism, diffusion-controlled termination, chain transfer and rate expression development. The models used to predict the experimental data obtained are also described in this chapter.

- Chapter 4 **Experimental Procedure and Product Characterization Techniques**

  Details of the methods and designs used to run the polymerization reactions and obtain experimental data via various characterization techniques are described in this chapter.

- Chapter 5 **Reactivity Ratio Experiments**

  This chapter describes the theory, design, experimental results and data interpretation involving low conversion (reactivity ratio) bulk and solution copolymerizations of BA and MMA.

- Chapter 6 **Full Conversion Experiments**

  This chapter describes the theory, design, experimental results and data interpretation involving low to high conversion bulk and solution copolymerizations of BA and MMA.

- Chapter 7 **Propagation and Depropagation Modeling**

  In this chapter, the effects of depropagation of butyl acrylate - methyl methacrylate - α-methyl styrene copolymer systems at high temperatures are presented. The theory involved in the modeling as well as the design and reactivity ratio estimation for the discrimination of models for each system is thoroughly discussed.

- Chapter 8 **Conclusions and Recommendations**

  This chapter outlines the major observations in the thesis and provides suggestions for procedural improvements as well as directions for future studies on the subject.

These chapters are supplemented with a section highlighting the references as well as an Appendix that contains the raw data tables for all the experiments performed.

CHAPTER 2

Literature Survey

Homopolymerization studies of methyl methacrylate (MMA) have been cited extensively in the literature. Less work has been performed on butyl acrylate (BA) and the BA/MMA copolymer system. Similarly, high temperature studies of either the homopolymerizations or the copolymerization of butyl acrylate (BA) and methyl methacrylate (MMA) have rarely been explored in the literature. This chapter will serve to briefly review the homopolymerization of both butyl acrylate and methyl methacrylate. This synopsis will be followed by a look at the research performed using the copolymer system.

2.1 Butyl Acrylate Homopolymerization

Most of the research on butyl acrylate homopolymerization to date has involved the estimation of propagation and termination rate constants. As a result, there were very few papers dealing with full conversion runs. One of the first systematic studies of BA homopolymerization was performed by Dubé et al. (1991b). A list of studies performed in this area are described in Table 2-1 (modified from Dubé, 1994). Table 2-1 indicates the type of reaction, data and conditions for each work cited. Very few high temperature and full conversion studies have been performed.

In 1995, McKenna explored the advantages in defining the rate constants for the homopolymerization of butyl acrylate. These free-radical solution polymerizations led to the investigation of the influence of oxygen inhibition on the observed rate of reaction. In this work, McKenna demonstrated the importance of taking the oxygen inhibition into account when performing kinetic studies.

Table 2-1 Butyl Acrylate Homopolymerization Literature

Reference	Reaction Type	Data Collected	Full Conversion	Conditions
Bengough and Melville, 1954	Bulk	x, M_n	Yes	AIBN 25 °C
Bengough and Melville, 1959	Bulk	x, k_p/k_t	No	AIBN 25 °C
Benson and North, 1959	Bulk & Solution	x, k_p , k_t	No	AIBN 30 °C
Bradbury and Melville, 1954	Bulk & Solution	x, k_p , k_t	No	AIBN 25 - 60 °C
Buback and Degener, 1993	Bulk	x, k_p , k_t	Yes	AIBN 25 - 80 °C
Buback et al., 1989	Bulk	k_p/k_t	No	50, 70 °C
Buback et al., 1994	Bulk	k_p/k_t	Yes	50 °C
Buback, 1990	Bulk	x, k_t	No	50 °C
Dubé et al., 1991b	Bulk	x	Yes	AIBN 50, 60 °C
Gladyshev and Rafikov, 1966	Bulk	x, k_p , k_t	Yes	25 °C
Kamachi et al., 1982	Solution	k_p , k_t	No	30 °C
Kaszas et al., 1983	Bulk & Solution	$k_p/k_t^{1/2}$	No	AIBN 50 °C
Liaw and Chung, 1982	Solution	k_p , k_t	No	AIBN 30 °C
Majury and Melville, 1951	Bulk	k_p/k_t	No	15 °C
Mckenna et al., 1995	Bulk	x, k_p , k_t	No	AIBN, Low Temp
Melville and Bickel, 1949	Bulk	k_p/k_t	No	BPO 25,35 °C
Nandi et al., 1982	Bulk	M_n	No	80 °C
Ogo and Yokawa, 1977	Bulk	k_p , k_t	No	30 °C
Ratzsch and Zschach, 1968	Solution	R_p	No	BPO 50 °C
Scott and Senogles, 1970	Bulk & Solution	x, R_p	Yes	AIBN 35, 40 °C
Scott and Senogles, 1974	Bulk & Solution	x, R_p	No	AIBN 10 °C
Subrahmanyam et al., 1992	Solution	x, M_n, M_w, R_p	Yes	BPO 70 °C
Wunderlich, 1976	Solution	Rp , MWD	No	30, 50, 70 °C
Yokawa et al., 1974	Bulk	k_p , k_t, R_p	No	30 °C

Examination of solvent effects on BA homopolymerization was performed by Kamachi et al. (1982). In this paper, the solvent effect was observed on the propagation

constant k_p and not k_t . This was stated to be due to the formation of complexes with aromatic solvents and could not be readily explained by the diffusion-controlled polymerization theory (described in Chapter 3). In 1983, Kaszàs et al., developed the hot radical theory to explain this trend. To date, there have been many questions regarding the validity of this theory. This illustrates the continuing need to explore solvent effects on the kinetics of polymerization processes.

Many studies have been directed at validating the mechanisms proposed by diffusion-controlled termination and propagation theory (Odian, 1991). This mechanism will be discussed in greater detail later in this thesis (see Chapter 3). The homopolymerization of BA has been considered to be diffusion-controlled from the beginning of the process (Scott and Senogles, 1970). This trend has been confirmed for termination (Russell et al., 1988; Buback et al., 1989). Other studies have suggested that BA homopolymerization was diffusion-controlled for conversions from 0 to 80 % (Buback, 1990; Buback and Degener, 1993; Buback et al., 1994).

BA has been described as dynamically rigid due to the bulky side groups (Mallya and Plamthottam, 1989). It was also observed that the homopolymer was insoluble. This was probably due to the transfer to polymer resulting in terminal double bond reactions which form polymer branches (Dubé et al., 1991b). This branching effect was supported by earlier molecular weight studies of styrene (STY) / BA copolymerization (Dubé et al., 1990) with direct evidence of chain transfer to polymer reactions provided by Lovell et al. (1991, 1992). This was attributed to the removal of tertiary hydrogens from BA repeat units which led to 10 to 20 branch points per 1000 carbon atoms in the polymer backbone.

The modeling of BA homopolymerization has been a subject of growing interest. Dubé et al. (1991b) performed an experimental investigation of the kinetics of the bulk free radical polymerization of butyl acrylate at 50 and 60 °C. Conversion levels were measured by gravimetry and were independently confirmed using replicate runs. The model was able to predict conversion for all the conditions studied. Recently, Gao and Penlidis (1996) introduced an experimentally verified free-radical polymerization simulator to model many homopolymer systems including BA and MMA homopolymerization. Recent versions of the program incorporated the modeling of BA/MMA copolymerizations. This thesis will complement this work by studying models for the high temperature copolymerization reactions of BA and MMA.

2.2 Methyl Methacrylate Homopolymerization

MMA is an important component of many commodity polymers and as a result, kinetic studies for this monomer are widely cited in the literature. A detailed list of some MMA homopolymerization studies are found in Table 2-2 (modified from Dubé, 1994). There are many full conversion studies shown in Table 2-2. However, very few high temperature polymerization studies have been performed to date.

Bulk polymerization studies performed by Nishimura (1966) confirmed the usefulness of obtaining MMA homopolymerization conversion and molecular weight data for modeling purposes. There were some questions as to the assumptions of isothermal behaviour in that report (Armitage et al., 1988). This inquiry was addressed in

a paper by Zhu and Hamielec (1991) who provided guidelines for isothermal reactions, and gave recommendations for proper ampoule dimensions, reaction temperatures and initiator concentrations.

Table 2-2 Methyl Methacrylate Homopolymerization Literature

Reference	Reaction Type	Data Collected	Full Conversion	Conditions
Achilias and Kiparissides, 1988	Bulk	x , M_w , M_n	Yes	AIBN
Achilias and Kiparissides, 1992	Bulk	x , M_w , M_n	Yes	AIBN 60 °C
Agarwal and Gupta, 1993	Solution	Not Available	Yes	BPO, Benzene
Armitage et al., 1988	Bulk	x , M_w , M_n	Yes	AIBN 50, 70, 90 °C
Benson and North, 1959	Bulk & Solution	x, k_p/k_t	No	AIBN 40 °C
Bresler et al., 1974	Bulk	k_p , k_t	No	Various Temperatures
Buback 1990	Bulk	x, k_t	No	0, 50 °C
Buback et al., 1994	Bulk	k_p/k_t	Yes	0, 50 °C
Carswell et al., 1994	Bulk	f, x, k_p , k_t	Yes	AIBN 60 °C
Davis et al., 1989	Bulk & Solution	k_p	No	AIBN 25 °C
Gladyshev and Rafikov, 1966	Bulk	x, k_p , k_t	Yes	25 °C
Hamer et al., 1981	Solution	Not Available	Yes	BPO, 27 °C
Hutchinson et al., 1993	Bulk	k_p	No	AIBN 20 - 90 °C
Jahanzad et al., 1993	Bulk	x, M_n, M_w	Yes	AIBN, NDM 60 - 90 °C
Louie et al., 1985a	Bulk & Solution	x, M_w	Yes	AIBN 45, 70 °C
Mackay and Melville, 1949	Bulk	k_p , k_t	No	35.9, 50.5 °C
Madruga and Malfeito, 1992	Bulk & Solution	x, M_n, M_w	Yes	AIBN, NDM 70 °C
Madruga et al., 1990	Bulk	x, M_w	Yes	AIBN, NDM 70 °C
Mahabadi and O'Driscoll, 1977a	Bulk	k_p , k_t	No	AIBN 15 - 30 °C
Ogo and Yokawa, 1977	Bulk	k_p , k_t	No	30 °C
Penlidis et al., 1992	Solution	x, M_n, M_w	Yes	65, 75 °C
Ponnuswamy et al., 1988	Solution	x, M_n, M_w	Yes	65, 70, 75 °C
Ramelow and Qio, 1995	Bulk	x, k_p , k_t	No	UV initiation
Schmidt et al., 1984	Solution	x	Yes	AIBN
Shen et al., 1991	Bulk	x, $R^{\cdot}$, k_p , f	Yes	60, 70, 80 °C
Shen et al., 1992	Bulk	x, $R^{\cdot}$, k_p , f	Yes	BPO 26, 50 - 80 °C
Soh and Sunberg, 1982b	Solution	x	Yes	AIBN 50 °C
Wang and Ruckenstein, 1993	Bulk	x	Yes	AIBN 80 °C
Yufand et al., 1997	Bulk	x	No	Zirconocene initiators
Zhu and Hamielec, 1991	Bulk	x, T	Yes	AIBN 60 - 90 °C
Zhu et al., 1990	Bulk	k_t , $R^{\cdot}$	Yes	AIBN 25 °C

Another major issue that involved MMA was the determination of propagation constants for this homopolymerization. Electron spin resonance was used to calculate k_p

(Ballard et al., 1986 ; Chang et al., 1992; Carswell et al., 1992 ; Cutting and Tabner, 1993) which seemed to concur with other techniques (Buback et al., 1988). Pulsed-laser polymerization, which gave similar results (Davis et al., 1989 ; Hutchinson et al., 1993), is now considered the state of the art method of obtaining propagation constants. Due to this new procedure, k_p and k_t values for MMA homopolymerizations are considered to be well known over a limited temperature range (0 to 90°C).

Chain transfer constants (see Chapter 3) for MMA have been collected to a significant degree. N-dodecyl mercaptan (NDM) was used as a chain transfer agent and was shown to modify the gel effect of the homopolymer, lowering the final molecular weight and the degree of branching (Madruga et al., 1990; Madruga and Malfeito, 1992). The use of NDM as a chain transfer agent was also discussed by Jahanzad et al. (1993) who developed a temperature dependent expression for the transfer reaction. The validity of the model has since been questioned due to its predictions that an increase in molecular weight results from an increase in the temperature. This model trend is contrary to classical kinetic theory.

The homopolymerization of MMA has been said to be best described by diffusion-controlled propagation and termination (Sundberg et al., 1981; Soh and Sundberg, 1982a and 1982b; Buback, 1990 and Buback et al., 1994). These studies have indicated that higher levels of conversion are reaction diffusion-controlled (Odian, 1991). Yet Zhu et al. (1990), observed two radical populations (free radicals and trapped radicals) at high conversions. This study went on to claim that these two populations have very different reactivities for both propagation and termination processes. Thus,

there is much work to be done to better understand the suitable mechanism for this system as well as the copolymer system with BA.

2.3 Butyl Acrylate - Methyl Methacrylate Copolymerization

Limited research has been done on BA / MMA copolymerization. A list of studies dealing with the copolymer system is found in Table 2-3. As mentioned, there are few high temperature studies cited (Table 2-3). In this section, some of the work performed are discussed and the areas that have been least explored are identified.

Bulk reactivity ratio estimates (low conversion runs) for the BA/MMA copolymer system have been obtained for low temperatures (Grassie et al., 1965; Bevington and Harris, 1967; Dubé 1994; Dubé and Penlidis, 1995). To date no reactivity ratios have been estimated for high temperature conditions.

There has only been limited work done involving the copolymerization of BA and MMA with a solvent. Brosse et al. (1983), performed solution polymerizations to observe solvent effects on the copolymer system at low conversions. In 1997, Fernandez-Garcia and Madruga, performed a kinetic study of high-conversion copolymerization of butyl acrylate with methyl methacrylate in solution. BA and MMA were copolymerized in benzene solution using AIBN as an initiator over a wide composition and conversion range. The overall copolymerization parameter ($k_p/k_t^{1/2}$) and the composition of the copolymer formed were measured as a function of conversion (Odian, 1991). Theoretical values of the coupled parameter $k_p/k_t^{1/2}$ calculated from the implicit penultimate unit

model and those of cumulative copolymer composition, determined from the terminal model, have been correlated with the results that were experimentally obtained (Gao and Penlidis, 1996; Fernandez-Garcia and Madruga, 1997).

Table 2-3 Methyl Methacrylate - Butyl Acrylate Co-polymerization Literature

Reference	Reaction Type	Data Collected	Full Conversion	Conditions
Benson and North, 1959	Bulk & Solution	x, k_p/k_t	No	AIBN 40 °C
Bevington and Harris, 1967	Bulk	r_{ij}	No	AIBN, 60 °C
Bresler et al., 1974	Bulk	k_p , k_t	No	Various Temperatures
Brosse et al., 1983	Solution	x, F_i , r_{ij}	No	H_2O_2 55 °C
Buback 1990	Bulk	x, k_t	No	0, 50 °C
Buback et al., 1994	Bulk	k_p/k_t	Yes	0, 50 °C
Carswell et al., 1994	Bulk	f, x, k_p , k_t	Yes	AIBN 60 °C
Davis et al., 1989	Bulk & Solution	k_p	No	AIBN 25 °C
Dubé and Penlidis, 1995	Bulk	x, F_i , r_{ij}, M_n, M_w	Yes	Various Temperatures
Dubé et al., 1997	Bulk	x	Yes	Various Temperatures
Fernandez-Gracia et al., 1997	Solution	x, F_i , r_{ij}	No	Benzene Solvent
Gladyshev and Rafikov, 1966	Bulk	x, k_p , k_t	Yes	25 °C
Grassie et al., 1965	Bulk	r_{ij}	No	AIBN, 60 °C
Hamer et al., 1981	Solution	NA	Yes	BPO, 27 °C
Hutchinson et al., 1993	Bulk	k_p	No	AIBN 20 - 90 °C
Hutchinson et al., 1997	Bulk	k_p , k_t	No	Pulsed Laser initiation
Jahanzad et al., 1993	Bulk	x, M_n, M_w	Yes	AIBN, NDM 60 - 90 °C
Louie et al., 1985a	Bulk & Solution	x, M_w	Yes	AIBN 45, 70 °C
Mackay and Melville, 1949	Bulk	k_p , k_t	No	35.9, 50.5 °C
Madruga and Malfeito, 1992	Bulk & Solution	x, M_n, M_w	Yes	AIBN, NDM 70 °C
Madruga et al., 1990	Bulk	x, M_w	Yes	AIBN, NDM 70 °C
Mahabadi and O'Driscoll, 1977a	Bulk	k_p , k_t	No	AIBN 15 - 30 °C
Ogo and Yokawa, 1977	Bulk	k_p , k_t	No	30 °C
Ponnuswamy et al., 1988	Solution	x, M_n, M_w	Yes	65, 70, 75 °C
Rajatapiti et al., 1996	Bulk	x, F_i , r_{ij}	No	AIBN, Low Temp
Schmidt et al., 1984	Solution	x	Yes	AIBN
Shen et al., 1991	Bulk	x, $R^{\cdot}$, k_p , f	Yes	60, 70, 80 °C
Shen et al., 1992	Bulk	x, $R^{\cdot}$, k_p , f	Yes	BPO 26, 50 - 80 °C
Soh and Sunberg, 1982b	Solution	x	Yes	AIBN 50 °C
Wang and Ruckenstein, 1993	Bulk	x	Yes	AIBN 80 °C
Wang and Ruckenstein, 1993	Bulk	x	Yes	AIBN 80 °C
Zhu and Hamielec, 1991	Bulk	x, T	Yes	AIBN 60 - 90 °C
Zhu et al., 1990	Bulk	k_t , $R^{\cdot}$	Yes	AIBN 25 °C

New techniques have emerged to allow for a more accurate study of the system. Hutchinson et al. (1997), used the pulsed-laser technique to study the penultimate copolymerization propagation kinetics of methyl methacrylate / n-butyl acrylate. The PLP/MWD technique was based upon analysis of the molecular weight distribution (MWD) of a polymer produced by pulsed-laser polymerization (PLP). The new method of analysis has proven to be a powerful probe for the examination of free-radical homopolymerization kinetics. The same method was applicable to the study of copolymerization propagation kinetics provided that proper calibrations were established for the measurement of copolymer MWDs. This was illustrated through an examination of the BA/MMA system. Statistical analysis indicated that although BA/MMA copolymer composition was well described by the terminal model, the propagation kinetics were not. Like many other systems recently examined, the data were well represented by the double prime implicit penultimate unit effect (Gao and Penlidis, 1996; Hutchinson et al., 1997). However, previous systems studied resulted in measured propagation rates that were lower than those predicted by the terminal model. As a result, it was found that the propagation rate of BA/MMA was greater than the terminal model predictions.

Estimates of reactivity ratios have been obtained for bulk copolymerizations of BA/MMA at low temperatures (Dubé and Penlidis, 1995). These parameters successfully predicted copolymer composition accurately through the full conversion range. An extensive review that included some BA/MMA work was performed by Dubé et al., (1997) on the mathematical modeling of multi-component polymerizations in batch,

semi-batch and continuous reactors. In 1996, Gao and Penlidis introduced a program that simulates the free-radical copolymerization of many systems including BA/MMA.

The advantages of operating at high temperatures (see Chapter 1) indicated that studies need to be performed in order to understand the process at these conditions. The special safety considerations, increase in the rates of depropagation, and solvent effects need to be examined in detail so that high temperature polymerizations may be performed industrially. To date, very few high temperature copolymerization studies have been performed in bulk or in solution. To that effect, this thesis will examine the bulk and solution (in toluene) free-radical polymerization kinetics of the BA/MMA copolymer system at high temperatures along the full range of conversion.

CHAPTER 3

Free Radical Polymerization Kinetics

3.1 Stages of Free Radical Polymerization

The copolymers used in this study were produced via free radical polymerization. This form of polymerization is driven by the production of polymer radicals that add to one another in a successive manner to elongate the polymer chain. There are three steps in free radical polymerization: initiation, propagation and termination.

Initiation occurs in two parts. This first involves the homolytic dissociation of an initiator, I, to yield a pair of initiator radicals, $R_I \bullet$, in the following manner:

$$I \xrightarrow{k_d} 2R_I^{\bullet} \tag{3-1}$$

The initiators used in this study were 2,2'-azobisisobutyronitrile (AIBN) and Trigonox B. These initiators underwent thermal, homolytic dissociation in order to generate initiator radicals. Not all initiator radicals go on to react with monomer. This effect is factored in through the use of an initiator efficiency, f_{int}. In systems where a large amount of solvent exists (usually near the beginning of a reaction), a solvent cage can form around the initiator radical pair. Once dissociation occurs in this cage, there is a strong possibility that the initiator radicals will recombine. This would lead to a decrease in the initiator efficiency and is termed as the cage effect (Odian, 1991). The second part of initiation

involves the addition of a newly formed radical to a monomer, M_j, to produce a monomer radical:

$$R_I^{\bullet} + M_j \xrightarrow{k_i} M_{1,j}^{\bullet} \tag{3-2}$$

This new molecule is termed a primary radical.

Propagation involves the sequential growth of the primary radical through the successive addition of hundreds to thousands of monomer molecules in the following manner:

$$M_{n,i}^{\bullet} + M_j \xrightarrow{k_p} M_{n+1,j}^{\bullet} \tag{3-3}$$

In equation 3-3, a monomer, M_j , adds to a radical of chain length n, ending in monomer i, $M_{n,i}^{\bullet}$, to form a radical of chain length n+1 ending in monomer j, $M_{n+1,j}^{\bullet}$. This step occurs quite quickly so that a long polymer chain (> 1000 monomer units long) is in a very short time (< 1 second). This model assumes that the kinetics of the propagation step are only dictated by the monomer radical at the end of the polymer chain. This mechanism is referred to as the terminal model. An alternative model that incorporates the effects of the last two monomers (at the end of a polymer radical) on the kinetics of the system is known as the penultimate model (Odian, 1991).

Termination involves the annihilation of the radical, ceasing propagation. There are many ways in which termination can occur. One type of termination is through combination (coupling):

$$M_{n,i}^{\bullet} + M_{m,j}^{\bullet} \xrightarrow{k_{tc}} M_{m+n} \tag{3-4}$$

This is a bimolecular reaction where two polymer radicals combined to form one larger polymer molecule without a radical center. A second type of termination occurs when the

two molecules mutually terminate their respective free radical centers leading to the formation of two polymers, one saturated and one unsaturated:

$$M_{n,i}^{\bullet} + M_{m,j}^{\bullet} \xrightarrow{k_{td}} M_m + M_n \tag{3-5}$$

The sum total termination step may be described as:

$$M_{n,i}^{\bullet} + M_{m,j}^{\bullet} \xrightarrow{k_t} Dead\ Polymer \tag{3-6}$$

Another type of termination occurs when the initiator radical combines with a polymer or monomer radical to form a polymer-initiator molecule as shown below:

$$M_{m,i}^{\bullet} + M_I^{\bullet} \xrightarrow{k_{tpr}} M_m - M_I \tag{3-7}$$

The process shown above is known as primary radical termination. The total rate of termination may be expressed as a function of termination by disproportionation and combination in the following manner:

$$k_t = k_{tc} + k_{td} + k_{tpr} \approx k_{tc} + k_{td} \tag{3-8}$$

Typically, the rate constant for primary radical termination is nearly zero.

In most cases, the rate of termination is said to be diffusion controlled (Mahabadi and O'Driscoll, 1977a, 1977b; North, 1974). There are three stages to the mechanism of diffusion-controlled termination which help define the conversion profile of a polymer system. The three stages are:

Translational Diffusion

Propagating polymer radicals need to diffuse towards each other in the bulk solution in order to react and terminate the polymerization. This stage depends on the viscosity of the solution as well as solvent effects.

$$M_n\cdot + M_m\cdot \underset{k_{t\overline{TD}}}{\overset{k_{tTD}}{\rightleftharpoons}} M_n\cdot \text{---} M_m\cdot \qquad (3\text{-}9)$$

As the viscosity of the solution increases, translational diffusion-controlled termination becomes dominant in determining the kinetics of the system.

Segmental Diffusion

This stage occurs after translational diffusion. Once the two polymer radicals are in close proximity, their radical ends need to rotate and join, in order to terminate the polymerization.

$$M_n\cdot \text{---} M_m\cdot \underset{k_{t\overline{SD}}}{\overset{k_{tSD}}{\rightleftharpoons}} M_n\cdot / M_m\cdot \qquad (3\text{-}10)$$

This stage is not very dependent on the viscosity of the solution.

Chemical Reaction

This stage occurs once the radicals are in close proximity to one another.

$$M_n\cdot / M_m\cdot \xrightarrow{k_{tCR}} \textit{Dead Polymer} \qquad (3\text{-}11)$$

At this point, termination depends on the properties of the radical molecules involved and not on any diffusion effects.

Using the mechanism described above, the rate of termination may be expressed in the following manner (Odian, 1991):

$$R_t = \frac{k_{tTD}\, k_{tSD}\, [M\cdot]^2}{k_{t\overline{TD}} + k_{tSD}} = k_t\, [M\cdot]^2 \tag{3-12}$$

with

$$k_{tCR} >> k_{t\overline{SD}}$$

and assuming a steady-state concentration of

$$[M_n\cdot \text{---} M_m\cdot] \quad and \quad [M_n\cdot / M_m\cdot] \tag{3-13}$$

One limiting case for this model occurs when translational diffusion is slow

$$k_{tSD} >> k_{t\overline{TD}}$$

In this case,

$$R_t = k_{tTD}\, [M\cdot]^2 \tag{3-14}$$

Another limiting case occurs when the segmental diffusion is slow

$$k_{tSD} << k_{t\overline{TD}}$$

so that

$$R_t = \frac{k_{tTD}\, k_{tSD}\, [M\cdot]^2}{k_{t\overline{TD}}} \tag{3-15}$$

Some work has suggested that segmental and translational diffusion are expected to be affected differently as the conversion increases (Dionisio and O'Driscoll, 1980; Mahabadi and O'Driscoll, 1977a, 1977b; Mahabadi and Rudin, 1979).

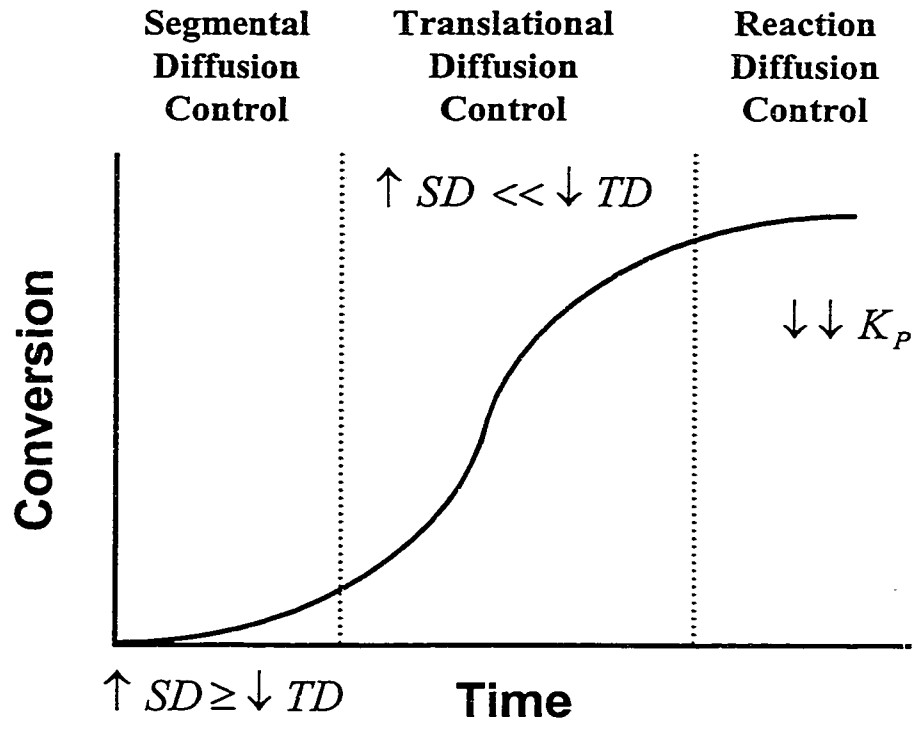

Figure 3-1 Typical S-shaped Conversion Profile

A typical s-shaped conversion curve is shown in Figure 3-1. The curve is split up into three regions that are defined by the relative rates of propagation and termination occurring in the reaction medium at one time.

The polymer medium is not viscous in the first region. As the conversion increases, the random coil size of the polymer decreases. This leads to a larger free radical concentration gradient across the polymer and so it is easier for polymer molecules to react together once translational diffusion occurs. This leads to an increase in segmental diffusion. Simultaneously, the increase in conversion also leads to an increase in the viscosity due to an increment in the amount of chain entanglement. The polymer radicals are impeded from moving quickly across the solution medium in order

to react. Thus, the rate of translational diffusion decreases. In most cases, the increase in the rate of segmental diffusion is balanced by the decrease in the rate of translational diffusion. Assuming that none of the limiting cases apply here, the rate constant of termination may be described in this manner,

$$k_t = Constant = \frac{k_{tTD}\, k_{tSD}}{k_{\overline{tTD}} + k_{tSD}} = A \tag{3-16}$$

so that the rate constant of segmental diffusion may be expressed in terms of the forward and reverse rate constants of translational diffusion. This expression may be used to calculate the various rate constants for the system.

$$k_{tSD} = \frac{A\, k_{\overline{tTD}}}{k_{tTD} - A} \tag{3-17}$$

There are some systems (i.e. styrene, methyl methacrylate) that exhibit a larger increase in segmental diffusion than a decrease in terminal diffusion (Abuin et al., 1978; High et al., 1979). At this point there is an increase in the termination rate constant and so a subsequent decrease in the rate of polymerization is observed. Since the rate of termination in this interval is dependent on the magnitude of segmental diffusion increase (relative to the decrease in translational diffusion), then the termination is said to be segmental-diffusion controlled.

In the second interval, the decrease in translational diffusion drops dramatically. The conversion and the viscosity have reached a point where the polymer radical movement is significantly hindered in the reaction medium (Lachinov et al., 1979). Thus, the decrease in translational diffusion is much larger than the increase in segmental diffusion. This results in a dramatic decrease in the rate of termination. Since the rate of

termination in this region is dependent on the magnitude of the decrease in the rate of translational diffusion (relative to the increase in segmental diffusion), then the termination is said to be translational diffusion-controlled. The rate constant of propagation also decreases in this interval. Nonetheless, the fact that propagation usually involves a polymer radical and a monomer (which can freely move around in a viscous medium) while termination requires the movement of two bulky polymer radicals, the magnitude of the rate constants relative to one another (Odian, 1991) is

$$k_t \approx \left(10^4 \text{ to } 10^5\right) k_p \tag{3-18}$$

Thus, due to the smaller size, the decrease in the rate constant of propagation is much less significant than that of the termination rate constant. This results in an increase in $k_p/k_t^{1/2}$ (Odian, 1991) and subsequently an increase in the rate of propagation. The initiator efficiency decreases linearly from the onset of the polymerization but does not have a great effect on the rate of propagation at that point (Russell et al., 1988; Sack et al., 1988). Thus, during this stage, the reaction medium turns to a gel-like state. This phenomenon is termed autoacceleration and may also be described as the gel, Trommsdorf or the Norrish-Smith effect. It turns out that the gel effect is "normal" behaviour for most polymerizations (Abuin and Lissi, 1977; Balke and Hamielec, 1973; Cardenas and O'Driscoll, 1976, 1977; Small, 1975; Turner, 1977; Yamamoto and Sugimoto, 1979). This gel effect is not a result of any non-isothermal conditions that would lead to an increase in propagation due to a localized increase in the reaction temperature (typical for exothermic polymerization). The actual gel effect phenomena occurs in isothermal conditions due to the factors described above. It is important to note

that the addition of a chain transfer agent to lower the molecular weight would shift the onset of the gel effect to higher conversions and moderate the increase of the rate throughout this period. The same effect is observed when a solvent is added to the system or the reaction temperature is decreased (Abuin and Lissi, 1977; Cardenas and O'Driscoll, 1976, 1977).

In the third interval, the rate constant of propagation significantly decreases so that $k_p/k_t^{1/2}$ begins to level off and then decreases through this period. The initiator efficiency, which has been decreasing linearly up until this point, drops dramatically (Russell et al., 1988; Sack et al., 1988). The combined rate constant and initiator efficiency trends usually lead to a decrease in the rate of propagation and a plateau effect in the conversion profile (refer to Figure 3-1). Since the viscosity of the solution and the conversion of monomer to polymer is very high, the polymer radicals are fixed in one place. At this stage, termination is proposed to occur in one or two different manners. The first is that the monomer (which is still relatively free to roam about in the solid-like medium) adds on to the stationary polymer free radical until its chain meets another radical and terminates the polymerization. Another theory proposed by Zhu et al. (1990) states that the polymer free radicals get trapped and the reaction cannot occur because there are no monomers or initiators present in those regions. Termination in this interval is said to be reaction diffusion-controlled. The phenomenon that describes the characteristics of the reaction medium at this stage is termed the glass effect. This behaviour is also characterized by the dramatic increase in the glass transition temperature of the polymer throughout the period. If the glass transition temperature increases to a point where its value is greater than the temperature of the reaction,

polymerization would stop before 100 % conversion is achieved (Russell et al., 1988; Sack et al., 1988). This is an important consideration in choosing the reaction medium and temperature for a particular system.

3.2 Copolymer Composition Based Theory

There are many models developed to simulate the polymerization rate kinetics for a copolymer system. One is the terminal model (described earlier in the chapter). This model assumes that only the terminal monomer (the one upon which the free radical resides) of a free radical polymer chain plays a role in the rate of polymerization (shown in Figure 3-2). The mechanism detailed in Figure 3-2 describes propagation and depropagation. The incorporation of depropagation in various models will be discussed in Chapter 7.

The mechanistic model, used to estimate the reactivity ratios for the copolymerization experiments, was developed by Mayo and Lewis (1948). This model will be discussed in greater detail along with the computer programs used to estimate the reactivity ratios.

The Mayo-Lewis model incorporates polymerization propagation as discussed earlier (also see equation 3-20 below). The equations used to model the copolymer system are generally described by:

$$M^{\bullet}_{n,i} + M_j \xrightarrow{k_{ij}} M^{\bullet}_{n+1,j} \qquad (3\text{-}19)$$

This case only incorporates propagation. The propagation occurs through homopolymerization and cross-polymerization as described in Figure 3-2. Homopolymerization involves the addition of monomer 'i' (either 1 or 2 in this case) to a polymer radical ending in the same monomer. Cross-polymerization involves the addition of monomer 1 to a polymer radical ending in monomer 2 or vice-versa. There are other models that incorporate the effects of depropagation (reverse depropagation) on the kinetics of the system (Wittmer, 1971). A detailed description of depropagation kinetics is found in Chapter 7.

Using this polymer reaction behaviour, Mayo and Lewis derived an expression for the instantaneous polymer composition as a function of the initial monomer concentrations and the reactivity ratios. This expression is defined as:

$$\frac{F_1}{F_2} = \frac{d[M_1]}{d[M_2]} = \frac{[M_1]}{[M_2]} \bullet \frac{r_1[M_1]+[M_2]}{[M_1]+r_2[M_2]} \tag{3-20}$$

with

$$r_1 = \frac{k_{11}}{k_{12}} \qquad and \qquad r_2 = \frac{k_{22}}{k_{21}}$$

The program that was used to estimate the reactivity ratios for this model was produced by Dubé et al. (1991a) and called RREVM. RREVM is a Fortran-based program that employes the Error-In-Variables Method (EVM) to obtain reactivity ratio estimates. The EVM method takes into account the experimental error in both dependent and independent variables. Using this method, there are no groups of variables that are considered to be free (independent) of error nor to have constant (dependent) error. All measured variables are considered on an equal basis, and represented as originating from

some true, but unknown, value which is contaminated with measurement error. The use of this method was prompted by a study conducted by Macfarlane et al. (1980) which revealed that linear methods had introduced error in the reactivity ratio estimation procedure. Patino-Leal et al. (1980), applied EVM to the estimation of reactivity ratios. This method has since been recommended over non-linear and linear methods (O'Driscoll and Reilly, 1987; Hamielec et al., 1989).

Homopolymerization

$$\text{---}M_1^{\bullet} + M_1 \underset{k_{\overline{11}}}{\overset{k_{11}}{\rightleftharpoons}} \text{---}M_1 - M_1^{\bullet}$$

$$\text{---}M_2^{\bullet} + M_2 \underset{k_{\overline{22}}}{\overset{k_{22}}{\rightleftharpoons}} \text{---}M_2 - M_2^{\bullet}$$

Cross-polymerization

$$\text{---}M_1^{\bullet} + M_2 \underset{k_{\overline{12}}}{\overset{k_{12}}{\rightleftharpoons}} \text{---}M_1 - M_2^{\bullet}$$

$$\text{---}M_2^{\bullet} + M_1 \underset{k_{\overline{21}}}{\overset{k_{21}}{\rightleftharpoons}} \text{---}M_2 - M_1^{\bullet}$$

Figure 3-2 Mechanism of Copolymerization

The second form of analysis was based on the same propagation mechanism described above. This model was developed by Meyer and Lowry in 1965. It is the

integrated form of the Mayo-Lewis equation described above. This form contains the conversion of monomer to polymer and is described as:

$$x = 1 - \left(\frac{f_{1\ell}}{f_1}\right)^{\alpha} \left(\frac{1-f_{1\ell}}{1-f_1}\right)^{\beta} \left(\frac{f_1 - \delta}{f_{1\ell} - \delta}\right)^{\gamma} \tag{3-21}$$

with

$$\alpha = \frac{r_2}{1-r_2}$$

$$\beta = \frac{r_1}{1-r_1}$$

$$\gamma = \frac{1-r_1 r_2}{(1-r_1)(1-r_2)}$$

$$\delta = \frac{1-r_2}{2-r_1-r_2}$$

The use of the Meyer-Lowry equation permits the estimation of reactivity ratios from full conversion experiments. The estimation of the parameters was performed through a Fortran 77 program developed by Burke et al., (1994). This program uses a non-linear least squares (which only incorporates the error in the dependent variables) method for obtaining the reactivity ratios.

The applicability of the Mayo-Lewis model was tested for this system in two ways. The first was that an Arrhenius-type expression was applied to the system using the reactivity ratios estimated as follows:

$$r_1 = \frac{A_{11}}{A_{12}} \exp\left(-\frac{E_{11}-E_{12}}{RT}\right) \quad \textit{and} \quad r_2 = \frac{A_{22}}{A_{21}} \exp\left(-\frac{E_{22}-E_{21}}{RT}\right) \tag{3-22}$$

This relationship indicates that the natural logarithm of a reactivity ratio is inversely proportional to temperature. This relationship has the algebraic form:

$$\ln r_{ij} \propto \frac{1}{T\,(Absolute)} \tag{3-23}$$

The use of this expression and its detailed description are found in Chapter 5.

The analysis performed using the Meyer-Lowry equation was compared to the reactivity ratio estimates from the differential form of the Mayo-Lewis model as a second test of the validity of the Mayo-Lewis equation for the prediction of polymer composition. This was performed by fitting the reactivity ratio values to an Arrhenius-type expression that was centered about the average temperature (Pritchard and Bacon, 1975). The equation is a derivation of equation 3-22 above, and is described as:

$$r_i = \frac{A_{ii}}{A_{ij}} \exp\left[-\frac{E_{ii}-E_{ij}}{R}\left(\frac{1}{T}-\frac{1}{T_o}\right)\right] \tag{3-24}$$

with

$$r_i = A \exp\left[-B\left(\frac{1}{T}-\frac{1}{T_o}\right)\right] \tag{3-25}$$

where

"i" , " j"	represent the monomers
A and B	represent grouped parameters
T_o	represents the centering temperature

The Arrhenius-type expression was fit to the reactivity ratio data using a non-linear equation solver program named Scientist® (discussed in greater detail in Chapter 7). Major discrepancies between the reactivity ratio estimates would indicate that composition drift in the samples were too large to use the differential form (Mayo-Lewis equation) rather than the integrated (Meyer-Lowry equation) model. Equation 3-22 was

also used to determine whether there was a solvent (toluene) effect on the reactivity ratios estimated.

3.3 Molecular Weight Modeling

The molecular weight is of great importance in defining polymer quality and final product performance. Therefore, understanding the basic mechanisms for the development of molecular weight as a reaction proceeds is of great use.

Estimation of the kinetic chain length of a polymer is one way of relating the molecular weight to the propagation rate (which we have already modeled). For termination by coupling, the relationship between the number-average molecular weight and the kinetic chain length for linear polymer chains is:

$$\overline{M}_n = \overline{M}_{monomer}\ \overline{X}_n = \overline{M}_{monomer}\ 2\nu \tag{3-26}$$

When termination occurs through disproportionation, the relationship is described as:

$$\overline{M}_n = \overline{M}_{monomer}\ \overline{X}_n = \overline{M}_{monomer}\ \nu \tag{3-27}$$

The kinetic chain length is related to the rate of propagation for a system initiated by the thermal homolysis of an initiator in the following manner:

$$\nu = \frac{R_P}{R_i} \approx \frac{R_p}{R_t} = \frac{k_p^2[M]^2}{2k_t R_p} = \frac{k_p[M]}{2\left(f k_d k_t [I]\right)^{1/2}} \tag{3-28}$$

It may be observed from the expressions above that the molecular weight is inversely proportional to the initiator concentration. Thus, any attempts to increase the reaction

rate by increasing the initiator concentration would lead to smaller molecules. This is an important consideration if one is trying to make a polymer of a specific molecular weight.

Another important factor in varying the molecular weight is the existence of radical displacement processes known as chain transfer reactions.

$$M_n \cdot + XA \xrightarrow{k_{tr}} M_n - X + A \cdot \tag{3-29}$$

In this case, XA may be a monomer, initiator, chain transfer agent, or other substance (i.e. polymer, solvent) with X as the atom or species transferred. The rate of chain transfer is expressed as

$$R_{tr} = k_{tr}[M \cdot][XA] \tag{3-30}$$

The species transferred may react with another monomer to reinitiate polymerization with a rate constant of k_p. Thus, through chain transfer, the polymer radical stops propagating at a smaller chain length. The effect of the chain transfer on the reaction rate depends on whether the rate of reinitiation is comparable to that of the original propagating radical. In this case, the kinetic chain length remains unaffected by the chain transfer but the degree of polymerization (X_n) decreases so that the molecular weight drops. The kinetic chain length remains constant but the amount of polymer molecules produced as the kinetic chain length varies. This degree of polymerization is then expressed as

$$\overline{X}_n = \frac{R_p}{(R_t/2) + k_{tr,M}[M \cdot][M] + k_{tr,S}[M \cdot][S] + k_{tr,I}[M \cdot][I]} \tag{3-31}$$

The various terms in the denominator relate to:

$(R_t/2)$ Rate of termination by coupling

$k_{tr,M}[M \cdot][M]$ Rate of transfer to monomer

$k_{tr,S}[M\cdot][S]$ Rate of transfer to chain transfer agent

$k_{tr,I}[M\cdot][I$ Rate of transfer to initiator

The chain transfer constants for the monomer, chain transfer agent and the initiator are given by :

$$C_M = \frac{k_{tr,M}}{k_p} \qquad C_S = \frac{k_{tr,S}}{k_p} \qquad C_I = \frac{k_{tr,I}}{k_p}$$

Thus,

$$\frac{1}{\overline{X_n}} = \frac{R_i}{2R_p} + C_M + C_S\frac{[S]}{[M]} + C_I\frac{[I]}{[M]} \tag{3-32}$$

with

$$\frac{1}{\overline{X_n}} = \frac{k_t R_p}{k_p^2[M]^2} + C_M + C_S\frac{[S]}{[M]} + C_I\frac{k_t R_p^2}{k_p^2 f k_d [M]^3} \tag{3-33}$$

There are various methods that may be used to calculate C_M , C_S , and C_I . A good description of these methods is found in Odian (1991). Chain transfer to polymer is very difficult to estimate (Yamamoto and Sigimoto, 1979). Chain transfer to solvent has not been studied in great detail (Odian, 1991). The controlled use of chain transfer agents when the chain transfer to monomer, initiator and other substances are small, have led to the production of polymers with precise molecular weights.

3.4 Polymerization Rate Expressions

The chain growth of the polymerization process resides in the propagation stage. Large amounts of polymers are formed relative to the number of initial free radicals

produced. This section details the rate expression for the system, highlighting all of the assumptions associated with the derivation.

The first assumption is that k_p and k_t are independent of chain length. This is based on the observation that the dependence of free radical formation on the molecular size diminishes considerably after dimers and trimers form in solution (Kerr, 1973). As mentioned earlier in the chapter, the propagation rate is quite high and leads to a large production of high molecular weight polymers. Thus, this assumption may be deemed valid for free radical polymerization. Monomers are consumed in the initiation as well as the propagation stage as discussed earlier in the chapter. This rate of monomer disappearance may be said to be approximately equal to the rate of propagation only:

$$-\frac{d[M]}{dt} = R_i + R_p \approx R_p \tag{3-34}$$

This is based on the larger number of molecules produced in the propagation stage rather than the initiation part of the reaction.

The next assumption is that all of the propagation steps are the same regardless of chain length. Thus, the rate of propagation may be expressed as:

$$R_p = k_p[M\cdot][M_t] \tag{3-35}$$

Since the concentration of monomer radicals is not easy to measure, a steady-state assumption of free radicals is made (Kondratiev, 1969, Wittmer, 1971). Thus, the rate of termination is said to be equal to the rate of initiation:

$$R_i \approx R_t = 2k_t[M\cdot]^2 \tag{3-36}$$

Isolating for the monomer free radical concentration and substituting the expression in the rate of propagation equation above leads to:

$$R_p = k_p[M_t]\left(\frac{R_i}{2k_t}\right)^{1/2} \tag{3-37}$$

Thus, doubling the initiator concentration doubles R_i but increases the rate of propagation by a factor of $\sqrt{2}$ only.

The rate of production of primary radicals by thermal homolysis of an initiator was described using the following expression:

$$R_d = 2f_{\text{int}}\, k_d[I] \tag{3-38}$$

In this case, f was the initiator efficiency and was defined as the fraction of the radicals produced in the decomposition reaction. The initiator efficiency may be dependent on the monomer concentration so that:

$$f_{\text{int}} = f'_{\text{int}}[M_t] \tag{3-39}$$

This leads to a first-order dependence of R_i on [M] and a 3/2-order dependence of R_p on [M]. Typically, the formation of the primary radical is a faster process than the homolysis reaction. Thus, we can state that the rate of decomposition, R_d is rate limiting and so is equal to the total rate of initiation R_i . The final equation for the rate of propagation is expressed as:

$$R_p = k_p[M_t]\left(\frac{fk_d[I]}{k_t}\right)^{1/2} \tag{3-40}$$

Now, the parameters may be estimated for a particular system at a set of conditions to model the rate of propagation.

CHAPTER 4

Experimental Procedure and Product Characterization Techniques

This chapter describes, in detail, the methods used to conduct the polymerization experiments and the manner in which the polymer products were characterized. Classical methods for the purification of the reagents were used (Stickler, 1987 ; Dubé et al., 1991b). The experimental method was very thorough and served to maximize the information content from the data. Particular emphasis was placed on reagent preparation and polymerization runs along the full range of conversion of monomer to polymer. The polymer products were characterized for percent conversion, cumulative copolymer composition and the cumulative number- and weight-average molecular weights. The systematic approach used to perform these experiments and the acquired data led to reliable, readily reproducible results.

4.1 List of Reagents

Reagent selection for the experimental runs outlined in this thesis, was based on criteria listed in Dubé (1994). This section will list the following reagents used throughout the runs. The monomers used for this work were:

- Butyl Acrylate (BA, Aldrich) with 40-80 ppm methyl ethyl hydroquinone (MEHQ)

- Methyl Methacrylate (MMA, Aldrich Chem Co.) with 20-30 ppm of hydroquinone (HQ)

The following list of solvents were used as packaged without any further purification :

Toluene (reagent grade, ACP Chemicals Inc.)

Acetone (reagent grade, ACP Chemicals Inc.)

Ethanol (denatured, ACP Chemicals Inc.)

Methanol (distilled, Aldrich Chem Co.)

Chloroform-D (Cambridge Isotope Laboratories)

Tetrahydrofuran (THF, HPLC grade, VWR Canlab Inc.)

Di-tert-butyl peroxide (Trigonox B, Akzo Nobel Chemicals Inc., initiator)

Azobisisobutyronitrile (AIBN, Aldrich Chem Co.)

1-Dodecanethiol (chain transfer agent, N-dodecylmercaptan, NDM, Acros Organics N.V.)

Sodium Hydroxide pellets (lab grade, ACP Chemicals Inc.)

Calcium Chloride Anhydrous (4-20 mesh, lab grade, ACP Chemicals Inc.)

AIBN initiator was used for reactions involving temperatures at or below 60 °C. The half-life for AIBN was too small for temperatures over 60 °C. At higher temperatures, Trigonox B, with a larger half-life under these conditions was used.

4.2 Experimental Design

The polymerization experiments performed were run to low (less than 5%) mass conversion and full mass conversion (0 to 100 wt%) of monomer to polymer. Two separate experimental designs were applied to these runs.

The purpose of the full conversion experiments was to obtain a profile of the conversion of monomer to polymer versus the time of reaction. Analysis by ^{1}H-NMR was employed to generate a profile of the cumulative copolymer composition as conversion increased. Finally the number- and weight-average molecular weights of the polymer products were analyzed as a function of conversion. For these types of experiments, a program that models this system (Dubé, 1991a) was used to obtain the approximate times to draw samples from the reaction bath. The goal was to draw samples at approximately every 8 to 10 % conversion increase. For that matter, 12 samples were usually taken for each full conversion run. The samples were drawn from the reaction bath at a greater frequency at the beginning of the run (when conversion was changing very quickly with respect to time) and less often near the end of the experiment (by this time the polymer solution was a solid near 100% conversion).

The low conversion runs were required in order to estimate reactivity ratios. These experiments also allowed for the estimation of parameters from the various alternative models that are discussed in Chapter 7. The low conversion was necessary to prevent significant composition drift from affecting the polymer composition measurements.

There were five criteria that the experimental design needed to meet in order to estimate the best reactivity ratios using the data acquired. These five conditions influenced the selection of the starting compositions of the monomer solution (before polymerization). A brief list of these conditions are listed below:

- Tidwell-Mortimer D-Optimal criterion (Tidwell and Mortimer, 1965)
- Equidistant starting monomer solution compositions (Burke et al., 1994)

- Required seven different starting monomer compositions (due to seven degrees of freedom) because some models used call for the estimation of up to six parameters.
- High temperature studies were necessary to investigate the impact of depropagation which occurs more frequently with an increase in temperature.
- Low conversion of monomer to polymer (less then 5 wt% on average).
- Use of a wide temperature range (60 to 140 °C) in order to estimate the temperature dependence of reactivity ratios.

The application of the conditions in the design of reactivity ratio experiments will be discussed in greater detail in Chapter 5.

4.3 Reagent Preparation

4.3.1 Initiator and Chain Transfer Agent Preparation

The initiators used in these experiments were azobisisobutyronitrile (AIBN) and Di-tert-butyl peroxide (Trigonox B) . The chain transfer agent, 1-Dodecanethiol (CTA) and the initiator, Trigonox B were used as packaged without further purification. AIBN was purified as follows.

First, a water bath was heated to 50 °C using a built in thermometer. A 250 ml beaker was filled with 150 ml of distilled methanol. The beaker was then submerged into the water bath and heated until it reached 40 °C (using a thermometer in the beaker). AIBN was then added until a saturated solution was produced. Next, the beaker was covered with a watch glass and placed in a freezer at -10 °C for 20 minutes in order to recrystalize the AIBN. The crystalline solution was then filtered using a Buchner funnel. The filtered crystals were placed in the 250 ml beaker with 140 ml of distilled methanol.

The production of a saturated solution was repeated two times as before. After the creation of the third saturated solution, the beaker was left to return to room temperature in order to produce larger crystals. Once at room temperature, the covered beaker was placed in the freezer for 30 minutes and then filtered one last time. The purified AIBN crystals were placed in a tinted bottle covered with a thick tape, labeled according to WHMIS standards and stored in a freezer at -10 °C. The initiator was allowed to heat to room temperature before being used for the polymerization reactions.

4.3.2 Monomer Preparation

There were three steps in monomer preparation. The first involved the removal of water and inhibitor from the monomers (these were normally supplied with inhibitors). The inhibitors introduced by the suppliers were:

40-80 ppm methyl ethyl hydroquinone (MEHQ) for Butyl Acrylate (BA, Aldrich)

20-30 ppm of hydroquinone (HQ) for Methyl Methacrylate (MMA, Aldrich)

The second step was to distill the monomer using a rotary evaporator. The final step involved the removal of oxygen (a free radical scavenger) from the reaction mixture. These steps are described in detail below.

4.3.2.1 Monomer Cleaning

Initially, the monomer (MMA) was taken out of the freezer and left to heat up to room temperature (BA was stored at room temperature). The monomers were then

washed three times with a 10% solution of sodium hydroxide (NaOH) to remove the inhibitor. This was done using a separatory funnel with a NaOH solution equivalent to one-tenth of the monomer volume. After every wash, the aqueous (bottom) portion of the emulsion was discarded. Next, the monomer was washed three times with distilled, deionized water in the same manner using an amount of water equivalent to one-tenth of the monomer volume. The monomer was then placed in an Erlenmeyer flask and a small amount of calcium chloride (to remove any residual water) was added. The flask was then closed with an aluminum wrapped rubber stopper and sealed with parafilm. The sealed solution was stored in a freezer at -10°C .

4.3.2.2 Monomer Distillation

The monomers were vacuum-distilled using a rotary evaporator. The monomers were removed from the freezer and left to thaw to room temperature. The distillation temperatures were 32°C for BA and 35°C for MMA. The first 20-50 ml of the distillate were discarded. Distillation continued until 20-50 ml of the undistilled solution was left. The distillations were performed, at most, 24 hours before polymerization in order to minimize the formation of dimers and trimers. After distillation, the purified monomers were stored in the freezer at -10 °C if necessary.

4.3.2.3 Solution Preparation and Oxygen Removal

Solution preparation involved the calculation of the amounts of monomers, solvents and initiators required to make up a mixture at a given feed mole fraction. The freshly distilled monomers were removed from the freezer and left to reach room temperature. The monomers and solvents were weighed out using 5 - 10 ml pipettes with the initiators and the chain transfer agent added using Eppendorf micropipettors. Once the monomer solution was made, it was pipetted into borosilicate glass ampoules (length 10 cm, outer diameter 1.7 cm, capacity 10 ml) to a total of approximately 1.5 ml .

Next, oxygen was removed from the reaction mixture (prior to polymerization) using the setup shown in Figure 4-1. Each ampoule was connected to the degassing manifold (Apeizon AP 100 high/low temperature vacuum grease was applied to ensure a good seal). The ampoules were submerged in a liquid nitrogen containing dewar and a vacuum was applied to the contents. The valve to the manifold was then closed and the contents were allowed to thaw. Oxygen bubbles were then seen to rise into the evacuated head space of the ampoules. The ampoules were refrozen and the procedure was repeated for a total of three freeze-pump-thaw cycles or until bubbling was no longer evident. Finally, the ampoules were flame-sealed and placed in ice water.

4.4 Polymerization Reaction Runs and Assays

There were four different types of polymerization experiments performed in this work:

- Bulk Reactivity Ratio BA/MMA Experiments
- Solution (in toluene) Reactivity Ratio BA/MMA Experiments

- Bulk Full Conversion BA/MMA Experiments
- Bulk and Solution (in toluene) Full Conversion BA/MMA Experiments

The reactivity ratio experiments were run to low conversion levels (typically less than 5 wt%). This was done in order to minimize the effects of composition drift. The full conversion experiments were run along the full range of conversion of monomer to polymer (0 to 100 wt%). The procedures for all of these runs were similar with a few exceptions as noted below.

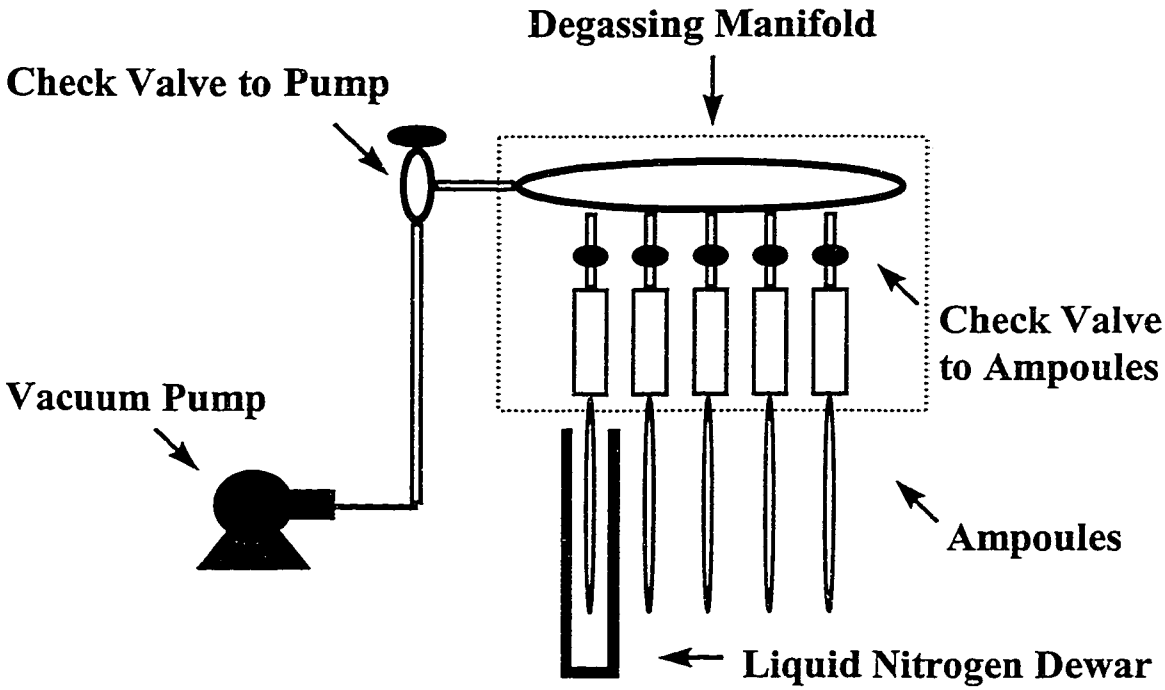

Figure 4-1 Polymerization Degassing Setup

A NESLAB EXACAL EX-250HT high temperature bath was employed to maintain the ampoules at the desired reaction temperature. Dow Corning 510 fluid was

used as the heat transfer medium in the bath to reduce vapour formation at elevated operating temperatures.

The oil bath was heated to the desired temperature. The ampoules were removed from the ice bath and then cloth dried. They were submerged in the reactor for a specified time. At recorded time intervals, the ampoules were removed, dried and directly placed in ice water to quench the reaction. Each unopened ampoule was then weighed, scored and broken. The contents were then poured into a pre-weighed crystallization dish and the ampoule was cleaned with acetone. A 10-fold excess of ethanol was then poured into the dish to precipitate the polymer and the mixture was then allowed to dry. In some full conversion experiments at conversions greater than, say 80 wt%, the unopened ampoules were placed in liquid nitrogen after being weighed. The ampoules were then broken while frozen and a piece of frozen polymer was placed in a pre-weighed crystallization dish and weighed immediately. The weight of the frozen polymer slug now represented the reaction medium before precipitation of the polymer. The polymer slug was dissolved in acetone and precipitated in a 10-fold excess of ethanol.

Upon drying, the crystallization dishes were placed in a vacuum oven. The samples remained in the oven for over 24 hours and were left to cool to room temperature for another period of 24 hours. The crystallization dishes (containing polymer) and the empty broken ampoules were then weighed. An overview of these procedures as well as the ensuing product characterization are shown in Figure 4-2.

4.5 Product Characterization

4.5.1 Gravimetric

A gravimetric analysis was used to determine the percent conversion of monomer to polymer. The weight conversion was calculated using the following formula for bulk and solution polymerization runs:

(4-1)

$$\%\ Conversion = \frac{(wt.of\ dried\ polymer\ and\ dish - wt.of\ empty\ dish)}{(wt.of\ ampoule\ and\ reaction\ mixture - wt.of\ ampoule)\times(1 - wt.\ fraction\ monomer\ in\ feed)} \times 100$$

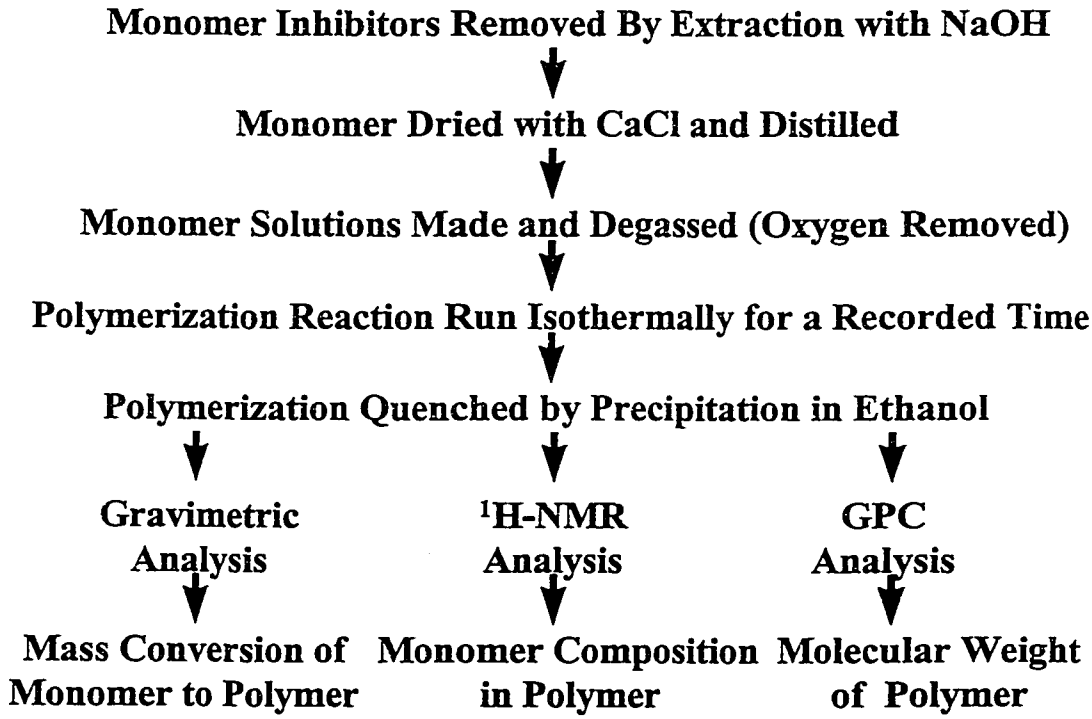

Figure 4-2 Polymerization Procedure Outline

4.5.2 Polymer Composition Measurement

Proton nuclear magnetic resonance (^{1}H-NMR) spectroscopy was used to determine the amount of each monomer chemically bound in the polymer. The polymer composition may be obtained in many ways including gas chromatography, UV spectroscopy, ^{1}H-NMR spectroscopy and elemental analysis. ^{1}H-NMR spectroscopy is both accurate and simple to perform. ^{1}H-NMR spectroscopy yields a measure of the extent to which electromagnetic radiation (radiant and magnetic energy) is absorbed or emitted by a sample of material. The absorption or emission of radiation depends on the wavelength. This relationship is known as the absorption/emission spectrum. In ^{1}H-NMR spectroscopy, a sample is placed in a magnetic field which causes the deflection of the hydrogen bonds to different degrees dependent on the amount of shielding (against the magnetic field) that results from the different atomic arrangements surrounding the bond. Once the magnetic field is turned off, the hydrogen bond relaxes and this energy is released. This released energy is measured and compared to a reference in the spectrum (deuterated chloroform, in our case). The absorption of electromagnetic radiation occurs in the radio frequency portion of the spectrum so that the radiant energy involved in the deflection is very small. The recorded spectrum of electromagnetic radiation absorbed contains peaks in which the ratio of the areas of the peaks are equivalent to the relative amounts of each proton (hydrogen bond) of a particular grouping. In our case, this grouping was identified as belonging to either BA or MMA due to its position from the reference peak. In the BA/MMA system the spectral peak of the -OCH_3 group in MMA

Butyl Acrylate = 4.02 ppm

Methy Methacrylate = 3.57 to 3.62 ppm

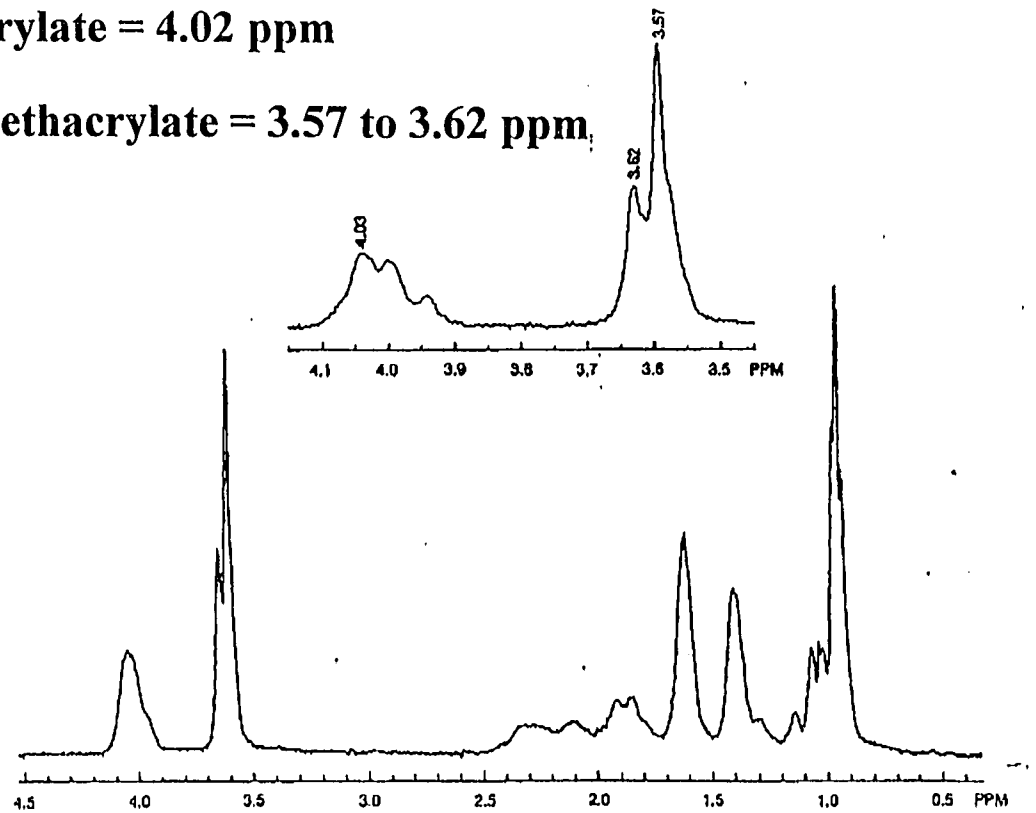

Figure 4-3 ^{1}H-NMR Spectrum For The BA/MMA System

was at ~3.6 ppm and the -OCH_2 group in BA was located at ~4.0 ppm. Sample spectra for this system are shown in Figure 4-3.

The acquisition of the NMR spectra was accomplished with a Bruker AMX500 ^{1}H-NMR spectrometer run using the following specifications :

- Deuterated chloroform as a reference and solvent
- Spectrometer frequency of approximately 500 Mhz
- Relaxation delay of 0.01 seconds
- Pulse of 3 microseconds
- Acquisition time of 4.6 seconds (on average)
- Number of scans averaged for readout was 16
- Time domain of approximately 65000 points
- Spectral window of 7042 Hz (13 to -2)

The procedure involved in acquiring the NMR spectra along with an explanation of the parameters just listed is found in Figure 4-4.

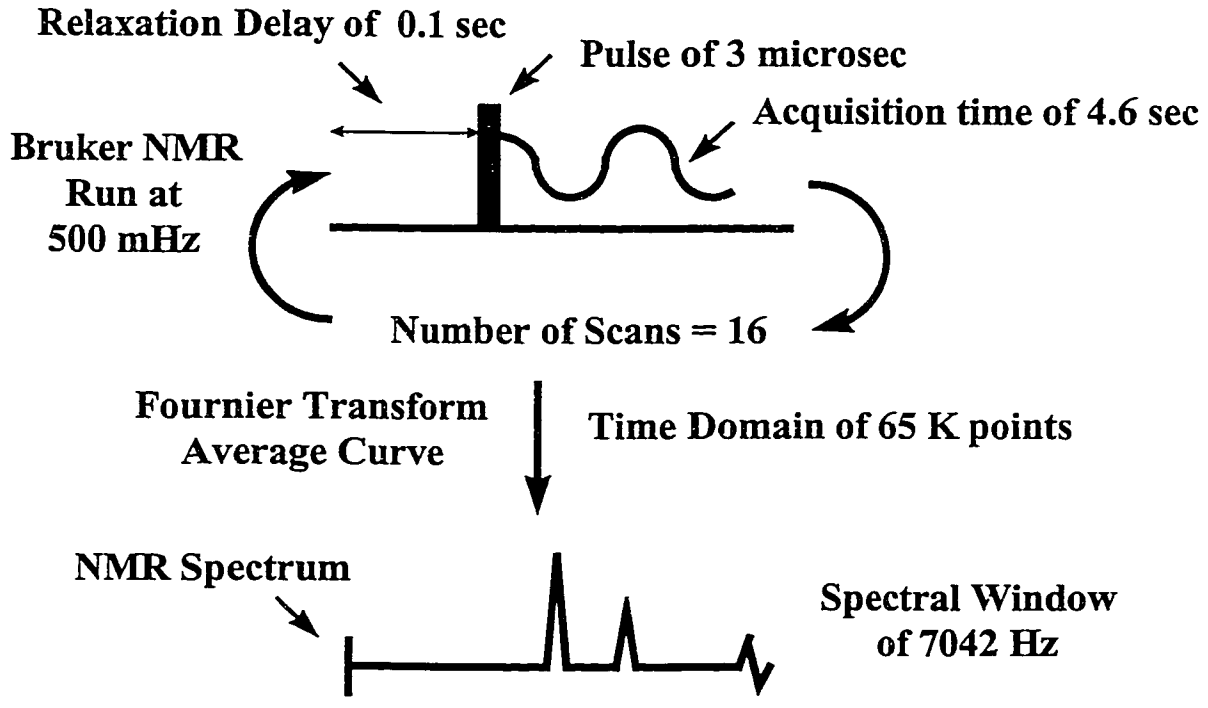

Figure 4-4 NMR Procedure And Specifications

Sample preparation for NMR analysis involved mixing a portion of the dried polymer with deuterated chloroform (chloroform-d) for a 2% w/v solution. As mentioned, the relative amounts of monomer bound in the polymer were estimated from the areas under the appropriate absorption peaks of the spectra. Thus, the mole fraction of the incorporation of monomer in the polymer was calculated as

$$F_{BA} = \frac{\frac{BA\ Area}{2}}{\frac{BA\ Area}{2} + \frac{MMA\ Area}{3}} \qquad (4\text{-}2)$$

and

$$F_{MMA} = \frac{\frac{MMA\ Area}{3}}{\frac{BA\ Area}{2} + \frac{MMA\ Area}{3}} \qquad (4\text{-}3)$$

4.5.3 Molecular Weight Measurement

A Waters Associates Gel Permeation Chromatograph was used to determine the number- and weight-average molecular weights of the polymer ($\overline{M}_n$ and $\overline{M}_w$, respectively) using a differential refractometer. This system is illustrated along with several key components in Figure 4-5. The detailed description of the system components are listed as follows:

- Rheodyne 7725I Injector with automatic relay
- Waters 610 Fluid Unit (pump)

- Waters Syragel Column container with HR6, HR4 and HR3 columns set up in the order specified.
- Waters 600 Pump Controller
- Waters 410 Differential Refractometer
- Digital Venturis 575 Personal Computer
- Millennium Chromatography Manager Version 2.15

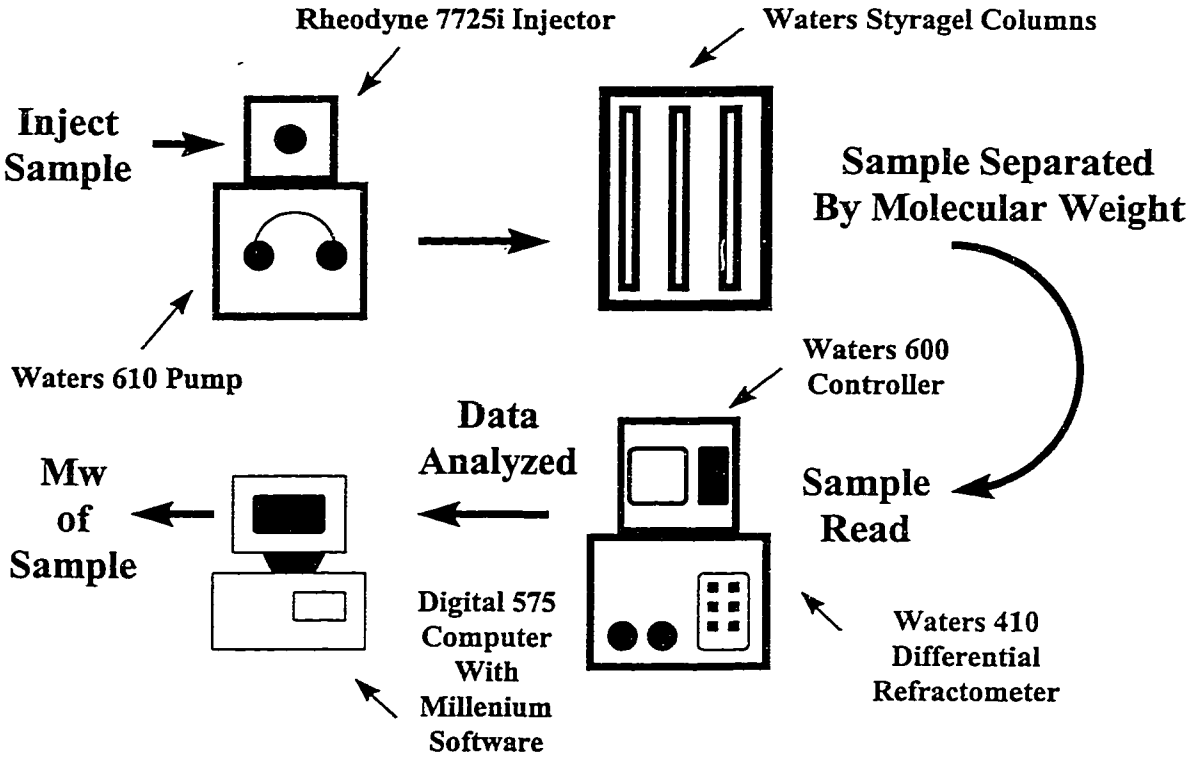

Figure 4-5 Gel Permeation Chromatograph Setup

A sample of polymer diluted in tetrahydrofuran to make a 0.01 g/ 100 ml solution was injected (Figure 4-5). This passed from the Rheodyne injector through the pump at 0.3 ml/min as controlled by the Waters 600 controller and the Millennium software. The sample was then fractionated in the gel columns which were kept at 38 °C and read by the differential refractometer. The raw data were then analyzed using the Millennium software and different molecular weight numbers were generated. The SYRAGEL

columns were packed with porous beads made up of a cross-linked polymer of styrene and divinyl benzene.

The GPC method separates the polymer sample based on its hydrodynamic volume. Hydrodynamic volume is directly proportional to the degree of solvation of the polymer molecules, the molecular weight and the amount of short- and long-chain branching of the polymer. Thus, the larger the hydrodynamic volume, the faster the polymer will elute through the columns. Polymers with a small hydrodynamic volume enter the pores of the column beads and are delayed, resulting in longer elution times. Upon leaving the column, the polymer passes through a differential refractometer. This refractometer consists of a mercury lamp that shines white light through two cells. One cell contains the polymer in solution and the other, the pure solvent (reference cell). The light beam is refracted and reflected back through both cells and the difference in the refractive index between the eluted polymer solution and the pure solvent is recorded. This Differential Refractive Index (DRI) reflects the proportion of polymer solution that has eluted through the columns at a particular time. The elution time and the magnitude of the DRI are registered and a curve is developed. The elution time of the largest peak is compared with a calibration curve (elution time vs. molecular weight). This calibration curve is generated using monodisperse polystyrene standards of various molecular weights. The comparison of the sample to this calibration curve is used to generate a molecular weight distribution chromatogram which allows for the calculation of different molecular weight numbers listed below:

- Mn Number-average molecular weight for the distribution
- Mw Weight-average molecular weight for the distribution

- Mw/Mn Polydispersity of the polymer
- Mz Z average molecular weight for this distribution
- Mz+1 Z+1 average molecular weight for this distribution

The basis of the calculation of these numbers is also described in Odian (1991) .

There are many errors associated with the calculation of these molecular weight averages. The hydrodynamic volume is not a function of the molecular weight but also of copolymer composition and polymer branching. For example, the amount of long- and short-chain branching affects the hydrodynamic volume and thus, polymers of the same molecular weight but different degrees of branching will have different elution times. Polymer chains of varying compositions (and likely different molecular weights) may have the same hydrodynamic volumes and elute at the same time. These two factors need to be taken into account in the interpretation of the molecular weight distribution generated and the numbers calculated from it (Garcia-Rubio et al., 1983 ; Hamielec and Meyer, 1986 ; Styring and Hamielec, 1989 ; Cotts and Siemens, 1991). The hydrodynamic volume is also dependent on the degree of solvation. Polymer solutions with similar molecular weights and differing degrees of solvation will elute at different times. Finally, the calibration curve generated for our study was based on polystyrene standards and not varying molecular weight samples of the BA/MMA copolymer. Since polystyrene and BA/MMA polymers of the same molecular weight do not elute at the same times, there is likely some error associated with generating molecular weight averages from a BA/MMA sample elution time compared to a polystyrene calibration curve. The use of BA/MMA standards (which are not commercially available) or a universal calibration curve could have reduced such errors. In addition, there are no

Mark-Hownink coefficients for BA/MMA available in the literature; thus, a universal calibration approach could not be used. Furthermore, due to composition drift, many of the polymer samples had a wide composition distribution. While absolute molecular weight values were not measurable, the relative trends in the molecular weight averages as the conversion increased were informative. Therefore, results obtained from the molecular weight characterization of the polymer samples were treated in a relative manner. Emphasis was placed on the interpretation of trends rather than the absolute molecular weight results.

CHAPTER 5

Reactivity Ratio Estimation Experiments

BA/MMA copolymerizations were performed in order to estimate the reactivity ratios described in Chapter 3. The experiments were performed in bulk and in solution in order to provide an opportunity to observe the effects of solvent on the kinetics of the system. Since high temperatures were used, issues related to depropagation were also investigated. The effects of depropagation are described in greater detail in Chapter 7.

5.1 Experimental Design

Low conversion (< 5 wt%) experimental runs were performed in order to obtain reactivity ratios for the BA/MMA copolymer system. The low conversion criterion was necessary in order to prevent composition drift from altering the values of the reactivity ratios estimated. Typically, composition drift occurs as conversion increases. The purpose of obtaining these reactivity ratios was to provide parameters for a mechanistic model of the system (Dubé et al., 1997). The next step involved testing the applicability of the models through adherence to the Arrhenius-type equations (see equation 3-22). The Arrhenius expression (see equation 3-24) and reactivity ratios estimated using data at various temperatures were also used to test model suitability.

There were five criteria that the experimental design needed to meet in order to estimate the best reactivity ratios using the acquired data. The five conditions influenced

the selection of the starting compositions of the monomer solution (before polymerization). The first condition was the Tidwell-Mortimer D-Optimal Criterion (Tidwell and Mortimer, 1965). This criterion was used to identify two starting compositions where there was the most variation in the Mayo-Lewis model for the BA/MMA system. These two points were calculated from previous reactivity ratios estimated for the system (see Table 5-1). The Tidwell-Mortimer criterion is considered to be part of an iterative procedure. The second condition involved the use of equidistant starting monomer feed compositions in order to discriminate between competing models (Burke et al., 1994). It was shown by McFarlane et al. (1980) that the Tidwell-Mortimer method produced better reactivity ratio estimates than the equidistant points scheme. The resulting simplicity and precision due to the use of the Tidwell-Mortimer criterion has led to its recommendation for use by many authors (O'Driscoll and Reilly, 1987; Hamielec et al., 1989; Dubé et al., 1991a; Burke et al., 1994). The third condition was based on the fact that some of the mechanistic models, which were applied to the system, required the estimation of six parameters. Thus, at least seven starting monomer solution compositions were required (number of parameters +1) in order to meet the degrees of freedom criteria and estimate the parameters for these models. The fourth condition involved the fact that depropagation (reverse polymerization) was potentially active at the reaction conditions of this study. The fifth condition was the low conversion requirement in order to avoid composition drift effects. There was some evidence presented that the conversion could go up to 40% without significant composition drift occurring. Nonetheless, the experimental design was implemented with a 5 to 10 wt% conversion limit.

Using these five conditions, the following experimental design was proposed for the BA/MMA reactivity ratio experiments :

- The temperature range was from 60°C to 140°C with experiments performed at 60, 80, 100, 120, and 140 °C respectively.
- Eight different monomer feed compositions were employed at each temperature.
- The two Tidwell-Mortimer starting points calculated were replicated for a total of four runs. The monomer feed compositions were calculated using the following expressions (Tidwell and Mortimer, 1965):

$$f_{10}^{\cdot} = \frac{2}{2 + r_1} \tag{5-1}$$

$$f_{10}^{\cdot} = \frac{r_2}{2 + r_2} \tag{5-2}$$

  The initial guesses for the bulk systems were based on reactivity ratios generated by Dubé and Penlidis (1995). The initial values for the solution runs were based on reactivity ratio estimates from a combination of literature values and preliminary (screening) experiments in our lab. The resulting Tidwell-Mortimer points are found in Table 5-1.
- The remaining six initial starting monomer compositions were equidistantly dispersed amongst the two Tidwell-Mortimer points (these were selected at 0.15, 0.25, 0.35, 0.60, 0.70, and 0.95 mole fraction of BA in the monomer feed).
- Experiments were performed to < 5 wt% conversion.

This design led to the polymerization of fourteen (14) samples for each reactivity ratio experiment at a given temperature. The solution polymerization runs were performed with 30 wt% toluene. The different reactivity ratio experiments performed in this work are displayed in Table 5-2.

Table 5-1 Monomer Feed Mole Fractions Based on the Tidwell Mortimer Criterion

Temperature T (°C)	Run Type	Starting Values (**) r (BA)	r (MMA)	Mole Fractions f_{BAo}'	f_{BAo}''
60	Solution	0.2646	1.5900	0.8832	0.4429
80	Solution	0.3361	1.9270	0.8561	0.4907
100	Solution	0.3562	1.7713	0.8488	0.4697
120*	Bulk	0.3351	1.6010	0.8232	0.4970
120	Solution	0.3856	1.6972	0.8384	0.4591
140	Solution	0.3809	1.6298	0.8400	0.4490

Note: * Reactivity Ratios are taken from Dubé (1994)
** Reactivity Ratios from Preliminary Screening Experiments

Table 5-2 Reactivity Ratio Estimation: Experimental Conditions

Condition Name	Temperature T (°C)	Run Type	Toluene (wt %)
RR60S30	60	Solution	30
RR80S30	80	Solution	30
RR100S30	100	Solution	30
RR120B	120	Bulk	0
RR120S30	120	Solution	30
RR120S50	120	Solution	50
RR140S30	140	Solution	30

5.2 Bulk Reactivity Ratio Results

A great deal of work has been performed on bulk BA/MMA reactivity ratio estimation. A synopsis of the major works was described earlier in Chapter 2. The emphasis of the present study is on solution polymerization reactivity ratio estimation. A bulk reactivity ratio run was performed at 120 °C in order to verify our experimental technique with a previous study (Dubé and Penlidis, 1995). The instantaneous mole fraction of BA bound in the copolymer ($\overline{F}_{BA}$) is plotted against the BA feed concentration (f_{BA}) in Figure 5-1. The data profile is almost identical to the bulk BA/MMA experiments performed by Dubé and Penlidis (1995). The Mayo-Lewis model predictions (Figure 5-1) using reactivity ratios estimated from this study and Dubé and Penlidis (1995) were also in good agreement. The standard deviation of the $\overline{F}_{BA}$ at the two Tidwell-Mortimer points was very small (less then 5 mole% $\overline{F}_{BA}$). Reproducibility of the literature data confirmed the validity of both the experimental and analytical techniques used in this study.

The reactivity ratios estimated from all of the runs in this study (using the Meyer-Lowry and Mayo-Lewis equations) as well as those acquired from preliminary studies are located in Table 5-3. The Mayo-Lewis and Meyer-Lowry models were fit to this data as shown in Figure 5-1. Predictions from both models fit the data equally well. This indicated that both the differential (Mayo-Lewis) and integral (Meyer-Lowry) model forms

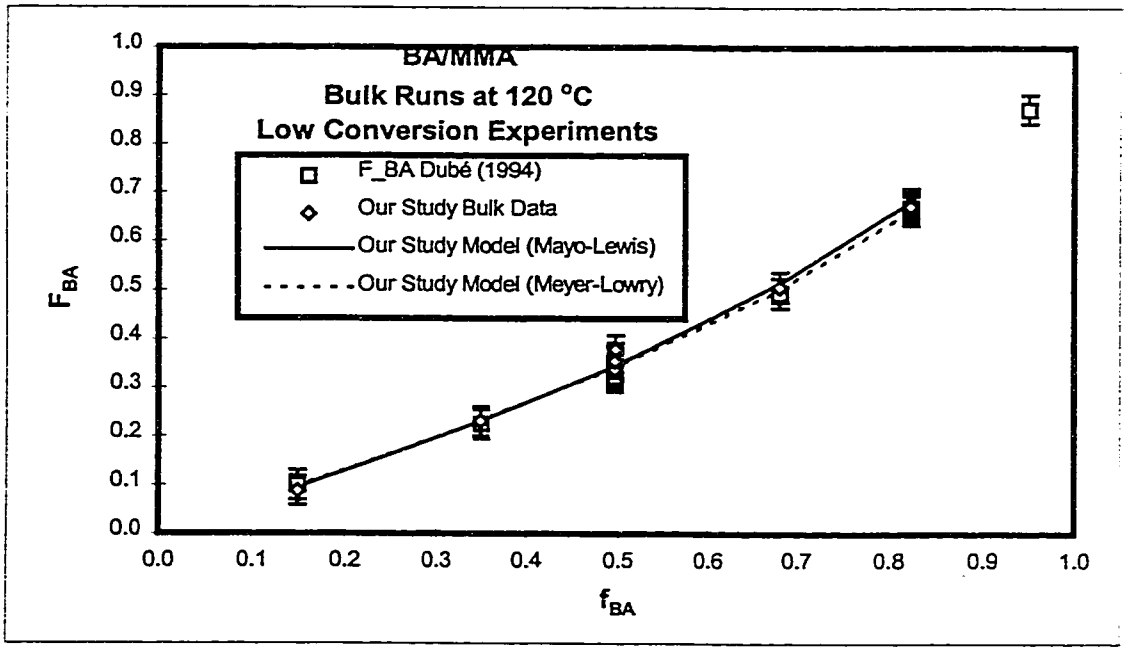

Figure 5-1 Comparisons of Bulk Reactivity Ratio Estimation Results to Literature Data

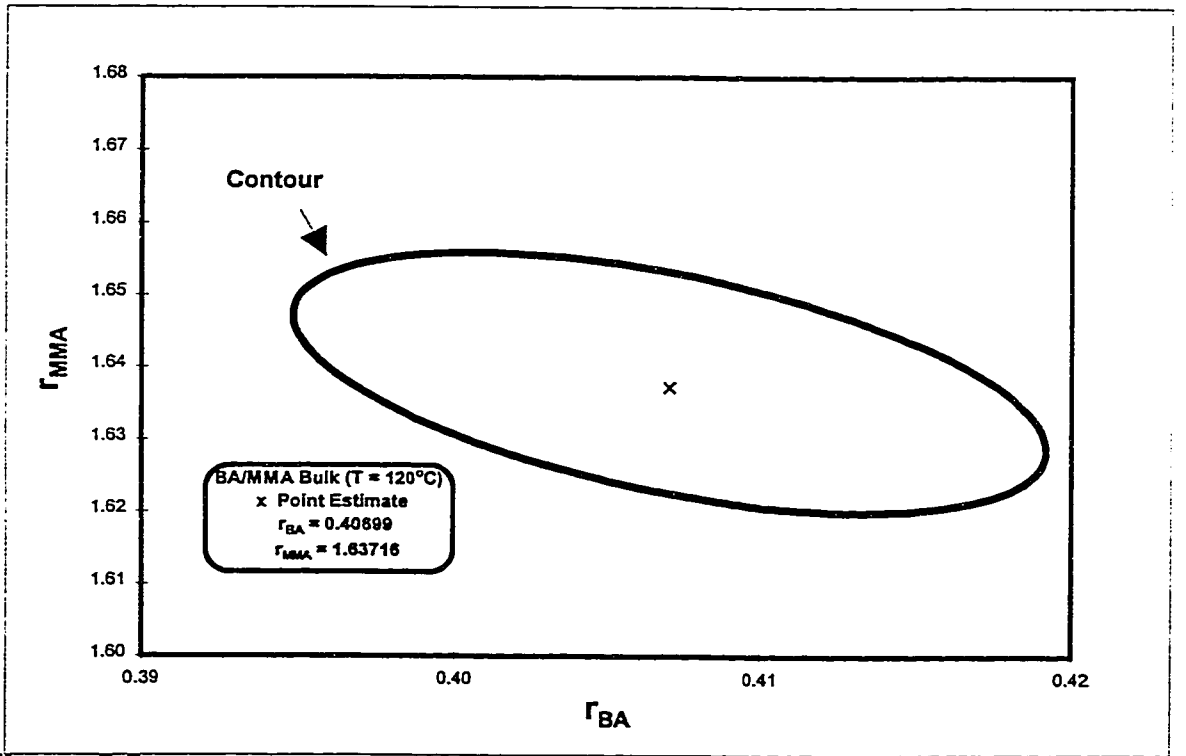

Figure 5-2 BA-MMA Reactivity Ratio Bulk Run 95% Posterior Probability Contour

will apply to this system. The use of the differential copolymer composition equation was justified due to the limited amount of composition drift at low conversions. This was also confirmed by Dubé and Penlidis (1995). Typically, composition drift was negligible (< 40 wt% conversion) so these reactivity ratio experiments with conversions under 5 wt% were not expected to exhibit composition drift. This observation was further validated by conclusions resulting from the full conversion experimental results (see Chapter 6).

The reactivity ratio results indicate the tendency of one monomer to homopropagate rather than cross-propagate. The BA/MMA bulk runs at 120 °C reveal a reactivity ratio for BA under 1 and a reactivity ratio of MMA greater than 1 (Figure 5-2). This indicates that BA tends to cross-propagate while MMA usually undergoes homo-propagation. H^1-NMR results measure relative amounts of monomers bound in the polymer as opposed to the sequence of monomers in the polymer (microstructure). The reactivity ratios allow one to predict the microstructure of the polymer. Alternatively, the microstructure can be measured using ^{13}C-NMR.

The reactivity ratio 95% posterior probability contour and reactivity ratio point estimates are plotted in Figure 5-2. The narrow elliptical shape of the region indicates the typical amount correlation between r_{BA} and r_{MMA}. Thus, observations of model suitability need to incorporate the reactivity ratio pairs and not simply individual parameter values. This indicates that the reactivity of one monomer effects the other. All contour plots generated from the reactivity ratio estimates exhibited this narrow elliptical shape.

5.3 Solution Reactivity Ratio Results

Low conversion BA/MMA solution copolymerization experiments were performed using toluene as solvent. The cumulative copolymer composition, $\overline{F}_{BA}$, is plotted versus the monomer feed composition, f_{BA}, in Figure 5-3 (similar plots at other reaction conditions may be found in Appendix A).

Table 5-3 Reactivity Ratio Estimates With Comparisons to Classical Data

Condition Name	Temperature T (°C)	Reactivity Ratios [A] (Based on Mayo-Lewis) r (BA)	r (MMA)	Reactivity Ratios [B] (Based on Meyer-Lowry) r (BA)	r (MMA)	Classical Reactivity Ratios (Preliminary Study) r (BA)	r (MMA)
RR60S30	60	0.1377	1.2046	0.1498	1.1845	0.2646	1.5900
RR80S30	80	0.2820	1.7350	0.2913	1.8285	0.3361	1.9270
RR100S30	100	0.2575	1.3278	0.2988	1.4905	0.3562	1.7713
RR120B*	120	0.4070	1.6379	0.3543	1.5805	0.3351	1.6010
RR120S30	120	0.3753	1.5469	0.3525	1.6046	0.3856	1.6972
RR120S50	120	0.3571	1.5433	0.3549	1.4611	NA	NA
RR140S30	140	0.3688	1.3802	0.3758	1.7381	0.3809	1.6298

Note: Refer to Table 5-2 for Condition Name Description
* Reactivity Ratios are taken from Dubé (1994)
[A] Reactivity ratios estimated using the Mayo-Lewis Model
[B] Reactivity ratios estimated using the Meyer-Lowry Model
NA Reactivity Ratio Estimate Not Available

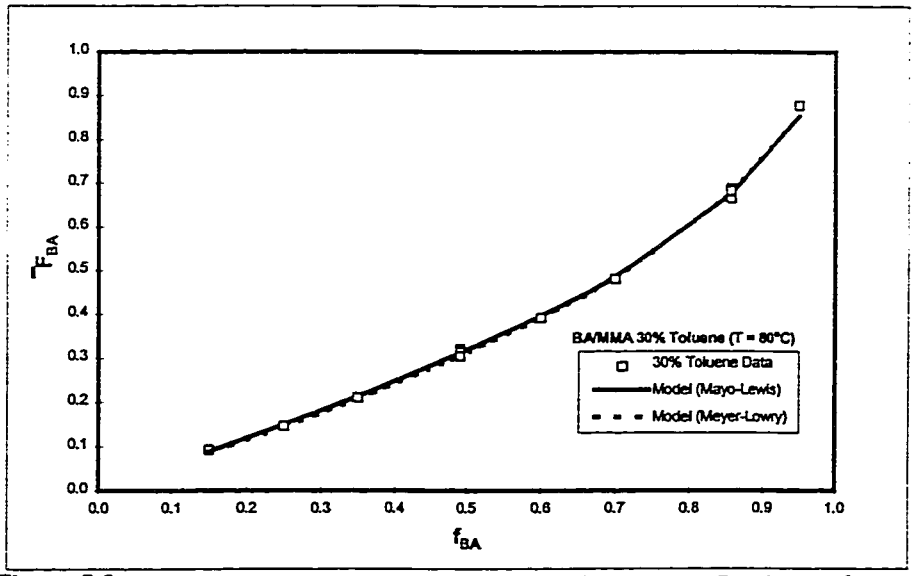

Figure 5-3 BA-MMA Reactivity Ratio 30% Toluene Composition Profile at 80 °C

There was little effect on the $\overline{F}_{BA}$ profile when temperature was increased from 60 °C to 140 °C nor as the initiator concentrations decreased. There was a change in the copolymer reactivity ratio values as temperature was varied (see Table 5-3). Since the values of the reactivity ratios have been mathematically proven to be independent of the initiator concentration (Odian, 1991), the change was attributed to the temperature effects only. As the temperature increased, the r_{BA} increased while the r_{MMA} decreased for both models (see Table 5-3). This indicated that the frequency of the homopropagation of BA and the cross-propagation of MMA were increasing as the temperature increased.

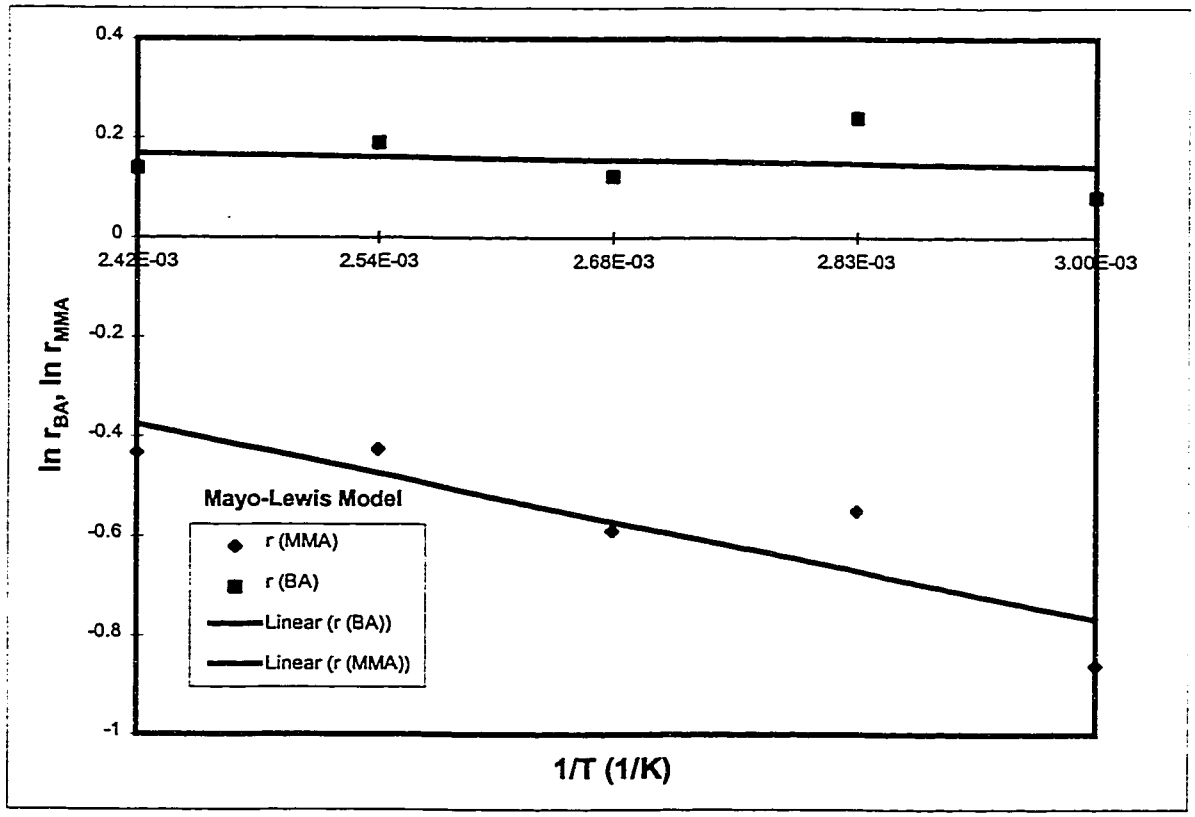

Figure 5-4 **BA-MMA 30 wt% Toluene Mayo-Lewis Model Suitability Test**

The natural logarithm of the reactivity ratio pairs estimated from the Mayo-Lewis and Meyer-Lowry models were linearly proportional to the inverse of the temperature (Figures 5-4 and 5-5). This linear relationships indicated adherence of both models to the Arrhenius type expressions shown in Chapter 3 (see equation 3-22).

It can be concluded that both the Mayo-Lewis and Meyer-Lowry models are suitable for the BA/MMA copolymer system. The two models also fit the experimental data very well as shown in Figure 5-3 (see Appendix A for somilar plots for the remainder of the experimental conditions). The modified Arrhenius-type expression (see equation 3-25) was utilized to fit the reactivity ratios derived from the Mayo-Lews and Meyer-Lowry models. The linear expressions are plotted with the BA and MMA reactivity ratio values in Figures 5-6 and 5-7, respectively. The Arrhenius-type expressions for the Mayo-Lewis and Meyer-Lowry derived reactivity ratios were almost identical. This further validates the observation made by Dubé and Penlidis (1995) regarding negligible composition drift at low conversions (< 40 wt%). 95% probability posterior contour plot were generated for the all BA/MMA solution runs (see Appendix A). All of the contours were elliptical and resembled the narrow and long shape found in Figure 5-2 (for the bulk experiments). The confidence intervals for every reactivity ratio estimate are shown in Figures 5-6 and 5-7.

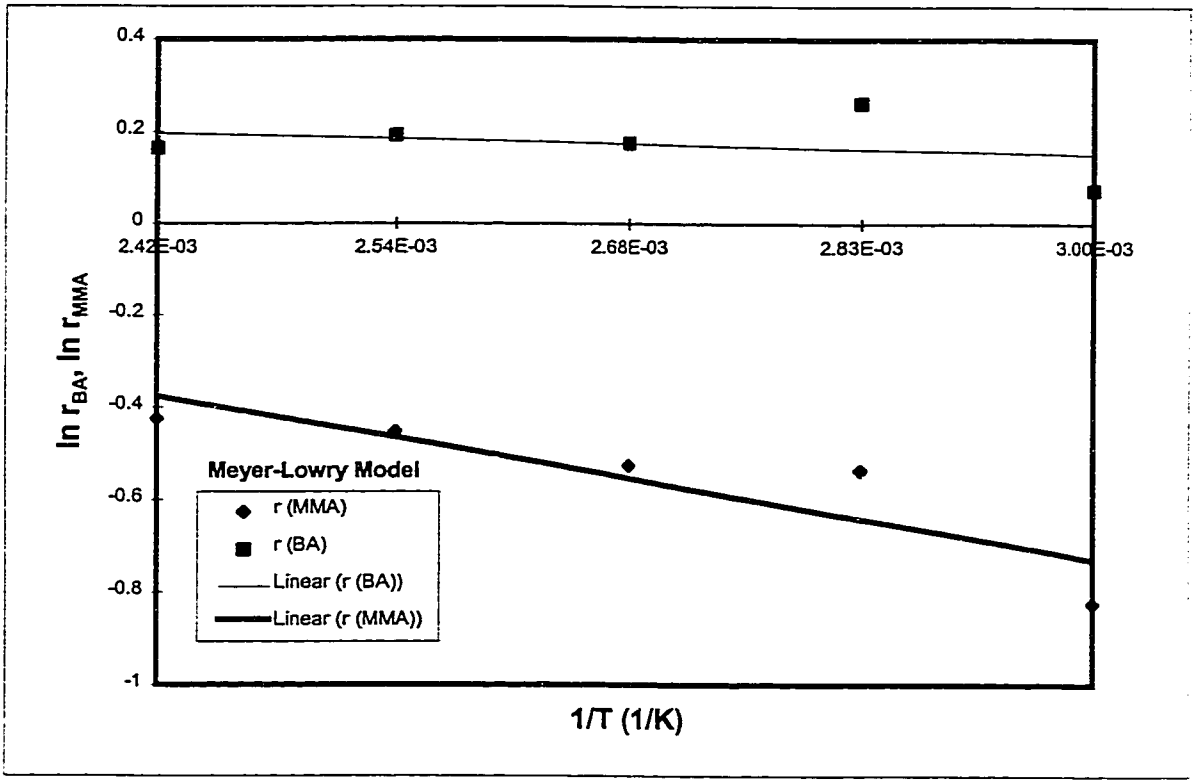

Figure 5-5 BA-MMA 30 wt% Toluene Meyer-Lowry Model Suitability Test

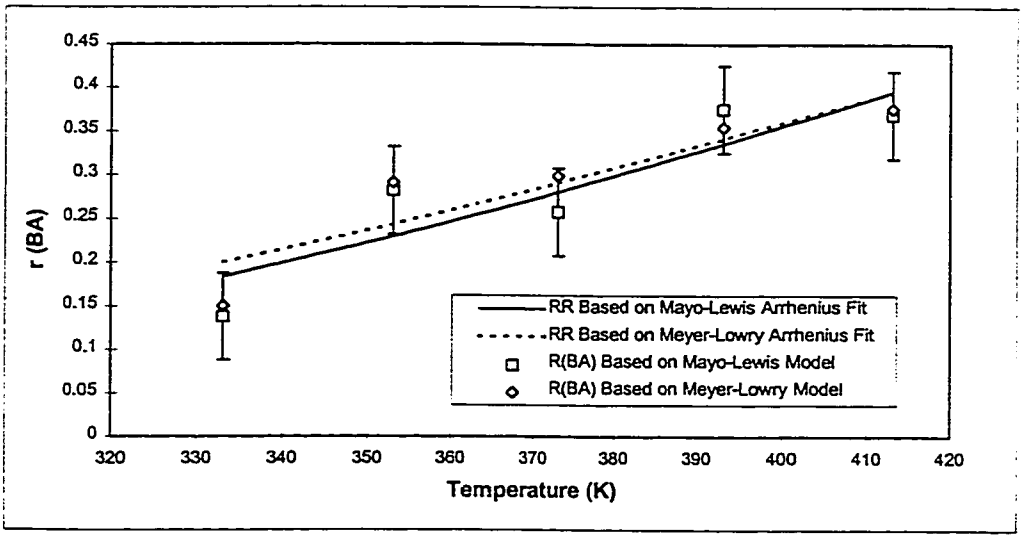

Figure 5-6 Comparison of BA Reactivity Ratio Estimates Based on the Mayo-Lewis and Meyer-Lowry Models Using Arrhenius-Type Expressions

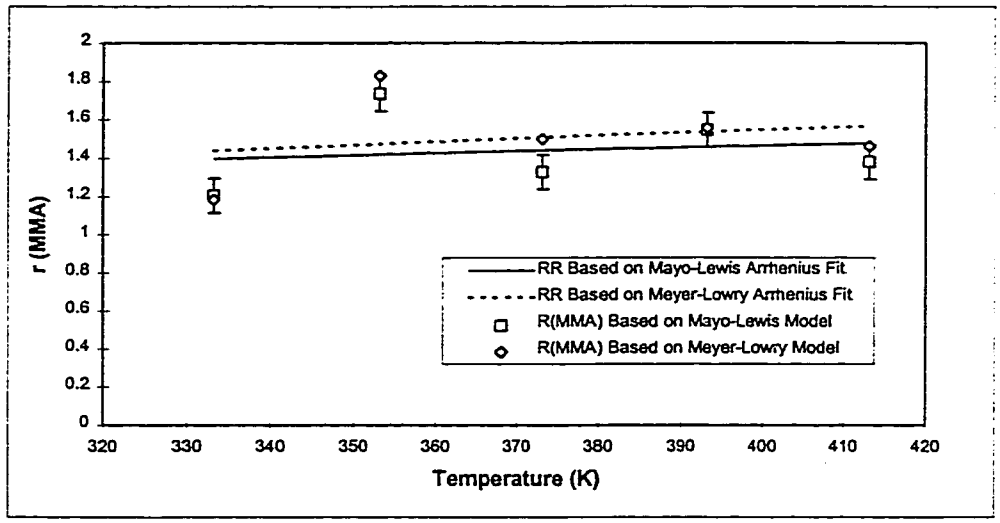

Figure 5-7 **Comparison of MMA Reactivity Ratio Estimates Based on the Mayo-Lewis and Meyer-Lowry Models Using Arrhenius-Type Expressions**

5.4 The Solvent Effect On Reactivity Ratio Results

Bulk and solution copolymerization experimental data in 0, 30, and 50 wt% toluene at 120 °C are compared in Figure 5-8. There seemed to be no effect of the solvent on the BA composition in the polymer as the conversion increased. A comparison of the reactivity ratios generated at these conditions using both Mayo-Lewis and Meyer-Lowry models indicated little or no solvent effects (Table 5-3). The small differences in the reactivity ratio estimates for each condition were attributed to the estimation procedure and experimental error.

Mayo-Lewis reactivity ratio estimates from 30 wt% toluene low conversion data and bulk results (Dubé and Penlidis, 1995) were fit to the Arrhenius-type expression (Equation 3-25). This was performed in order to determine the effects of solvent on reactivity ratio values. At higher temperatures (> 120°C), only slight differences were

observed in the reactivity ratios estimated from bulk and solution (30 wt% toluene) data (as shown in Figures 5-9 and 5-10). Similarities in the bulk and solution composition profiles at 120°C confirm the negligible solution effect at that temperature (refer to Figure 5-8). Differences in the reactivity ratio estimates derived from bulk and solution data were significant at lower temperatures (< 120°C). This indicates that the presence of a solvent will affect the reactivity ratio values at lower temperatures.

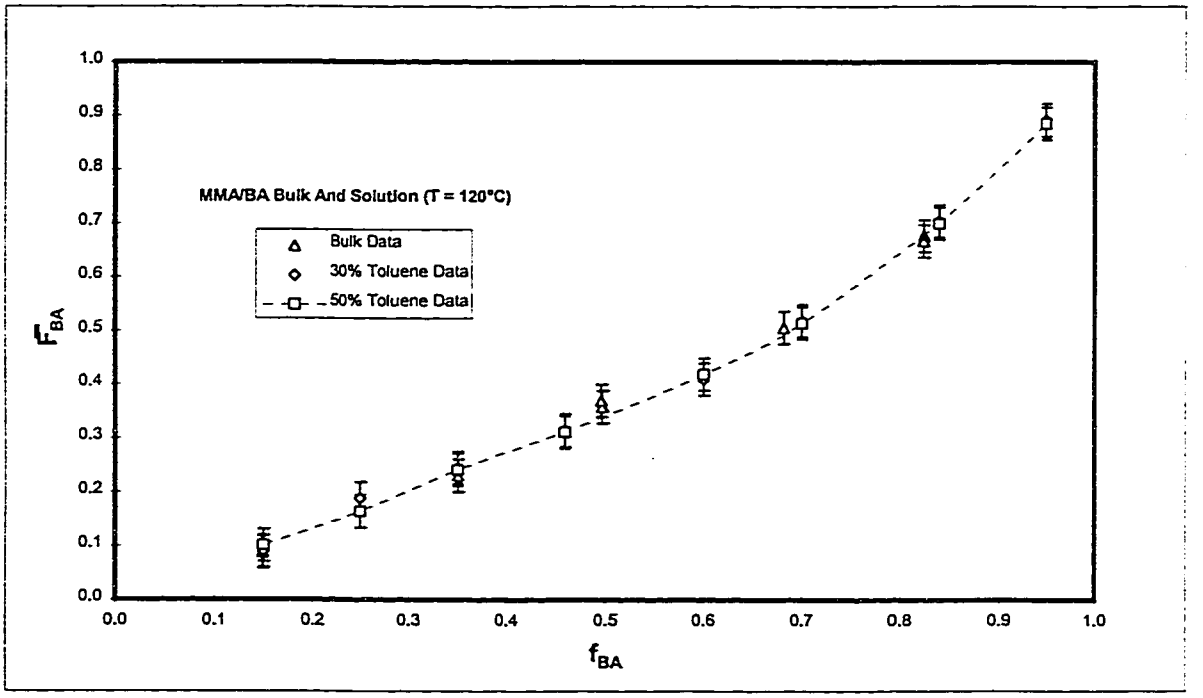

Figure 5-8 Effect of Solvent on BA/MMA Copolymer Composition

As a result of these observations, it may be concluded that the solvent will not affect the BA/MMA copolymer composition and reactivity ratios at higher temperatures. There appears to be a solvent effect on reactivity ratios at lower temperatures (< 120°C).

The effects of the solvent on the composition drift, molecular weight and conversion profiles will be discussed in Chapter 6.

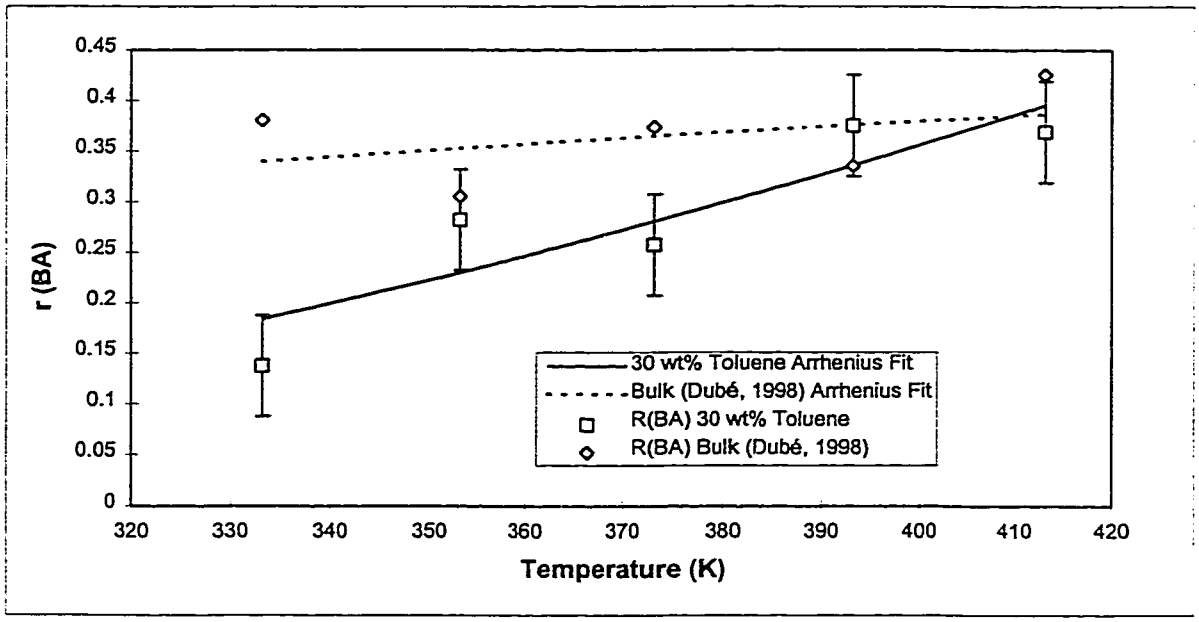

Figure 5-9 **Determination of Solvent Effect on BA Reactivity Ratio Estimates Using Arrhenius-Type Expressions**

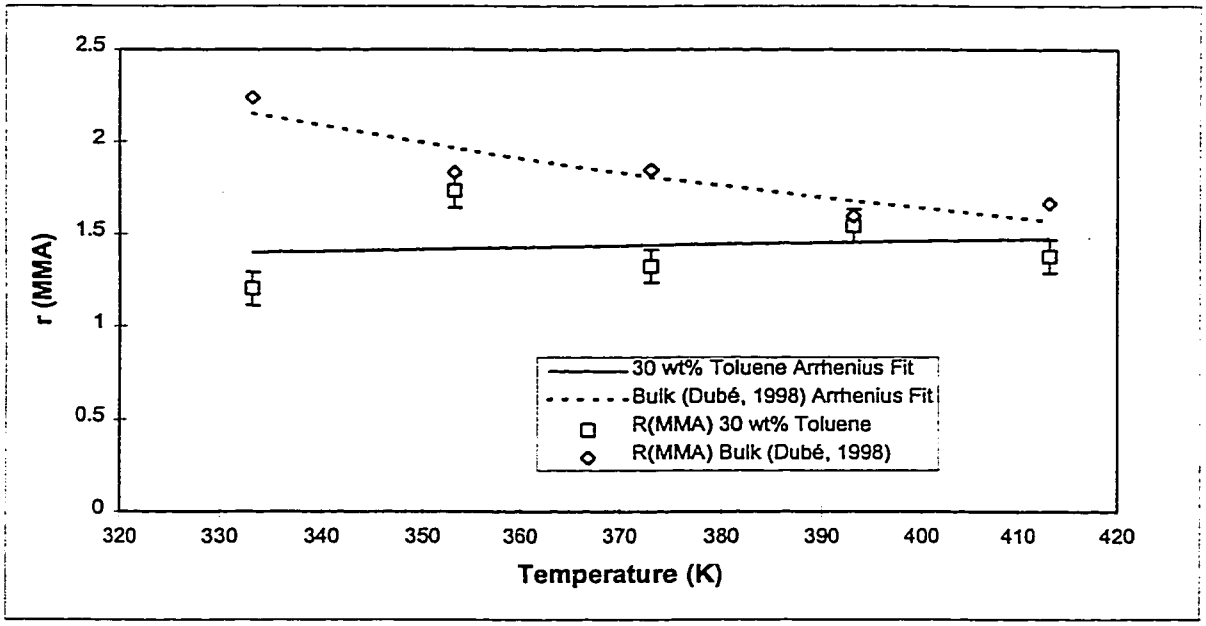

Figure 5-10 **Determination of Solvent Effect on MMA Reactivity Ratio Estimates Using Arrhenius-Type Expressions**

CHAPTER 6

Full Conversion Experiments

BA/MMA copolymerization experiments were run to high conversion levels (approximately 100 wt%). These experiments were performed in order to address the following objectives:

- Obtain bulk and solution conversion vs. time profiles for different reaction conditions.
- Observe how composition of the polymer changes as conversion increases in order to determine the moment when composition drift becomes significant.
- Observe how the molecular weight changes as the polymer conversion increases.
- Determine the effects of solvent on the copolymerization kinetics.
- Compare the effects of temperature on polymerization rates and profiles.
- Test whether reactivity ratios (from low or high conversion data) may be used to predict composition.

The conversion, cumulative copolymer composition and cumulative average molecular weight profiles were compared to classical free-radical polymerization kinetic trends.

6.1 Design of Experiments

The experiments were designed using the following criteria:

- Experimentation at previously unexplored higher temperatures (90 and 115°C).
- The solution runs were performed with 30 wt% toluene. Additional experimental runs at 23 wt% toluene were run to help confirm the solvent effects observed.

- An initial BA mole fraction of 0.439 was used (it corresponds to a 1:1 weight ratio of the BA and MMA monomers). This feed concentration is typically used in industry.
- An initial BA mole fraction of 0.148 was chosen in order to minimize the composition drift.

These criteria were used to set up a set of experiments highlighted in Table 6-1. The times at which the samples (ampoules) were drawn were determined through the use of model predictions (Dubé et al., 1997).

Table 6-1 Full Conversion Experimental Conditions and Reactivity Ratio Estimates

Condition Name	Mass Ratio BA:MMA	Temperature	Run Type	Toluene (wt %)	Trig B (initiator) [mol/L]	NDM (CTA) [mol/L]	Reactivity Ratios (Meyer-Lowry) r (BA)	r (MMA)
FC1045BT90	10 / 45	90	Bulk	0	0.0453	0.0058	3.7675	3.4427
FC79180BT115	79 / 180	115	Bulk	0	0.0061	0.0058	0.4939	1.9824
FC1045S23T115	10 / 45	115	Solution	23	0.0058	0.006	1.2352	2.2556
FC79180S23T90	79 / 180	90	Solution	23	0.045	0.006	1.1281	3.7131
FC1045S23T90	10 / 45	90	Solution	23	0.045	0.006	0.3105	1.7958
FC1045S30T115*	10 / 45	115	Solution	30	0.045	0.006	0.6353	1.5460
FC79180S30T90	79 / 180	90	Solution	30	0.045	0.006	0.7494	2.9570
FC1045S30T90	10 / 45	90	Solution	30	0.045	0.006	1.1992	2.2693

Note : The * experiment was repeated twice

6.2 Full Conversion Bulk Results

The main objectives of this section are to draw conclusions from the bulk full conversion BA/MMA experimental runs. Emphasis was placed on the study of the effects of temperature and initiator concentration. The applicability of the Terminal model for the BA/MMA system was also examined.

Two bulk BA/MMA runs were performed and their reaction conditions are shown in Table 6-1. The conversion profiles for both runs are shown in Figure 6-1. Both curves

followed the typical s-shaped curve for diffusion-controlled polymerization reactions (discussed in Chapter 3). The initial gradual increase in the conversion (for the FC1045BT90 condition) is typical for segmental diffusion-controlled polymerization. The onset of the gel effect was observed to occur at 350 min for that condition (FC1045BT90). At higher conversions, reaction diffusion-control became significant and a plateau effect was observed. The addition of BA and the increase in the temperature to 115°C (FC78190BT115) hastened the onset of the gel effect (refer to Figure 6-1). BA was expected to increase the propagation rate due to its propensity to increase the frequency of branching reactions. This will eventually increase the molecular weight of the BA/MMA copolymer as well as the reaction medium viscosity. Higher temperature conditions will also accelerate the rate of propagation which leads to the early onset of the gel effect. The outcome of increasing the propagation rate as well as the reaction medium viscosity on the gel effect is discussed in greater detail in Section 6.3 .

As expected, the composition of BA in the polymer was lower for the low BA feed composition than for the higher one (Figure 6-2). This figure also indicates that composition drift is significant only after 40 to 50 wt% conversion. This experimentally verified the observation made by Dubé and Penlidis (1995) with respect to negligible composition drift at lower compositions. It also validated the use of the terminal model to predict composition.

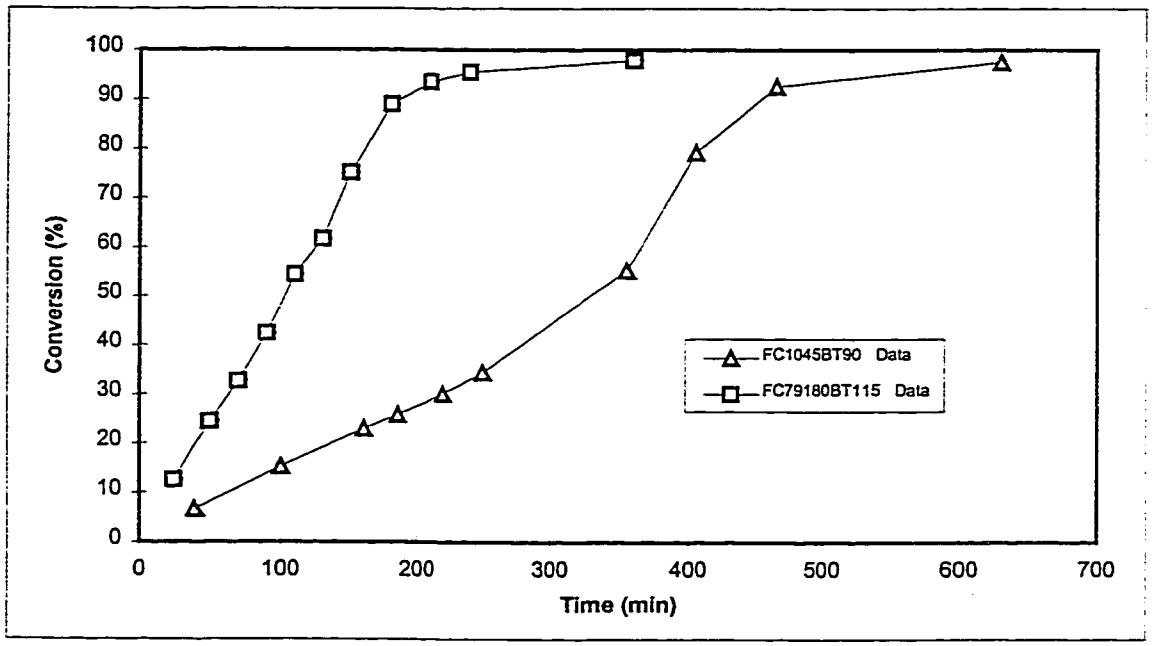

Figure 6-1 **Full Conversion BA-MMA Bulk Profiles**

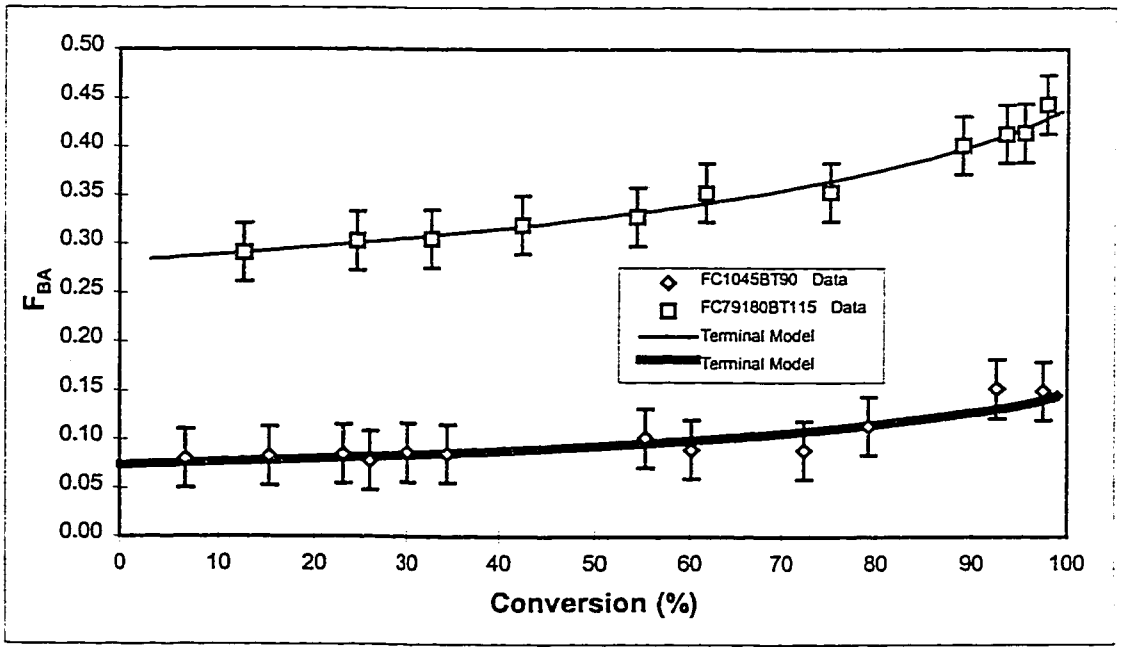

Figure 6-2 **BA-MMA Bulk Composition Profiles**

The reactivity ratios estimated using the Meyer-Lowry model are listed in Table 6-1. The reactivity ratios were then applied to the Terminal model (Dubé and Penlidis, 1995) to predict the composition profiles. The Terminal model fit all of the composition

experimental data very well (Figure 6-2). This confirmed that the reactivity ratios estimated using the Meyer-Lowry model and high conversion data may be used in the Terminal model to predict full conversion profiles.

The molecular weight profiles for the FC1045BT90 and FC79180BT115 runs indicated little or no increase along the full conversion range (refer to Figure 6-3 for a sample and Appendix C for the remainder of the results). This was due to the presence of the chain transfer agent which helped keep the molecular weight constant through chain transfer reactions (see equation 3-26 and 3-33). The number-average molecular weights were approximately 110,000 and 155,000 Daltons for the FC1045BT90 and FC79180BT115 runs. The presence of BA will increase the propagation rate due to its propensity to participate in branching reactions (Dubé, 1994).

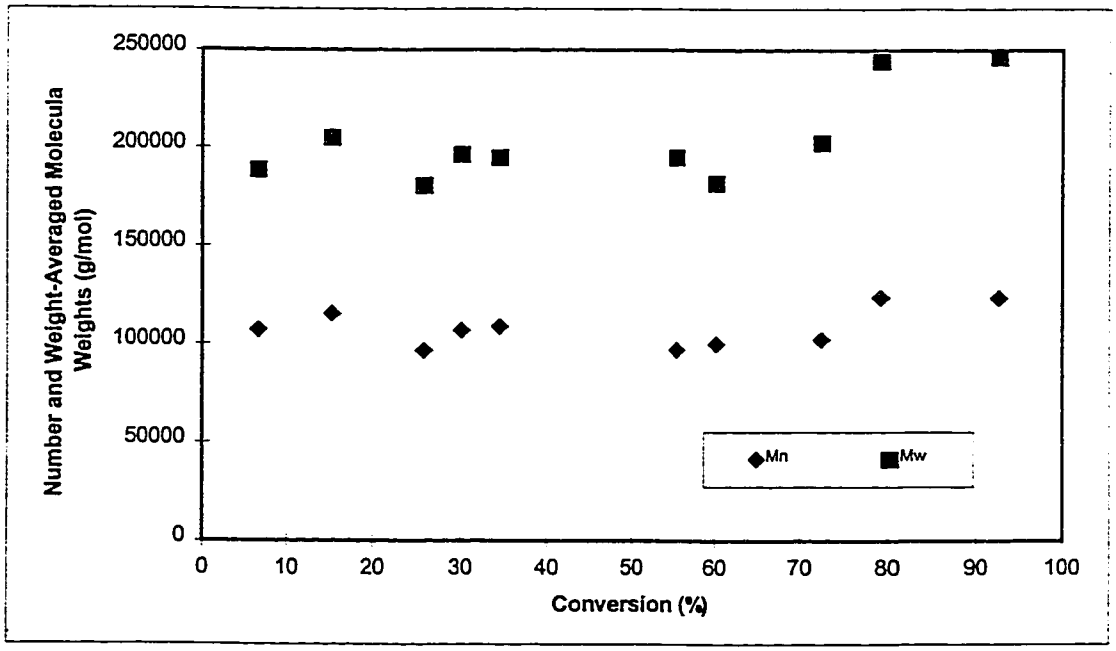

Figure 6-3 **BA-MMA 10/45 Bulk Molecular Weight Profile At 90 °C**

6.3 Full Conversion Solution Results

Full conversion BA/MMA copolymerization experiments in toluene were investigated at various conditions (see Table 6-1). The main focus of this section is to determine the temperature and initiator concentration effects on the BA/MMA system along the full conversion range. The effect of the toluene solvent on the polymerization kinetics will be discussed in a separate subsection.

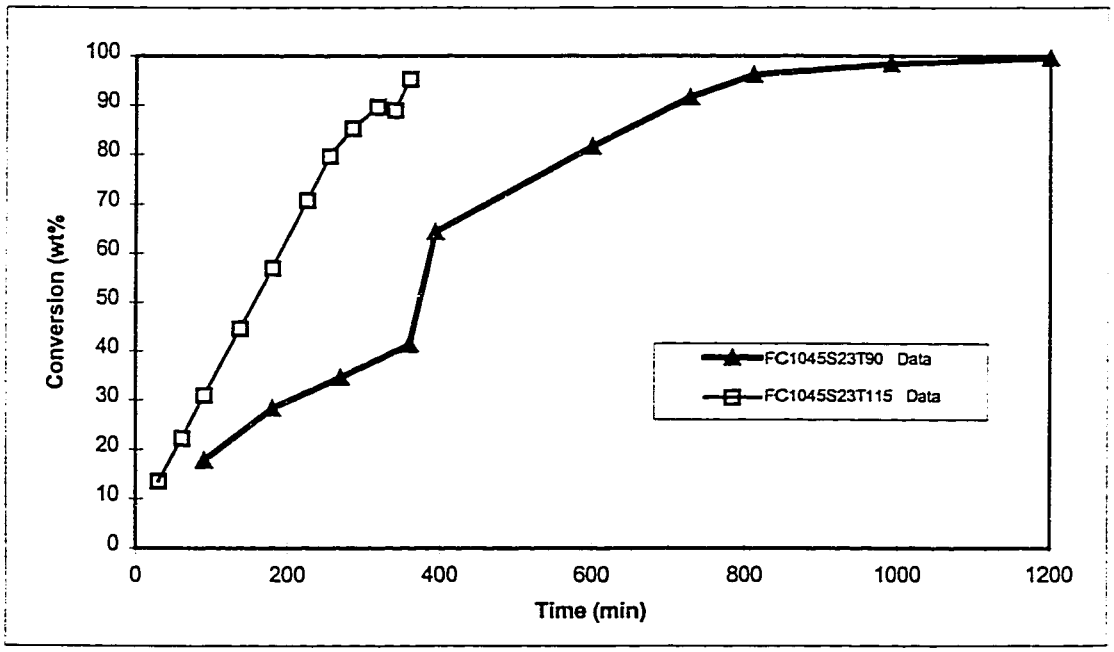

Figure 6-4 **BA-MMA 10/45 23% Toluene Conversion Profiles**

Representative conversion versus time profiles for a sample run performed using 23 wt% toluene is found Figure 6-4 with the remainder of the plots in Appendix C. These profiles followed the same s-shape (typical for diffusion-controlled

polymerization) curve exhibited by the bulk full conversion runs. The FC1045S23T115 condition exhibited an gel effect almost immediately (Figure 6-4). The translational diffusion-controlled region characterized by the gel effect occurred once the reaction medium viscosity increased to a particular point where translational diffusion decreases rapidly. This results in the large decrease of the termination rate constant relative to the propagation rate constant leading to a dramatic increase in the rate of polymerization and the gel effect. The early onset of the gel effect for the FC1045S23T115 relative to the FC1045S23T90 condition was due to a rapid increase in the viscosity of the solution at higher temperature where the propagation rate, and hence, the molecular weight was greater (Figure 6-4). This shortened the segmental-diffusion controlled region at the high temperature condition. As expected, higher temperature conditions (irregardless of weight ratio of initial solution) led to the early onset of the gel effect. The quick dynamics of the higher temperature condition were dramatic, considering 10 times less initiator was used, compared to the low temperature condition (see Table 6-1). The solvent and chain transfer agent concentrations were equal at 23 wt% toluene and 6.01 x 10^{-3} mol/L (Table 6-1), so they would not have had an effect on the trend observed.

The three systems (at 23 wt% toluene) also revealed little composition drift at lower conversions (refer to Figure 6-5 for a sample and Appendix C for the remainder of the results) as discussed in the previous section dealing with the bulk runs. The reactivity ratios estimated using the Meyer-Lowry model and 23 wt% toluene full conversion data are listed in Table 6-1. As with the bulk runs, the reactivity ratios were incorporated into the Terminal model in order to predict composition. The Terminal model fit all of the full conversion experimental data very well (refer to Figure 6-5 for a representative run

and Appendix C for the remainder of the results). This reconfirms that the Terminal model was suitable for the BA/MMA copolymer system for high conversion experiments (as discussed in Chapter 5).

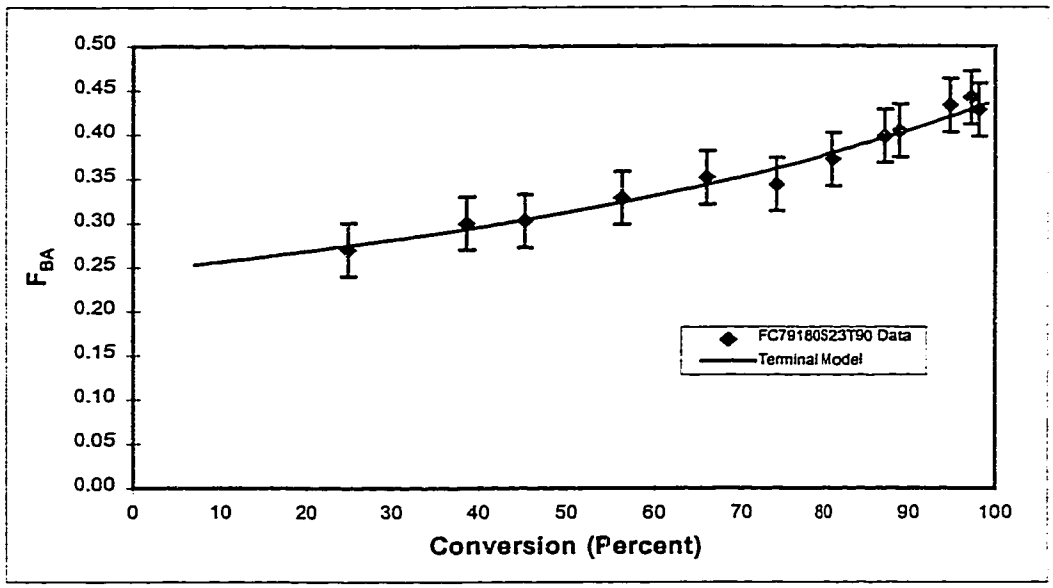

Figure 6-5 **BA-MMA 79/180 23% Toluene Composition Profile At 90 °C**

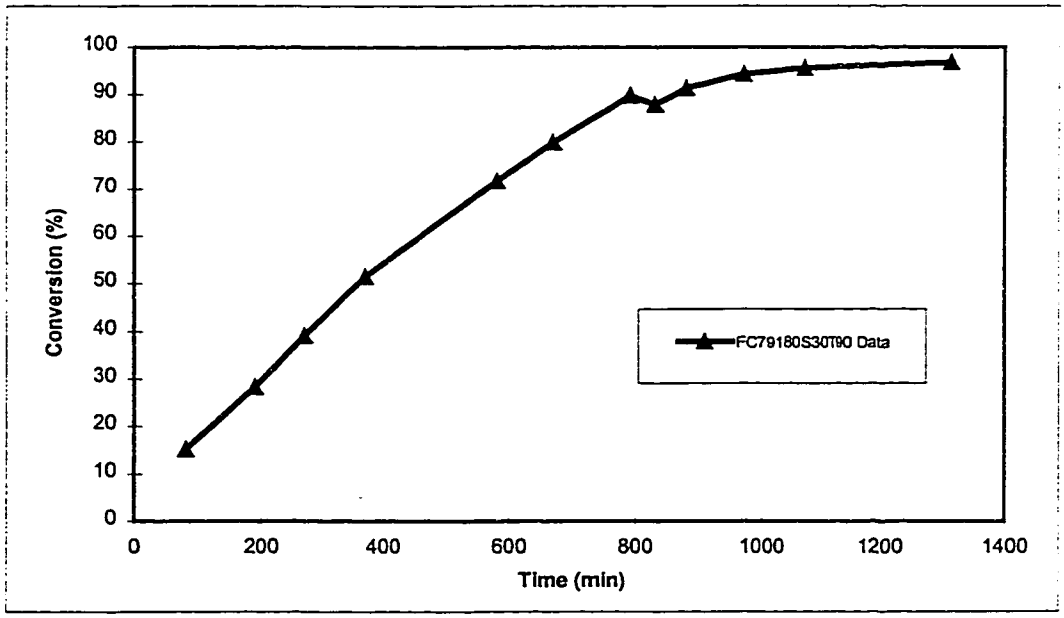

Figure 6-6 **BA-MMA 79/180 30% Toluene Conversion Profile At 90 °C**

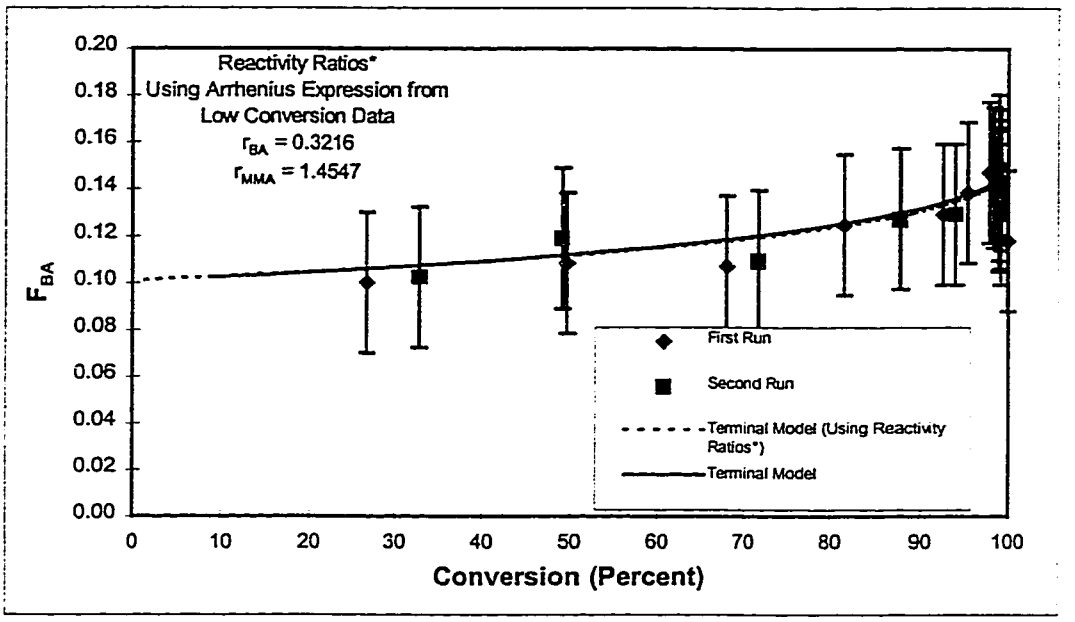

Figure 6-7 **BA-MMA 10/45 30% Toluene Composition Profile At 115 °C**

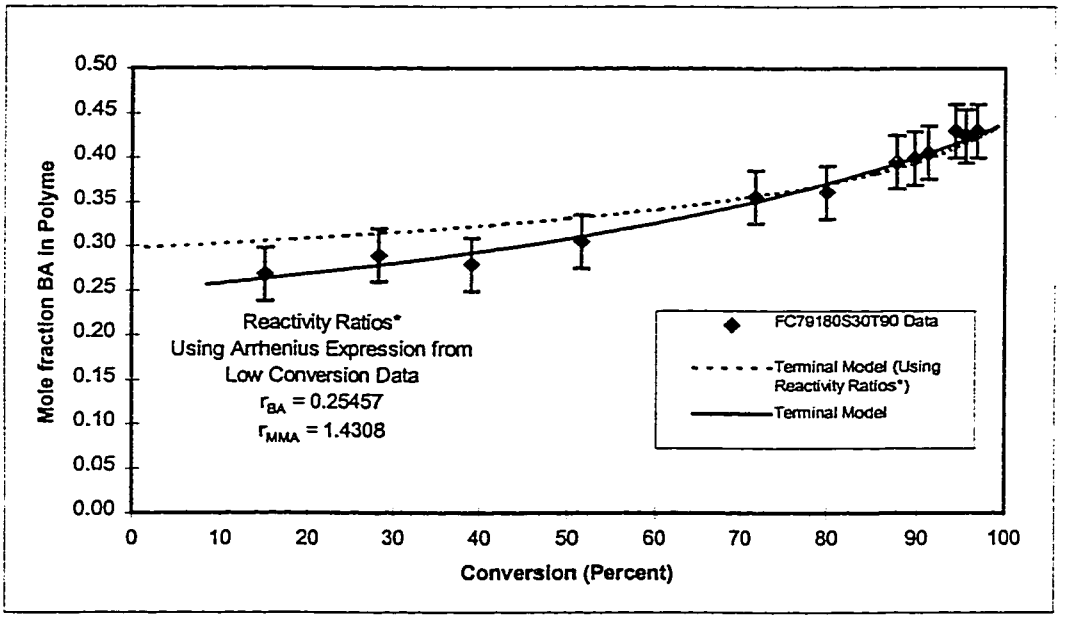

Figure 6-8 **BA-MMA 79/180 30% Toluene Composition Profile At 90 °C**

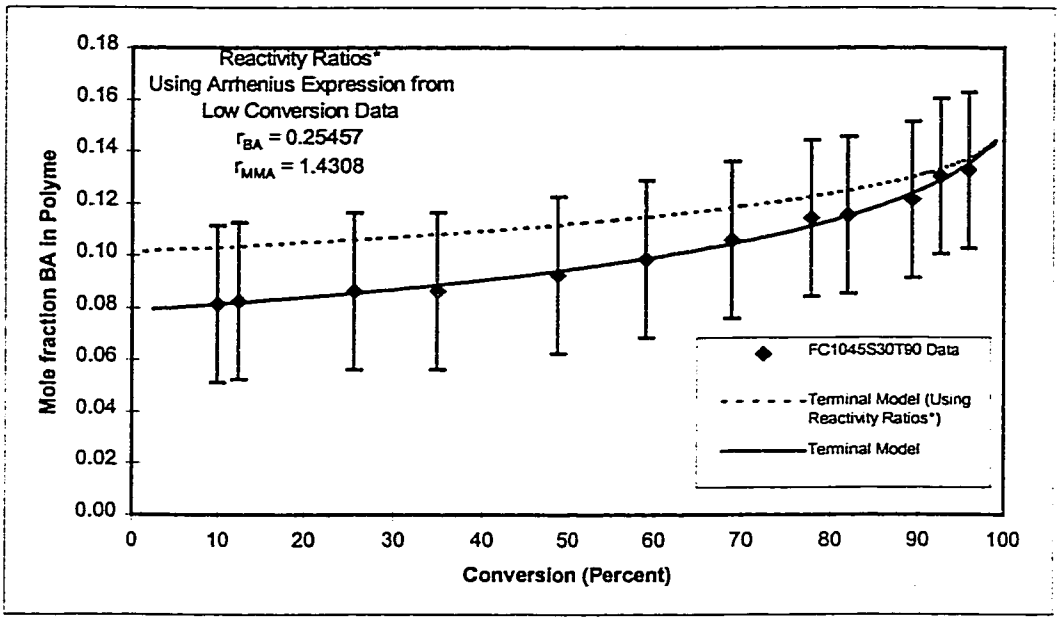

Figure 6-9 BA-MMA 10/45 30% Toluene Composition Profile At 90 °C

The 30 wt% toluene conversion profiles resembled the 23 wt% toluene runs (refer to Figure 6-6 for a representative run and Appendix C for the remainder of the results). The composition drift occurred at conversions over 50 wt% (see Figures 6-7 to 6-9) as seen for the bulk and 23 wt% toluene systems. Two types of reactivity ratios were incorporated into the Terminal model in order to predict copolymer composition. The first type was derived from full conversion data (termed r_{high}) and utilized the Meyer-Lowry equation. The second type of reactivity ratio (r_{low}) was obtained from the Arrhenius expression developed using low conversion data (described in Chapter 5) and the Mayo-Lewis model. The Terminal model predicted the FC1045S30T115 (at 115°C) composition data very well using both r_{low} or r_{high} (Figure 6-7). At lower temperatures (90°C), the r_{low} did not predict the composition as well as the r_{high} (see Figures 6-8 and 6-9).

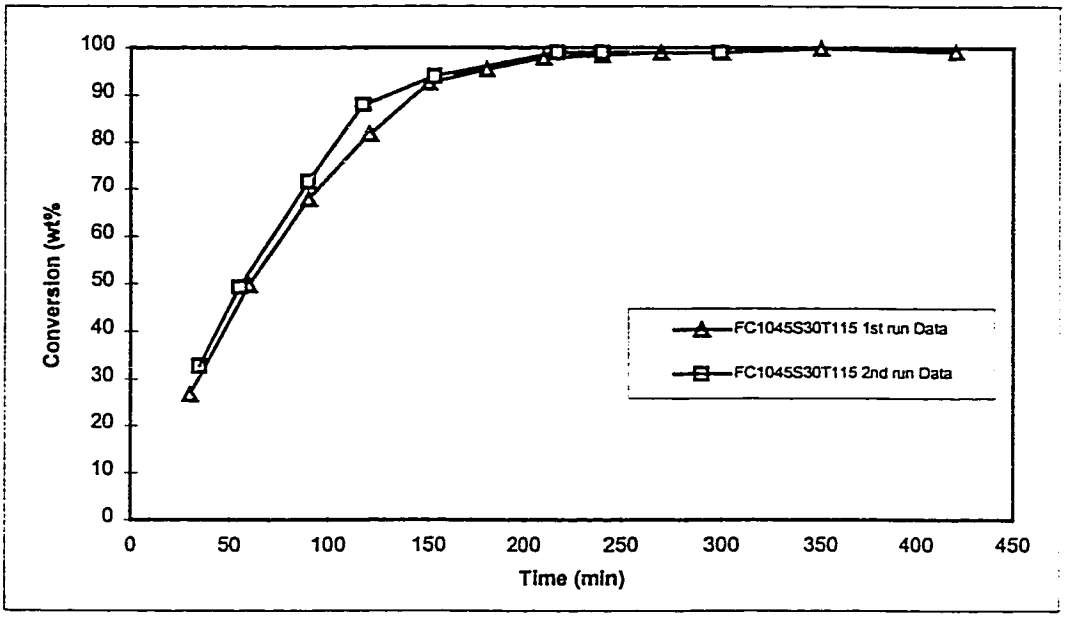

Figure 6-10 BA-MMA 10/45 30% Toluene Conversion Profile At 115 °C

The precision of the experimental data obtained for this thesis is well illustrated in Figure 6-10. In this case the FC1045S30T115 was repeated with almost identical conditions (Figure 6-10). The two runs were made months apart with the entire procedure repeated completely two times. The conversion profile was consistently lower for the first run due to the small differences in the initiator and initial monomer concentrations (see Appendix D). The small deviations in the composition and conversion data were much less than expected for the complexity of the procedure outlined for these experiments. This allowed us to conclude that our full conversion results were readily reproducible with a high degree of precision.

The molecular weight profiles for the full conversion solution runs (Table 6-1) indicated little or no increase along the full conversion range (refer to Figure 6-11 for a sample and Appendix C for the remainder of the results). This was due to the presence of

the chain transfer agent which helped keep the molecular weight constant through chain transfer reactions (equation 3-33). The number-averaged molecular weights were approximately (values averaged over full conversion range)

FC1045S23T90	115,000	Daltons
FC79180S23T90	109,000	Daltons
FC1045S23T115	100,000	Daltons
FC1045S30T90	120,000	Daltons
FC79180S30T90	80,000	Daltons
FC1045S30T115	75,000	Daltons

for the BA/MMA copolymer products. The generation of the molecular weight values (through integration under the MWD peaks, refer to Chapter 4 for details) led to deviations of +/- 10,000 Daltons.

6.4 The Solvent Effect On The Full Conversion Results

The solvent effect on the conversion versus time profiles 10-45 BA/MMA at 90°C conditions (0, 23, 30 wt% toluene) are shown in Figure 6-11. The onset of the gel effect was delayed as the toluene concentration in the reaction medium increased. This was due to the relative decrease of the reaction medium viscosity for similar conversions at higher solvent concentrations. This resulted in a delay of the onset of the gel effect which required the medium to attain a particular viscosity in order to occur (Chapter 4). These effects are not evident in Figure 6-12 for the 79-180 BA/MMA condition (23 and 30 wt% toluene) used at 90°C . The presence of BA may have countered the slight solvent effect (from 23 to 30 wt% toluene) so that no delay in the onset of the gel effect was observed.

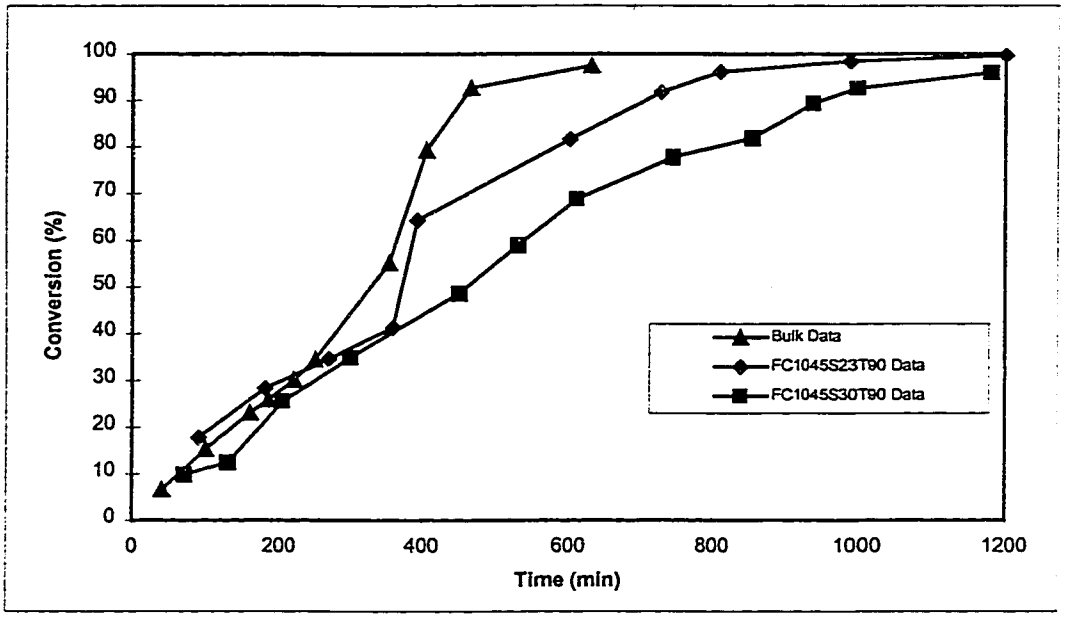

Figure 6-11 BA-MMA 10/45 Solvent Effect On The Conversion At 90 °C

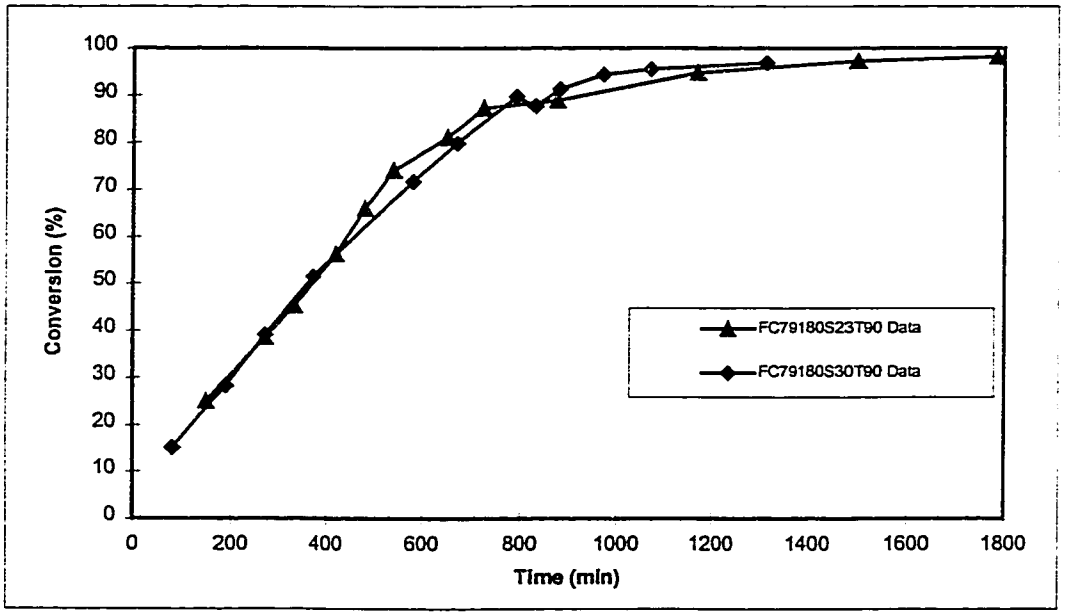

Figure 6-12 BA-MMA 79/180 Solvent Effect On The Conversion At 90 °C

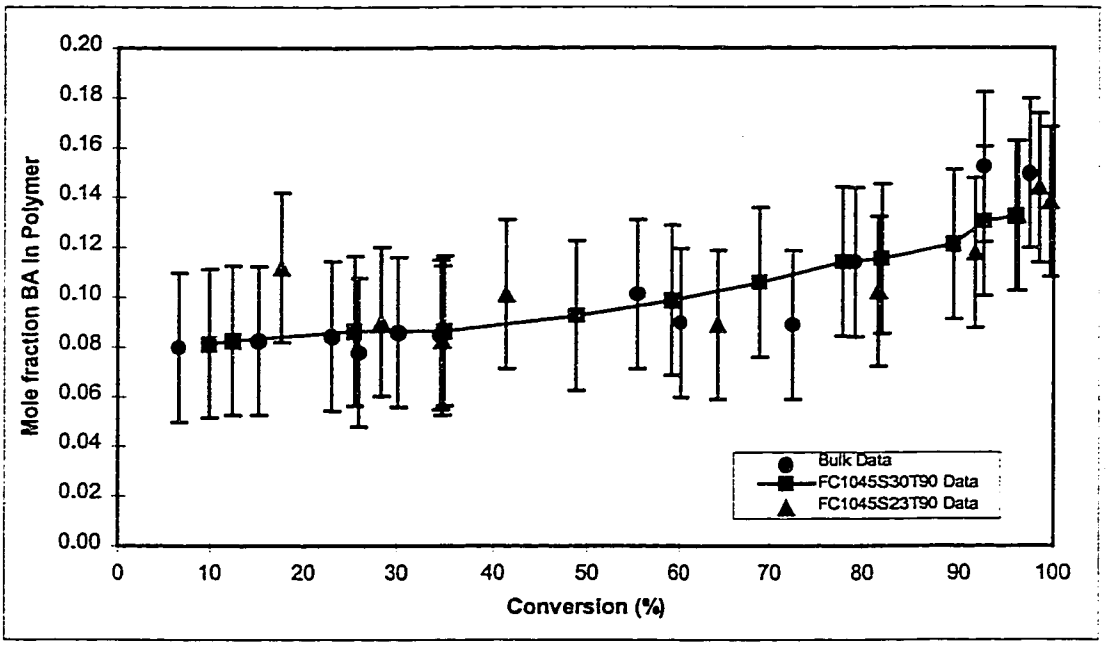

Figure 6-13 **BA-MMA 10/45 Solvent Effect On Composition At 90 °C**

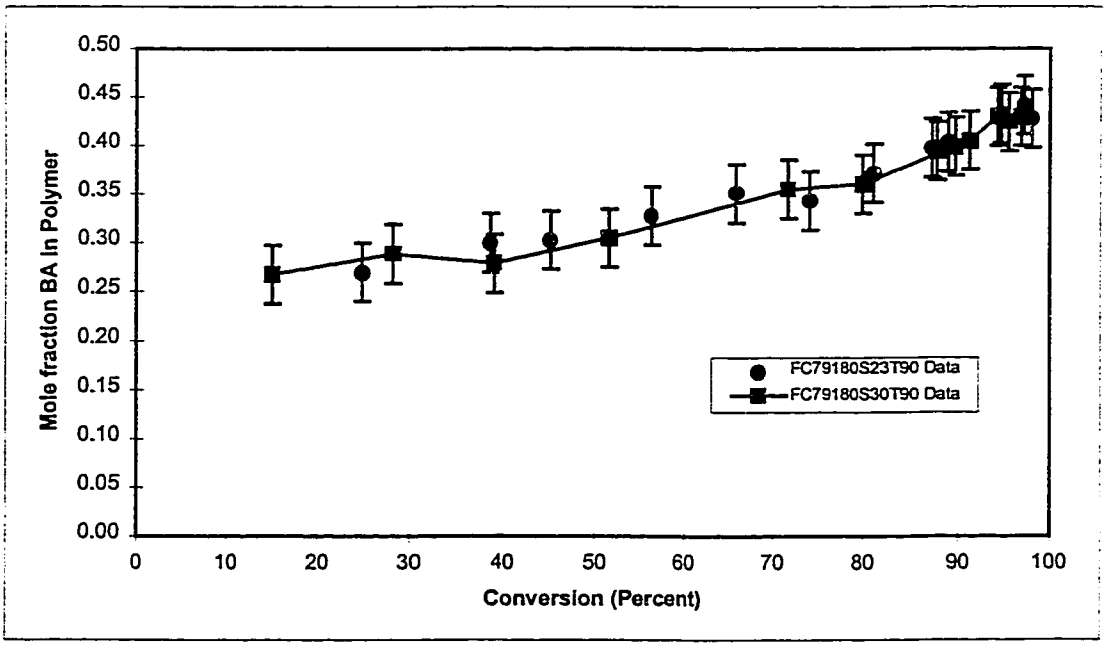

Figure 6-14 **BA-MMA 79/180 Solvent Effect on Composition At 90 °C**

The composition of BA in the polymer as the conversion increased was not affected by the presence of the solvent for all conditions as expected (refer to Figures 6-13 and 6-14). Since these profiles were primarily dictated by the reactivity ratios (which help define the kinetics of the system) then, only changing the temperature would have a significant effect on the results. This result was confirmed by similar observations made using low conversion reactivity ratio estimation experiments (see Chapter 5).

CHAPTER 7

Model Discrimination: Depropagation Kinetics

Depropagation is the reverse reaction of propagation. Depropagation occurs in many instances depending on the temperature of reaction, and the type of monomers used. The rate of depropagation increases with the reaction temperature and thus, its effects on reaction kinetics need to be considered when modeling high temperature polymerizations. In this study, depropagation was examined by using low conversion (reactivity ratio estimation) data to estimate parameters for various models that include depropagation. This allowed us to determine the kinetic mechanisms for the polymerization of the butyl acrylate / methyl methacrylate, butyl acrylate / α-methyl styrene (AMS), and the methyl methacrylate / α-methyl styrene copolymer systems.

In Chapter 5, it was seen that by using an Arrhenius-type expression to describe the dependence of the reactivity ratios on temperature, the applicability of a particular model to the system may be determined. In that chapter, only the forward propagation reactions were considered in the models (e.g. Mayo-Lewis model). Testing the suitability of various models that incorporate depropagation (using the Arrhenius-type expression), will permit us to infer whether depropagation is occurring in that copolymer system.

In this chapter, we first describe the different models, which include depropagation, that were used to predict copolymer composition. Next, the computer-aided statistical methods used to estimate the reactivity ratios from the different models are discussed. Each model was based on a different polymerization mechanism. The

reactivity ratios estimates were then fit to an Arrhenius-type expression, to discriminate between the different models. This assisted us in establishing whether depropagation kinetics were active.

7.1 Model Theory

Depropagation is defined as the reverse of propagation. The rate of depropagation increases as the temperature rises. At a certain temperature, the rate of depropagation is equivalent to the rate of propagation. The temperature at this point is termed the ceiling temperature (T_c). It is usually expressed as:

$$T_C = \frac{E_p - E_d}{R\ln(A_p[M]/A_d)} = -\frac{\Delta H}{R\ln(A_p[M]/A_d)} \qquad (7\text{-}1)$$

where

E	Energy of activation
A	Collision frequency factor
H	Enthalpy

Above the ceiling temperature, the polymer radical will tend to depolymerize in the presence of monomer.

The mechanism through which depropagation is expected to occur was shown previously in Figure 3-2. This mechanism used a terminal model approach which assumed that only the reactions on the terminal end of a polymer are considered to have a significant effect on the reaction rate and copolymer composition. This assumption has

been previously applied to the MMA-AMS copolymer system (Wittmer, 1971). Four models were considered for the model discrimination exercise discussed herein. The parameters estimated from these models are shown with their respective reaction conditions in Table 7-1.

Table 7-1 Reactivity Ratio Estimate Comparisons Among Various Propagation and Depropagation Models

Copolymer System	Temperature	Reactivity Ratios (Mayo-Lewis Model)		Reactivity Ratios (D1 Model)		Reactivity Ratios (D2 Model)		Reactivity Ratios (D3 Model)	
	T (°C)	r_1	r_2	r_1	r_2	r_1	r_2	r_1	r_2
BA (1) / MMA (2)	60	0.3257	2.043	NA	NA	1.763	17.305	NA	NA
	80	0.3095	1.841	NA	NA	1.8916	15.717	NA	NA
	100	0.3736	1.848	NA	NA	8.065	50.27	NA	NA
	120	0.3731	1.616	NA	NA	1.872	13.728	NA	NA
	140	0.4558	1.768	NA	NA	0.72436	6.4705	NA	NA
	ln (r) vs. 1/T Fit	Linear	Linear	NA	NA	Non-Linear	Linear	NA	NA
BA (1) / AMS (2)	60	0.1183	0.6207	NA	NA	0.1016	2.844	NA	NA
	80	0.1412	0.4090	NA	NA	0.0958	4.92E+12	NA	NA
	100	0.1641	0.1400	NA	NA	0.1266	7.45E+15	NA	NA
	120	0.1774	0.0806	NA	NA	0.1314	4.98E+13	NA	NA
	140	0.2122	0.0964	NA	NA	0.1490	1.70E+14	NA	NA
	ln (r) vs. 1/T Fit	Linear	Non-Linear	NA	NA	Linear	Non-Linear	NA	NA
MMA (1) / AMS (2)	60	0.5740	0.6628	0.4113	3.584	0.4133	3.679	0.4134	3.679
	80	0.4705	0.1649	0.6280	5.478	0.6605	4.612	0.6669	4.620
	100	1.098	0.0262	1.129	0.4824	1.271	0.1295	0.1289	0.1285
	120	1.7367	0.0207	0.7627	6.668	1.928	0.1118	1.999	0.0999
	140	2.8912	-0.0534	0.878	0.09582	6.064	9.46E-16	7.142	9.46E-16
	ln (r) vs. 1/T Fit	Linear	Non-Linear	Linear	Non-Linear	Linear	Non-Linear	Linear	Linear with one point deviation

Note : Refer to Table 7-2 for a list of the parameters used in every model

The Mayo-Lewis model has been previously described in Chapter 3. The depropagation models proposed by Wittmer (1971) were based on mass balances on the monomers and the monomer radicals using the mechanism proposed below. These mass balances are expressed in the following manner:

$$\frac{d[M_1]}{dt} = -k_{11}[M_1^\bullet][M_1] + k_{\overline{11}}[M_{11}^\bullet] - k_{21}[M_2^\bullet][M_1] + k_{\overline{21}}[M_{21}^\bullet] \tag{7-2}$$

$$\frac{d[M_2]}{dt} = -k_{22}[M_2^\bullet][M_2] + k_{\overline{22}}[M_{22}^\bullet] - k_{12}[M_1^\bullet][M_2] + k_{\overline{12}}[M_{12}^\bullet] \tag{7-3}$$

$$\frac{d[M_1^\bullet]}{dt} = -k_{12}[M_1^\bullet][M_2] + k_{\overline{12}}[M_{12}^\bullet] - k_{21}[M_2^\bullet][M_1] + k_{\overline{21}}[M_{21}^\bullet] \tag{7-4}$$

$$\frac{d[M_2^\bullet]}{dt} = +k_{12}[M_1^\bullet][M_2] + k_{\overline{12}}[M_{12}^\bullet] - k_{21}[M_2^\bullet][M_1] + k_{\overline{21}}[M_{21}^\bullet] \tag{7-5}$$

where

$k_{ij}[M_i^\bullet][M_j]$	Represents the generation or consumption (based on positive and negative sign respectively) of a polymer radical ending in "j" from a polymer radical ending in "i".
$k_{\overline{ij}}[M_{ij}^\bullet]$	Represents the generation or consumption of a polymer radical ending in "j" due to the depropagation of a polymer radical ending in "i" followed by "j".
$k_{ji}[M_j^\bullet][M_i]$	Represents the generation or consumption of a polymer radical ending in "j" due to the propagation of a polymer radical ending in "j".
$k_{\overline{ji}}[M_{ji}^\bullet]$	Represents the generation or consumption of a polymer radical ending in "j" due to the depropagation of a polymer radical ending in "j" followed by "i".

Now using the following conditions:

- The Bodenstein principle that assumed that the free radical concentration was constant.

$$\frac{d[M_1^\bullet]}{dt} = \frac{d[M_2^\bullet]}{dt} = 0 \tag{7-6}$$

- Monomer free radical concentrations (i.e. radicals of chain length 1) were equal to zero.

$$[M_1^\bullet](1\,mer) \approx [M_2^\bullet](1\,mer) \approx 0 \tag{7-7}$$

- Schulz-Flory (Vollmert, 1962) distribution function assumed.

The following expression was derived for the case where all forms of depropagation are possible (Model D1).

Model D1

$$\frac{F_1}{F_2}=\frac{d[M_1]}{d[M_2]}=\frac{1+\dfrac{r_1\dfrac{[M_1]}{[M_2]}-r_1\dfrac{K_1}{[M_2]}\left(1-x_1\right)}{1-q_1\dfrac{y_1}{[M_2]}\bullet\dfrac{[M_2]+q_2x_1}{[M_1]+q_1y_1}}}{1+\dfrac{r_2\dfrac{[M_2]}{[M_1]}-r_2\dfrac{K_2}{[M_1]}\left(1-y_1\right)}{1-q_2\dfrac{x_1}{[M_1]}\bullet\dfrac{[M_1]+q_1y_1}{[M_2]+q_2x_1}}} \tag{7-8}$$

with

$$1-x_1=\frac{r_1\left([M_1]+K_1\right)+[M_2]}{2r_1K_1}-\sqrt{\left(\frac{r_1\left([M_1]+K_1\right)+[M_2]}{2r_1K_1}\right)^2-\frac{[M_1]}{K_1}}$$

$$1-y_1=\frac{r_2\left([M_2]+K_2\right)+[M_1]}{2r_2K_2}-\sqrt{\left(\frac{r_2\left([M_2]+K_2\right)+[M_1]}{2r_2K_2}\right)^2-\frac{[M_2]}{K_2}}$$

$$K_1=\frac{k_{\overline{11}}}{k_{11}}\qquad K_2=\frac{k_{\overline{22}}}{k_{22}}\qquad q_1=\frac{k_{\overline{12}}}{k_{21}}\qquad q_2=\frac{k_{\overline{21}}}{k_{12}}$$

and the parameters are described as

r	represents the reactivity ratio
K	represents the homo-depropagation equilibrium constant
q	represents the cross-depropagation equilibrium constant

In the special case where only the homopolymerization of M_1 is reversible, the rate constants $k_{\overline{12}}$, $k_{\overline{21}}$, $k_{\overline{22}}$ are equal to zero. Thus, the parameters K_2, q_1, q_2, are all equal to zero. As a result, equation 7-8 reduces to the following expression (termed Model D2).

Model D2

$$\frac{F_1}{F_2}=\frac{d[M_1]}{d[M_2]}=\frac{1+r_1\frac{[M_1]}{[M_2]}-r_1\frac{K_1}{[M_2]}\left(1-x_1\right)}{1+r_2\frac{[M_2]}{[M_1]}} \tag{7-9}$$

The D3 model case occurs when the homo-depropagation of both monomers are significant. Only the cross-depropagation rate constants ($k_{\overline{12}}, k_{\overline{21}}$) are equal to zero. Thus, parameters q_1 and q_2 are also zero. The final depropagation D3 model (Table 7-1) is expressed as:

Model D3

$$\frac{F_1}{F_2}=\frac{d[M_1]}{d[M_2]}=\frac{1+r_1\frac{[M_1]}{[M_2]}-r_1\frac{K_1}{[M_2]}\left(1-x_1\right)}{1+r_2\frac{[M_2]}{[M_1]}-r_2\frac{K_2}{[M_1]}\left(1-y_1\right)} \tag{7-10}$$

Determination of the parameters for these models for each case was very difficult to achieve due to numerical difficulties encountered in the non-linear estimation program (Scientist®). Thus, following the method of Wittmer (1971), the parameters K_1, K_2, q_1 and q_2 were set as constants from literature estimates. The resultant parameters used and the reactivity ratios estimated are shown in Table 7-2.

Table 7-2 Parameter Values For Depropagation Models

Temperature T (°C)	K (MMA) [mol/L]	K (AMS) [mol/L]	K (BA) [mol/L]	q (MMA)	q (AMS)	q (BA)
60	0.001	7.1	0	0.1	0.1	0
80	0.1	12.9	0	0.5	0.1	0
100	0.119	22.9	0	1	0.1	0
120	0.262	35	0	7	0.1	0
140	0.54	54	0	15	0.1	0

Note : Parameter Data from Wittmer (1965)

7.2 Design of Parameter Estimation Runs

The ML model was solved through the use of the RREVM program (Dubé et al., 1991a). This program employed the Error-In-Variables (EVM) technique (see Chapter 3 for a detailed description of the program and its use) to converge on the estimates. Four sets of initial reactivity ratios were generated via a two level factorial grid design. All sets of initial reactivity ratios converged to approximately identical final estimates.

The D1, D2 and D3 models were solved using a non-linear least squares technique (NLS) found in the Scientist Software package from Micromath. This technique utilized a modified Powell algorithm (Micromath, 1995) to find a local minimum (possibly the global minimum) of the sum of the squared deviations between observed data and model calculations. Convergence was usually achieved very quickly. Failure was usually a consequence of the initial parameter estimates being so far removed from the solution

that Scientist® could not determine which direction to search. The usual behaviour was that the algorithm took anywhere up to several dozen iterations to converge on a solution. The minimization algorithm was tuned to indicate convergence after it detected an unchanging sum of squares value. Scientist® frequently took an extra 5 to 10 iterations near the solution in order to ascertain convergence. The Powell algorithm and the least squares fitting process are described in greater detail in Micromath (1995).

A grid of initial values of reactivity ratios were established using a two-level factorial design. The high starting value was 1.5 and the lower was 0.4 for both reactivity ratio parameters. The K and Q parameters were set to specific values (Wittmer, 1971) as shown in Table 7-2. The final reactivity ratio estimates generated from the different starting values were, for the most part, in agreement with one another. The tolerance for the error-squared value was set at 1×10^{-16}. Upon reaching this value, the program stopped iterating. The search algorithm was constrained to a minimum step of 1×10^{-5} and a maximum step size of 100.

7.3 Parameter Estimation Results

As a rule, the Mayo-Lewis model converged very quickly and yielded estimates of high precision using different starting points. In addition, the reactivity ratio estimates were physically realizable and thus conclusions centered around these estimates can be regarded with a high level of confidence. On the other hand, the Wittmer (1971) depropagation models (D1, D2, D3) were difficult to work with. The symmetric, square

root containing, highly complex formulas made parameter estimation very challenging. In order to test the viability of the Powell algorithm used to obtain parameter estimates, benchmark runs were performed. In this case, each model had a set of data made up that corresponded to a specified pair of reactivity ratios (with fixed parameters K and q). The bench mark data were then used by the Powell non-linear least squares (NLS) method (Micromath, 1995) to obtain parameter estimates. The reactivity ratios obtained were in excellent agreement with the ones specified for the data. This confirmed that the Powell NLS method was able to obtain the correct parameter estimates using different starting points. The variability of the estimates from the specified reactivity ratios increased as the initial starting values were significantly varied. Thus, the high and low initial reactivity ratios limits need to be carefully chosen when setting the two-level factorial design grid for the model runs.

Another concern revolved around the reliability of the data from Wittmer (1971). The MMA-AMS system was compared to data from Dubé (1994). There were disagreements between data obtained from Dubé (1994) and Wittmer (1971) for the 60 and 120°C cases but results for the 80 and 100°C conditions were similar. These discrepancies are worth noting. For example, re-estimation of reactivity ratios using Wittmer's (1971) MMA/AMS data at 80°C was performed. The results, shown in Figure 7-1, reveal that our re-estimation of the parameters, using the D2 model, resulted in a better fit than the reactivity ratios estimated in his paper. Also, the D2 model fit generated using his data and reactivity ratios did not match up with the composition profile displayed in his work (Wittmer, 1971). This led to the observation that there may have been some error in the work presented by Wittmer (1971). Nonetheless, a re-

derivation of the depropagation models in Wittmer (1971) led to exactly the same equations. While the data may be questionable, the theory is solid.

The following list represents the series of observations made when estimating the parameters for the various depropagation models:

- The 1 x 10^{-16} tolerance stipulated in the Powell NLS method did not seem to adhere to all of the converged runs performed. In some trials, the deviations of the predicted model to the experimental data were much too large for the tolerance to have been met.
- Some of the converged runs resulted in irregular fits of the model to the data (as seen in some of the runs to be discussed).
- The Simplex parameter estimation method (Micromath, 1995) produced different parameter estimates than the Powell NLS procedure. The Simplex method used a multi-dimensional surface technique to find the local minima. The convergence of the Simplex method to various values near the starting points indicated that the multi-dimensional surface of the depropagation equations were very flat. This meant that local minima may be found very quickly irregardless of the starting points used. The NLS method found the global minima without any surface technique. For this reason, the Powell NLS method was used to estimate the parameters for the depropagation models.
- Irregular fits resulted when the K and q parameters were allowed to vary. In some cases, the results indicated that the depropagation of AMS was less than MMA which was contrary to classical literature and incorrect. For this reason, the K and q parameters were fixed in the same fashion as Wittmer (1971).
- MMA-AMS data at 80°C along with K and q parameters for the 60°C condition were used to obtain reactivity ratio estimates. The reactivity ratios obtained were irregular (some had magnitudes of 10^{-15}). When the correct K and q parameters were used for the 80°C case, the reactivity ratios estimated were in excellent agreement with the experimental data. This meant that there was

some physical relevance to the reactivity ratios estimated using these models and methods.

These observations played a major role in all the parameter estimation methods used and the conditions specified to obtain reasonable model predictions to the data.

7.3.1 Depropagation Models Sensitivity Analysis

In order to gain a better understanding of the depropagation model equations and the challenges of obtaining meaningful parameter estimates, a sensitivity analysis was performed.

The first case involved the use of the D2 model (equation 7-9). Benchmark data for the MMA-AMS system were used. The homodepropagation equilibrium constant of AMS (K (AMS)) was varied from 0 mol/L to 100 mol/L. Reactivity ratios were estimated for several values of K (AMS). The results, shown in Figure 7-2, reveal that for a wide range of reactivity ratio pairs and different K (AMS) values, similar fits of model to the data may be achieved. This implies that the value of K (AMS) is rather insensitive to composition data. It is likely that rate data would be necessary for model discrimination in this case.

The results of this analysis, led to a more in depth look at the sensitivity of every parameter used in the depropagation models. Therefore, the full depropagation model (D1, equation 7-8) was chosen to perform the study. Benchmark data were generated

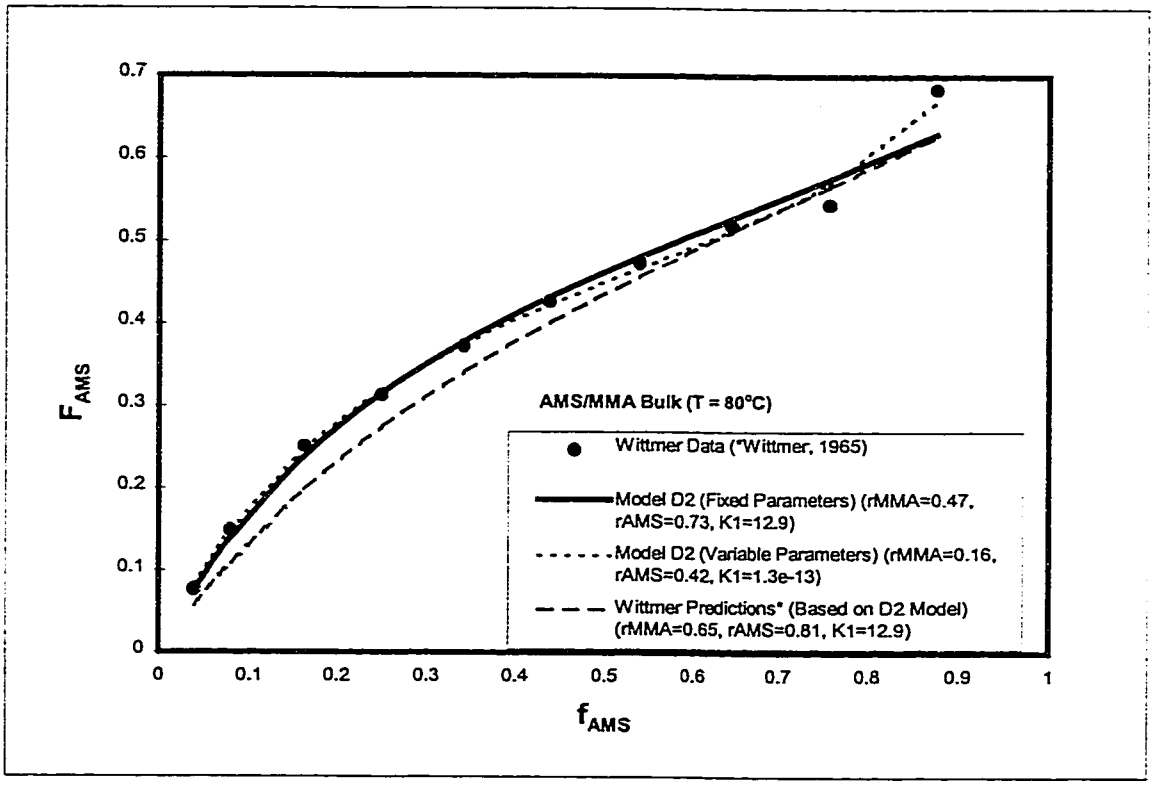

Figure 7-1 MMA-AMS Wittmer (1965) Composition Profile Comparison At 80 °C

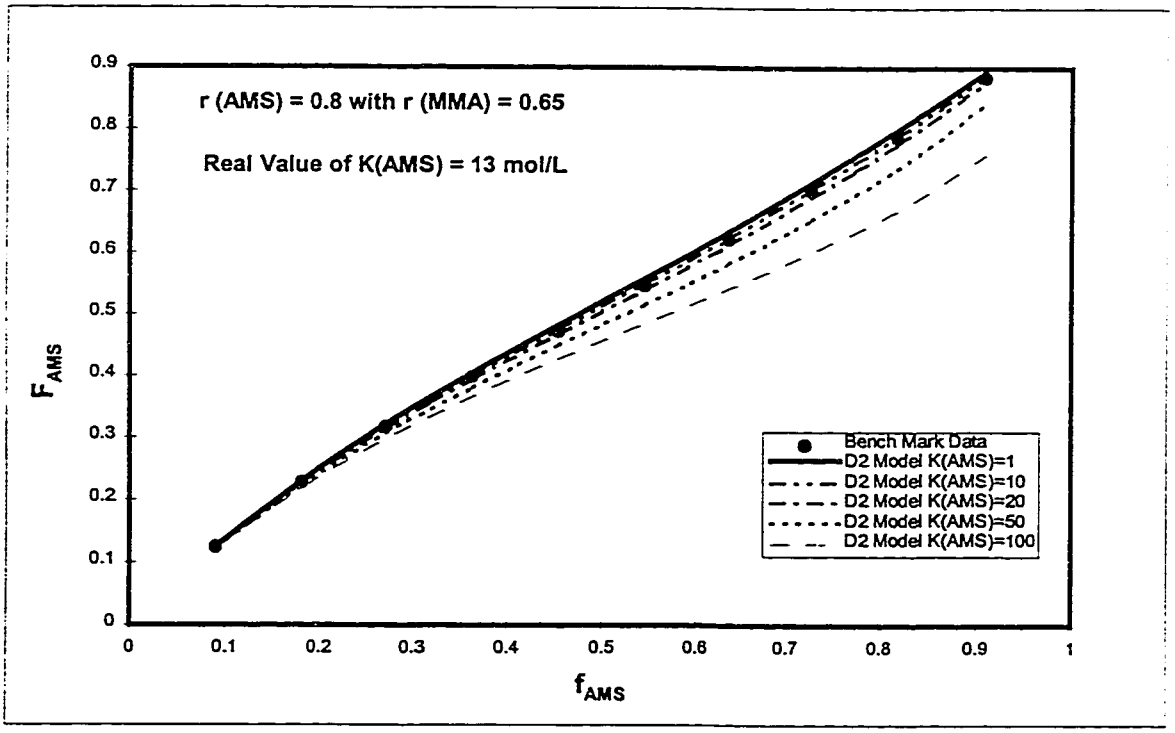

Figure 7-2 AMS-MMA Benchmark Sensitivity Analysis Runs [Varying K (AMS)]

using a fixed set of parameter values. In each case, only one parameter was varied along a specified range and the model fits were discussed.

The first case, involved the variation of r (MMA) as shown in Figure 7-3. Figure 7-3 reveals that even slight variations (greater than 0.2) in r (MMA) resulted in large deviations from the benchmark data. Thus, the model was relatively sensitive to variations in r(MMA). This trend was also found for r (AMS) as shown in Figure 7-3. A sensitivity analysis using the Mayo-Lewis equation resulted in similar sensitivities for the reactivity ratio values.

In varying the value for K (MMA), less deviation was observed from the data (Figure 7-4). In fact, noticeable deviations of the model from the data occurred only at 50 mol/L with the true value of K (MMA) being 0.2 mol/L. This trend was also observed for K (AMS) as shown in Figure 7-4. This suggests that the model (D1) is reasonably insensitive with respect to the homodepropagation equilibrium constants. Similar conclusions were arrived at for the parameters q(AMS) and q(MMA) as shown in Figure 7-5.

As a result of this sensitivity analysis, it was concluded that the homo- and cross-depropagation equilibrium constants should be fixed and only the reactivity ratios would be estimated.

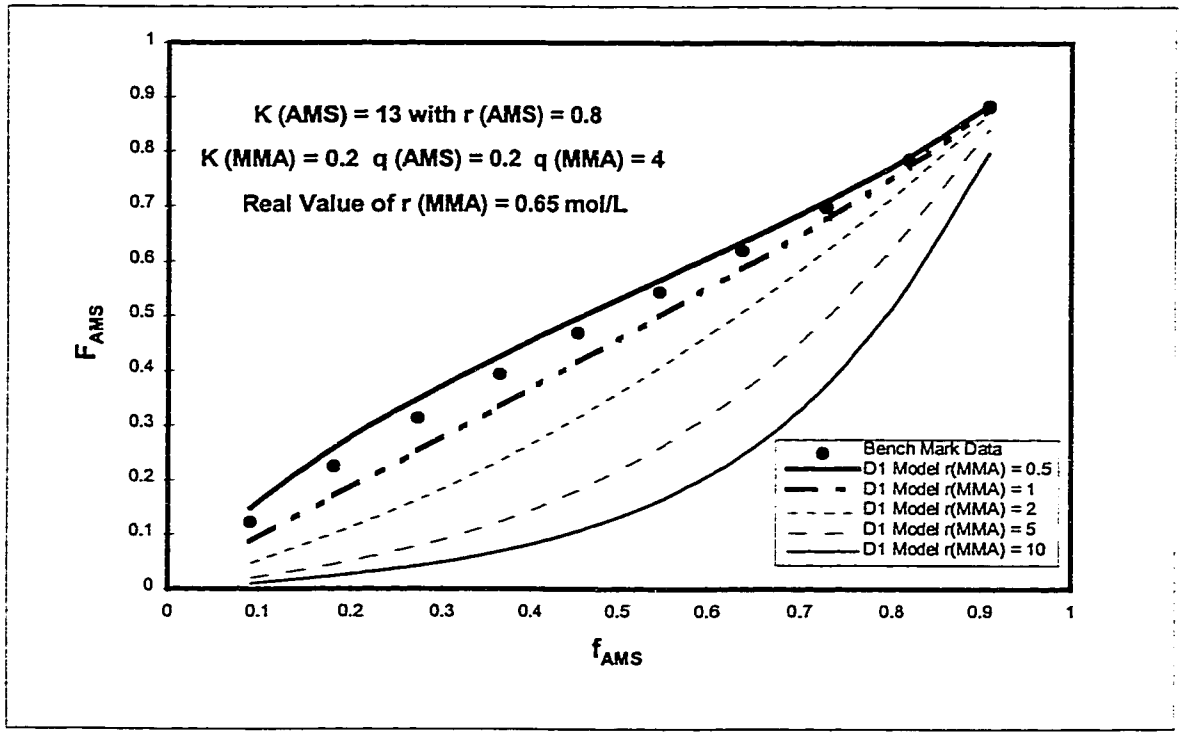

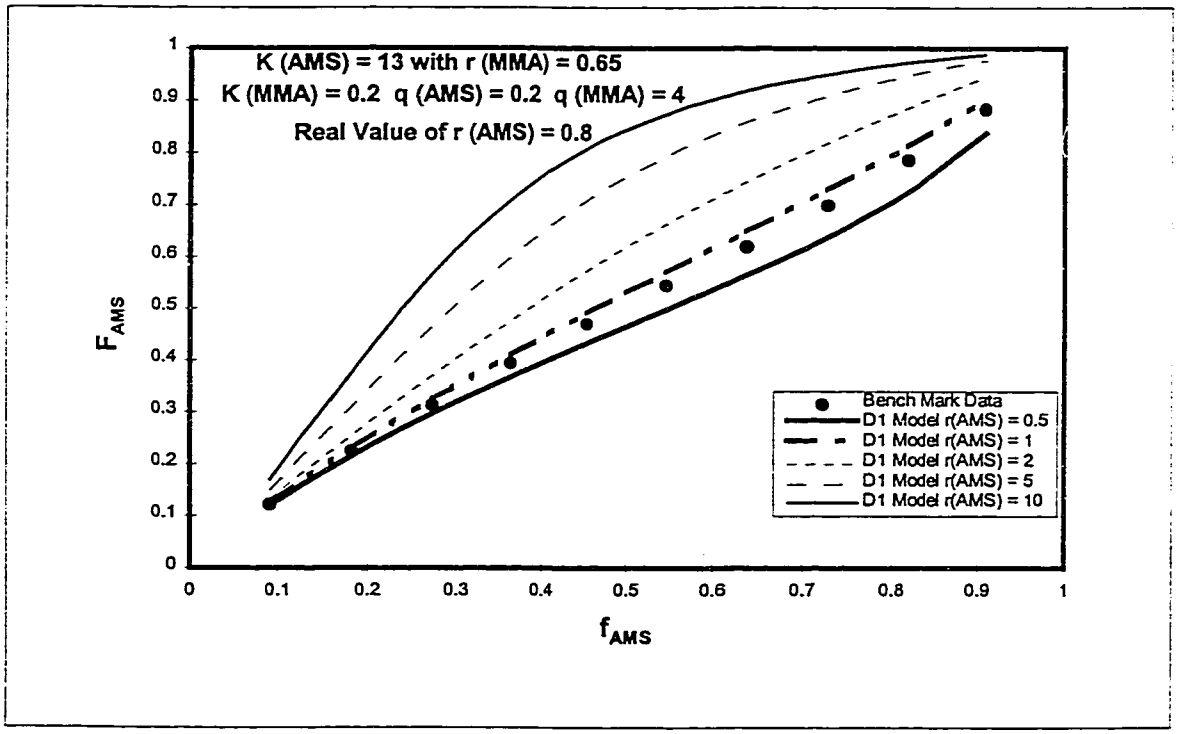

Figure 7-3 **Sensitivity of D1 Model for the Reactivity Ratio Parameters**

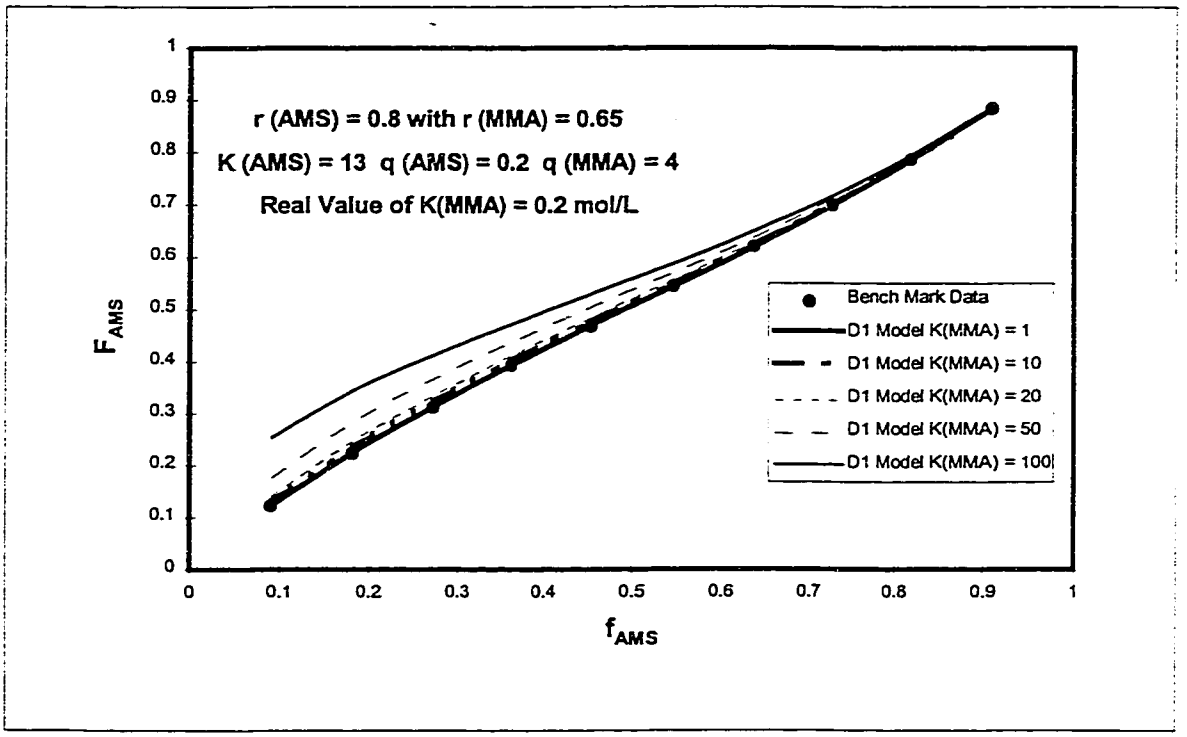

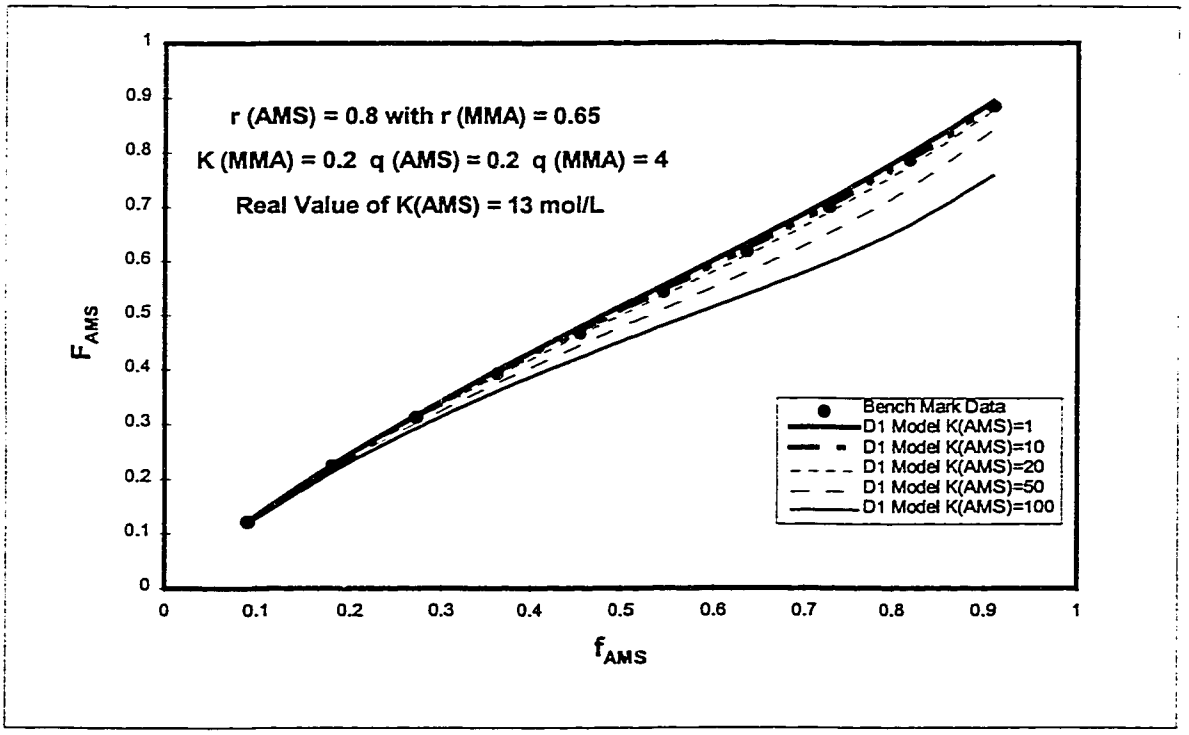

Figure 7-4 **Sensitivity of D1 Model for the Homo-Depropagation Constants**

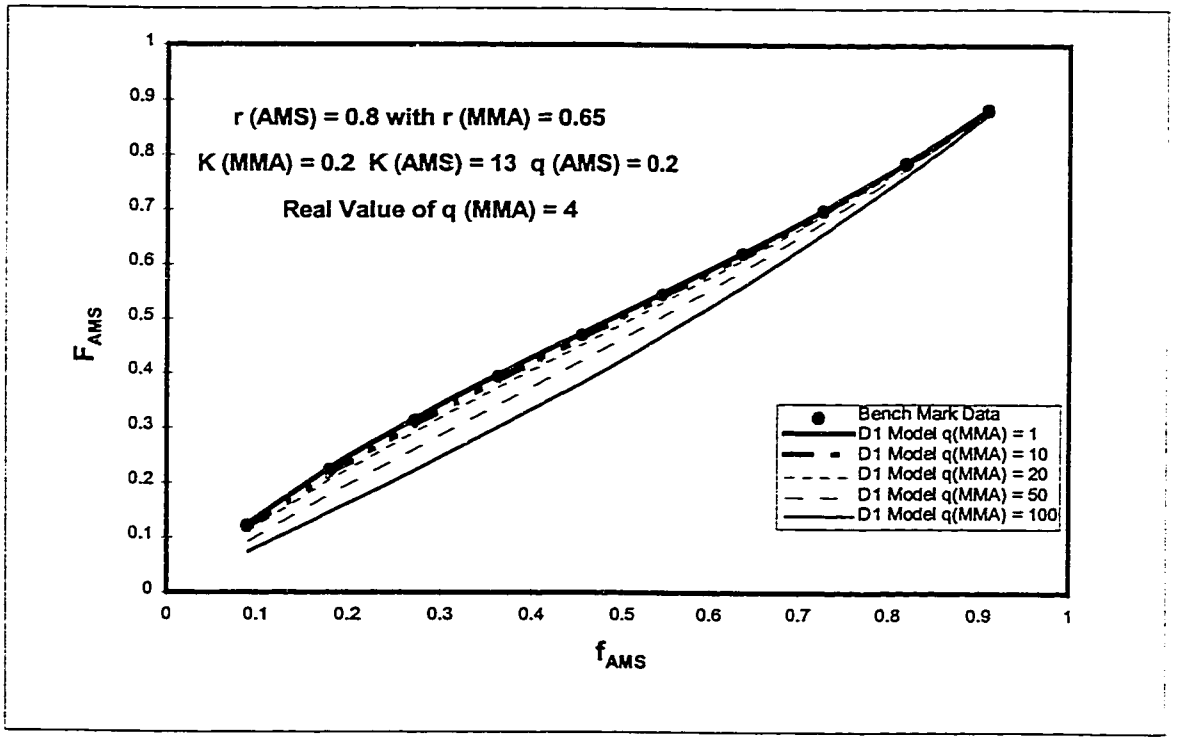

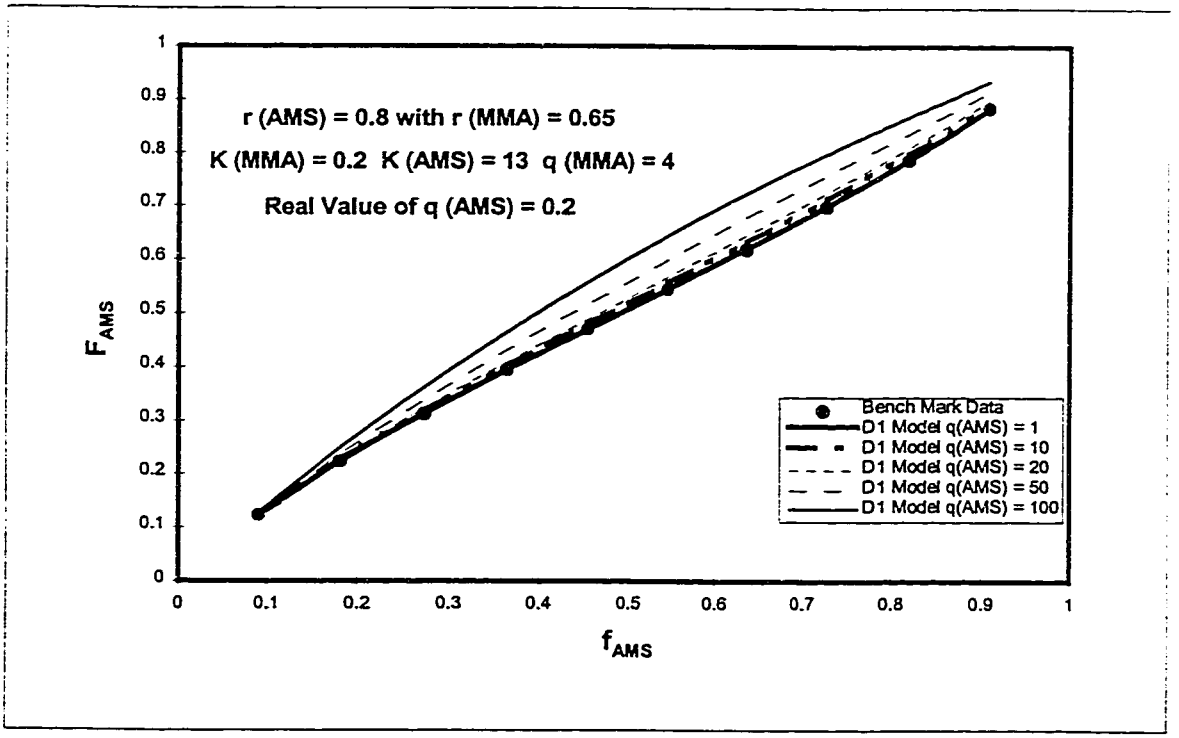

Figure 7-5 **Sensitivity of D1 Model for the Cross-Depropagation Constants**

7.3.2 Butyl Acrylate / Methyl Methacrylate Parameter Estimation Results

The Mayo-Lewis and D2 models were applied to this copolymer system at temperatures of 60 to 140°C. The D1 and D3 models did not apply because the homo- and cross-depropagation constants for BA are zero (refer to Table 7-2). This is due to the high ceiling temperature of BA. The bulk low conversion data used for this study were obtained from Dubé (1994).

The Mayo-Lewis model fit the data very well for all temperature conditions (refer to Appendix E). This implied that the estimation of proper reactivity ratio values for this system was successful. Plots of the natural logarithm of the reactivity ratios versus the inverse of the temperature (termed Arrhenius test) revealed linear fits (as indicated in Table 7-1 and Appendix E). Conversely, the D2 model fit the data very poorly at all conditions. The Arrhenius test indicated that the system is not suitable for the D2 model. The test results may not be valid due to the poor estimation of the reactivity ratios using the D2 model.

7.3.3 Butyl Acrylate / α-Methyl Styrene Parameter Estimation Results

As in the BA/MMA case, only the Mayo-Lewis and D2 model were applied to the BA/AMS copolymer system. The Mayo-Lewis model fit the data (Dubé, 1994) very well at all temperature conditions (60 to 140°C). The non-linear relationship exhibited when the Arrhenius test was performed revealed the unsuitability of the Mayo-Lewis model for the BA/AMS system (described in Table 7-1 and Appendix E). This is likely due to the

low ceiling temperature of AMS (60°C), which indicated that significant depropagation will occur at higher temperatures. The D2 model fits of the BA/AMS system were very poor (Appendix E). This is likely why this model did not pass the Arrhenius test (refer to Table 7-1 and Appendix E).

7.3.4 Methyl Methacrylate - Alpha Methyl Styrene Parameter Estimation Results

The relatively low ceiling temperatures of both MMA and AMS was indicative of the non-zero homo- and cross-depropagation constants for these monomers (Table 7-2). Thus, the Mayo-Lewis, D1, D2 and D3 models were applied to this system. All of the models fit the MMA/AMS system very well except for the 140°C condition for the D2 and D3 models (Appendix E). In these two cases the r_{AMS} estimate was very low (9.46×10^{-16}) indicating an erroneous estimate (Table 7-2). This means that model discrimination may be applied to the system for appropriate reactivity ratio estimates were obtained in most cases.

The application of the Arrhenius test to the reactivity ratios estimated using the Mayo-Lewis model revealed a non-linear relationship (Table 7-1 and Appendix E). this implies that significant depropagation is occurring in the MMA/AMS system. The unsuitability of the Mayo-Lewis model for the MMA/AMS system was also exhibited by D1 and D2 model results (Table 7-1). This indicates that no significant cross-depropagation was occurring (D1) and that AMS is not the only monomer that is homo-depropagating at higher temperatures. The D3 model did pass the Arrhenius test with the

exception of the erroneous reactivity ratio estimate at 140°C. This implies that both AMS and MMA were homo-depropagating in this copolymer system.

CHAPTER 8

Conclusions and Recommendations

This chapter summarizes the major conclusions made throughout the thesis and relates them back to the objectives of this study. Recommendations are made to help guide future research in this area.

The two main thesis objectives are to study the BA/MMA copolymer system at elevated temperatures and determine the effect of solvent on polymerization kinetics. In order to achieve these general goals, a list of specific objectives were developed. They are listed as follows:

- Estimate reactivity ratios using various models and verify the predictions with high and low conversion experimental data.
- Determine the effect of temperature on the composition, conversion profiles, reactivity ratios.
- Analyze the effect of toluene solvent on the conversion profiles, reactivity ratios, composition.
- Explore copolymer systems (through model discrimination) that consist of at least one monomer that depropagates at elevated temperatures.

8.1 Conclusions

Low and high conversion data were obtained at many temperatures in order to obtain a good understanding of the types of polymerization kinetics involved in the BA/MMA system. BA/MMA reactivity ratios were estimated in order to obtain a mechanistic model representing the data collected. These initiatives led to the following observations:

- The s-shape of the full conversion profiles were indicative of a diffusion-controlled polymerization reaction mechanism.

- Reactivity ratio and full conversion results were confirmed with classical data. This led to the conclusion that the system developed is reliable.

- The shape of the 95% contour plots for bulk and solvent reactivity ratios indicated the dependence of r_{MMA} to r_{AMS}.

- The Mayo-Lewis and Meyer-Lowry models fit the bulk and solution reactivity ratio data equally well. This implied that very little composition drift was occurring in these low conversion runs. This fact was confirmed by composition profiles which revealed composition drift commencing at 40 to 50% conversion.

- Reactivity ratios derived from low conversion data were successfully used to predict copolymer composition along the full conversion range at elevated temperatures.

- The full conversion results were almost identical for two runs (at the same conditions) but were performed months apart. The two results showed very low conversion and composition profile deviations. The error was much less then expected given the complexity of the procedure outlined for these experiments. This allows us to conclude that our full conversion results are readily reproducible with a high degree of precision

- Reactivity ratios derived from high conversion data were successfully used to predict copolymer composition along the full conversion range for all conditions.

A study of the effects of temperature on BA/MMA copolymerization resulted in the following conclusions:

- As the temperature increased, the r_{BA} increased while the r_{MMA} decreased for both models. This indicated that the frequency of the homopropagation of BA and the cross-propagation of MMA were increasing as the temperature increased.

- Higher temperature conditions (irregardless of weight ratio of initial solution) led to a faster onset of the gel effect, where 100% polymerization was achieved quickly.

The study in to the effect of solvent on the polymerization reactions led to the following conclusions:

- The use of a toluene solvent delays the onset and intensity of the segmental-diffusion-controlled region due to the difficulty of polymers to translationally diffusing in order to terminate the reaction.

- There are no effects of the solvent on the polymer composition profiles at higher temperatures (> 120°C) for the reactivity ratio estimation experiments. This was confirmed in the solvent full conversion runs as well.

- There was an effect of the solvent on the reactivity ratio values estimated for the BA/MMA system. This effect was small at higher temperatures (> 120°C) and significant at lower temperatures (< 120°C).

An examination of depropagation and model discrimination techniques led to the following observations:

- The Mayo-Lewis and depropagation models are very sensitive with respect to the reactivity ratios.

- The depropagation models are reasonably insensitive with respect to the homo- and cross-depropagation equilibrium constants K and q .

- The insensitivity of the parameters to the composition data implies that rate data may be necessary to perform appropriate model discrimination.

- The Mayo-Lewis model was found to be suitable for the BA-MMA copolymer system. This implies that the depropagation of MMA and BA are negligible in this system.

- No model was found suitable for the BA-AMS system. It was noted that due to the low ceiling temperature of AMS, the D2 model should have fit the system. This would imply that only AMS will depropagate at higher temperatures in this system. The deviation of the results from this observation has been largely due to the difficulty of obtaining good reactivity ratio estimates for the depropagation models.

- The D3 model is found to be suitable for the MMA-AMS copolymer system. This implies that the only homodepropagation of AMS and MMA may be assumed to be significant at these temperature ranges. Little or no cross-depropagation is occurring in this system.

These observations lead to the overall conclusion that the study of high temperature polymerization will generally require the incorporation of depropagation in the

mechanistic models used to simulate copolymer systems at these conditions. The use of a solvent in the system will not alter the copolymer composition at high temperatures (>120°C). It may effect the reactivity ratio estimates and will certainly delay the onset of the gel effect.

8.2 Recommendations

The following are a list of suggestions that were formulated throughout the period in which this work has been performed:

- The acquisition of rate data may be useful in discriminating between the various depropagation models. The use of full conversion data would give reliable results. This would require the integration of the differential versions of the depropagation models.

- The effect of grease on the polymerization reaction kinetics needs to be performed. The grease was used in several different parts of the monomer purification procedure (i.e. when degassing the ampoules) and may have contaminated some of the results obtained.

- Examine alternative methods of obtaining accurate molecular weights.

- The effects of the use of other solvents maybe explored to see if there are changes in the kinetics of the system. The solvent effect on the reactivity ratios (and probably the composition) at lower temperatures may be diminished when using different reagents.

- Comparisons of bulk and solution composition profiles at lower temperatures (< 120°C) will help verify the solvent effect observed on the reactivity ratio values at those temperatures.

- Estimation of the reactivity ratios at lower temperatures (< 60°C) in order to verify that the solvent effect is greater at those conditions as indicated by trends in Figures 6-11 to 6-14.

These suggestions were made in the hopes of directing future work in high temperature multi-component polymerization.

CHAPTER 9

References

Abuin, E.B. and Lissi, E.A., (1977). Methyl methacylate polymerization at high conversion II. Factors determining the onset of the gel effect. J. Macromol. Sci. Chem. (A11) 287.

Abuin, E.B.; Lissi, E.A.; Marquez, A., (1978). Methyl methacrylate polymerization in the presence of polystyrene. J. Polym. Sci. Polym. Chem. Ed. (16) 3003.

Achillas, D. and C. Kiparissides, (1988). Modeling of diffusion-controlled free-radical polymerization reactors. J. Appl. Polym. Sci., 35, 1303-1323.

Achillas, D. and C. Kiparissides, (1992). Development of a general mathematical framework for modeling diffusion-controlled free-radical polymerization reactions. Macromolecules, 25, 3739-3750.

Agarwal, B. and S.K. Gupta, (1993). Parameter estimation for solution polymerization of methylmethacrylate. J. Polym. Engng., 12, 257-281.

Armitage, P.D., S. Hill, A.F. Johnson, J. Mykytiuk and J.M.C. Turner, (1988). Bulk polymerization of methyl methacrylate: Part 1: Some kinetic and modeling considerations for isothermal reactions. Polymer, 29, 2221-2228.

Balke, S.T.; Hamielec, A.E., (1973). Bulk polymerizations of methyl methacrylate J. Appl. Polym. Sci. (17) 905.

Ballard, M.J., R.G. Gilbert, D.H. Napper, P.J. Pomery, P.W. O'Sullivan and J.H. O'Donnell, (1986). Propagation rate coefficients from electron spin resonance studies of the emulsion polymerization of methyl methacrylate. Macromolecules, 19, 1303-1308.

Bengough, W.I. and H.W. Melville, (1954). A thermocouple method of following the non-stationary state of chemical reactions. I. The evaluation of velocity coefficients of vinyl acetate, methyl methacrylate, and butyl acrylate polymerization reactions. Proc. Roy. Soc., A225, 330-345.

Bengough, W.I. and H.W. Melville, (1959). A thermocouple method of following the non-stationary state of chemical reactions. III. The evaluation of velocity coefficients and energies of activation for the propagation and termination reactions for the initial and later stages of the polymerization of butyl acrylate. Proc. Roy. Soc., A249, 445-454.

Benson, S.W. and A.M. North, (1959). A simple dilatometric method of determining the rate constants of chain reactions. J. Amer. Chem. Soc., 81, 1339-1345.

Bevington, J.C. and D.O. Harris, (1967). Reactivities of acrylates and methacrylates, J. Polym. Sci.: Polym. Lett. Ed., 5, 799-802.

Bradbury, J.H. and H.W. Melville, (1954). The co-polymerization of styrene and butyl acrylate in benzene solution. Proc. Roy. Soc. Lond., A222, 456-470.

Bresler, S.E., E.N. Kazbekov and V.N. Shadrin, (1974). Study of radical polymerization by means of ESR, 2. Homogeneous polymerization of methyl methacrylate and vinyl acetate. Makromol. Chem., 175, 2875-2880.

Brosse, J.-C., J.-M. Gauthier and J.-C. Lenain, (1983). Synthèse par voie radicalaire de polymères à extrémités hydroxylées, 11. Etude de la copolymérisation du méthacrylate de méthyle avec divers acrylates et méthacrylates. Détermination des rapports de réactivité. Makromol. Chem., 184, 505-517.

Buback, M., (1990). Free-radical polymerization up to high conversion. A general kinetic treatment. Makromol. Chem., 191, 1575-1587.

Buback, M. and B. Deneger, (1993). Rate coefficients for free-radical polymerization of butyl acrylate to high conversion. Makromol. Chem., 194, 2875-2883.

Buback, M., B. Deneger and B. Huckestein, (1989). Conversion dependence of free-radical polymerization rate coefficients from laser-induced esperiments, 1. Butyl acrylate. Makromol. Chem., Rapid Commun., 10, 311-316.

Buback, M., L.H. Garcia-Rubio, R.G. Gilbert, D.H. Napper, J. Guillot, A.E. Hamielec, D. Hill, K.F. O'Driscoll, O.F. Olaj, J. Shen, D. Solomon, G. Moad, M. Stickler, M. Tirrell, M.A. Winnik, (1988). Consistent values of rate parameters in free-radical polymerization systems. J. Polym. Sci.: Part C Polym. Lett., 26, 293-297.

Buback, M., B. Huckestein and G.T. Russell, (1994). Modeling of termination in intermediate and high conversion free radical polymerizations. Macromol. Chem. Phys., 195, 539-554.

Burke, A.L., T.A. Duever and A. Penlidis, (1994). Model discrimination via designed experiments: Discriminating between the terminal and penultimate models based on triad fraction data. Macromol. Theory Simul., 3, 1005-10031.

Cardenas, J.N. and O'Driscoll, K.F., (1976). High conversion polymerization I. theory and application to methyl methacrylate. J. Polym. Sci. Polym. Chem. Ed. (14) 883.

Cardenas, J.N. and O'Driscoll, K.F., (1977). High conversion polymerization II. Influence of chain transfer on the gel effect. J. Polym. Sci. Polym. Chem. Ed. (15) 1883, 2097.

Carswell, T.G., D.J.T. Hill, D.I. Londero, J.H. O'Donnell, P.J. Pomery and C.L. Winzor, (1992). Kinetic parameters for polymerization of methyl methacrylate at 60°C. Polymer J., 24, 1037-1048.

Carswell, T.G., D.J.T. Hill, D.I. Londero, J.H. O'Donnell, P.J. Pomery and C.L. Winzor, (1992). Kinetic parameters for polymerization of methyl methacrylate at 60°C. Polymer, 33, 137-140.

Chang, H.-R., H.-Y. Parker and D.G. Westmoreland, (1992). Continuous ESR measurement of propagating free-radical concentrations for batch emulsion polymerization of methyl methacrylate. Macromolecules, 25, 5557-55558.

Cotts, P.M. and R. Siemens, (1991). Characterization of random copolymers by size exclusion chromatography with a light scattering detector. Polymer, 32, 3052.

Cutting, G.R. and B.J. Tabner, (1993). Radical termination and radical concentrations during the batch emulsion polymerization of methyl methacrylate studied by electron spin resonance spectroscopy. Macromolecules, 26, 951-955.

Davis, T.P., K.F. O'Driscoll, M.C. Piton and M.A. Winnik, (1989). Determination of propagation rate constants for the copolymerization of methyl methacrylate and styrene using a pulsed laser technique. J. Polym. Sci.: Poly,. Lett., 27, 181-185.

Dionisio, J.M. and O'Driscoll, K.F., (1980) High conversion polymerization. VI. Detailed examination of the kinetic model. J. Polym. Sci. Polym. Chem. Ed., (18) 241.

Dubé, M.A., (1994). A systematic approach to the study of multi-component polymerization kinetics. Ph.D. Thesis, University of Waterloo.

Dubé, M.A., R. Amin Sanayei, A. Penlidis, K.F. O'Driscoll and P.M. Reilly, (1991a). A microcomputer program for estimation of copolymerization reactivity ratios. J. Poly,. Sci.: Part A: Polym. Chem. 29, 703-708.

Dubé, M.A., A. Penlidis, (1995). Systematic approach to the study of multi-component polymerization kinetics - The butyl acrylate/methyl methacrylate/vinyl acetate example: 1. Bulk copolymerization. Polymer J., 36(3) 587-598.

Dubé, M.A., A. Penlidis and K.F. O'Driscoll, (1990). A kinetic investigation of styrene/butyl acrylate copolymerization. Can. J. Chem. Eng., 68, 974-987.

Dubé, M.A., K. Rilling and A. Penlidis, (1991b). A kinetic investigation of butyl acrylate polymerization. J. Appl. Polym. Sci., 43, 2137-2145.

Dubé, M A. J B P. Soares, A. Penlidis, A E. Hamielec, (1997). Mathematical modeling of multi-component chain-growth polymerizations in batch, semi-batch, and continuous reactors: A review. Industrial & Engineering Chemistry Research, 36(4) 966-1015.

Fernandez-Garcia, M. and E.L. Madruga, (1997). Kinetic study of high-conversion copolymerization of butyl acrylate with methyl methacrylate in solution. J. Polym. Sci. Part A-Polym. Chem., 35(10), 1961-1965.

Gao, J. and A. Penlidis, (1996). A comprehensive simulator/database package for reviewing free-radical homopolymerizations. J. Macro. Sci.: Reviews in Macro. Chem. and Phy., C36(2), 199-404.

Garcia-Rubio, L.H., J.F. MacGregor and A.E. Hamielec, (1983). Size exclusion chromatography of copolymers. ACS Advances in Chem. Series, no. 203, polymer Characterization: Spectroscopic, chromatographic, and Physical Instrumental Methods, C.D. Craver Ed., 311-344.

Gladyshev, G.P. and S.R. Rafikov, (1996). Bulk polymerization of vinyl monomers at high extents of reaction. Russ. Chem. Revs., 35, 405-415.

Grassie, N., B.J.D. Torrance, J.D. Fortune and J.D. Gemell, (1965). Reactivity ratios for the copolymerization of acrylates and methacrylates by nuclear magnetic resonance spectroscopy. Polymer, 6, 653-658.

Hamer, J.W., t.A. Akramov and W.H. Ray, (1981). The dynamic behaviour of continuous polymerization reactors - II. Non-isothermal solution homopolymerization and copolymerization in a CSTR. Chem. Eng. Sci., 36, 1897-1914.

Hamielec, A.E. and H. Meyer, (1986). Online molecular weight and long chain branching measurement using SEC and low-angle laser light scattering. Unknown origin. In "Developments in Polymer characterization" Volume 5. J.V. Dawkins (Ed.), Elsevier Applied Science Publishers, London.

Hamielec, A.E., J.F. MacGregor and A. Penlidis, (1989). Copolymerization. In "Comprehensive Polymer Science". G. Allen and J.C. Bevington (Eds.), Pergammon Press, Toronto, Chapter 2, 17-32.

High, K.A.; Lee, H.B.; Turner, D.T., (1979). Autoacceleration of free-radical polymerization 4. Pre-dissolved polymer. Macromolecules (12) 332.

Hutchinson, R.A., M.T. Aronson and J.R. Richards, (1993). Analysis of pulsed-laser-generated molecular weight distributions for the determination of propagation rate coefficients. Macromolecules, 26, 6410-6415.

Hutchinson, R.A., J.H. McMinn, D.A. Paquet, S Jr. Beuermann, C. Jackson, (1997). Pulsed-laser study of penultimate copolymerization propagation kinetics for methyl methacrylate/n-butyl acrylate. Indus. & Eng. Che. Res., 36(4), 1103-1113.

Jahanzad, F., M. Kazemi, S. Sajjadi and F. Afshar Taromi, (1993). N-Dodecyl mercaptan transfer constant in polymerization of methyl methacrylate. Polymer, 34, 3542-3544.

Kamachi, M., M. Fujii, S.-I. ninomiya, S. Katsuki and S.-I. Nozakura, (1982). Solvent effect on radical polymerization of butyl acrylate. J. Polym. Sci.: Polym. Chem. Ed., 20, 1489-1496.

Käszas G., T. F`ldes-Berezsnich and F. Thd`s, (1983). Kinetics of radical polymerization XXXIX. Investigation of the polymerizations of butyl acrylate and methyl acrylate in solution. Eur. Polym. J., 19, 469-473.

Kerr, J.A., (1973), Rate processes in the Gas Phase. (Chapt. 1) in "Free Radical". Vol 1., Kochi, J.K. John Wiley and Sons, New York.

Kondratiev, V.N. (1969), "Chain Reactions" Chapt. 2 in "Comprehensive Chemical Kinetics" Vol. 2, C.H. Bamford and C.F.H. Tipper, Eds., American Elsevier, New York.

Lachinov, M.P.; Simonian, R.A.; Georgieva, T.G.; Zubov, V.P.; Kabanov, V.A., (1979). Effects of $ZnCl_2$ on the rate of thermal decomposition of azobisisobutyronitrile. J. Polym. Sci. Polym. Chem. Ed., (15) 1777.

Li, Y., D.G. Ward, S.S. Reddy, S. Collins, (1997). Polymerization of methyl methacrylate using zirconocene initiators: Polymerization mechanisms and applications. Macromol., 30(7), 1875-1883.

Liaw, D.-J. and K.-C. Chung, (1982). Determination of the absolute rate constants in the radical polymerization of n-butyl acrylate and cyclohexyl acrylate. J. Chin. Inst. Chem. Eng., 13, 145-149.

Louie et al., B.M., G.M. Carratt and D.S. Soong, (1985). Modeling the free radical solution and bulk polymerization of methyl methacrylate by oxygen injection. I. Modeling study. J. Appl. Polym. Sci., 30, 3189-3223.

Lovell, P.A., T.H. Shah and F. Heatley, (1991). Chain transfer to polymer in emulsion polymerization of n-butyl acrylate studied by ^{13}C N.M.R. spectroscopy and G.P.C. Polym. Commun., 32, 98-103.

Lovell, P.A., T.H. Shah and F. Heatley, (1992). Correlation of the extent of chain transfer to polymer with reaction conditions for emulsion polymerization of n-butyl acrylate. In `Polymer Latexes. Preparation, characterization, and Applications`. E.S. Daniels, E.D. Sudol and M.S. El-Aasser (Eds.), ACS Symp. Ser. 492, 188-202.

Mackay, M.H. and H.W. melville, (1949). Rate coefficients in the polymerization of methyl methacrylate. Part 1. Trans. Farad. Soc., 45, 323-338.

Madruga, E.L., J. San Roman and P. Benedi, (1990). High conversion polymerization of methyl methacrylate in the presence of n-dodecylmercaptan. J. Appl. Polym. Sci., 41, 1133-1140.

Madruga, E.L., and J.J. Malfeito, (1992). Effect of chain transfer agent and the reaction medium on the limiting conversion of methyl methacrylate free-radical polymerization. Eur. Polym. J., 28, 863-866.

Mahabadi, H.K., and O'Driscoll, K.F., (1977a). Termination rate constant in free-radical polymerization. J. Polym. Sci. Polym. Chem. Ed., (15) 283.

Mahabadi, H.K., and O'Driscoll, K.F., (1977b). concentration dependance of the termination rate constant during the initial stages of free-radical polymerization. Macromolecules, (10) 55.

Mahabadi, H.K., and Rudin, A., (1979). Effect of solvent on the termination rate constant in the initial stages of free radical polymerization. J. Polym. Sci., (17) 1801.

Majury, T.G. and H.w. Melville, (1951). A dielectric constant method of following the non-stationary state in polymerization. III. The determination of rates of polymerization and of radical lifetimes. Proc. Roy. Soc., A205, 496-516.

Mallya, P. and S.S. Plamthottam, (1989). Termination rate constant in butyl acrylate batch emulsion polymerization. Polym. Bull., 21, 497-504.

Mayo, F.R., C. Walling, F.M. Lewis and W.F. Hulse, (1948). Copolymerization. V. Some copolymerization of vinyl acetate. J. Amer. Chem. Soc., 70, 1523-1525.

McFarlane, R.C., P.M. Reilly and K.F. O'Driscoll, (1980). Comparison of the precision of estimation of copolymerization reactivity ratios by current methods. J. Polym. Sci. Polym. Chem., 18, 251-257.

McKenna, T F., C. Graillat, J. Guillot, (1995). Contributions to defining the rate constants for the homo- and copolymerization of butyl acrylate and vinyl acetate. Polymer Bulletin, 34 (3), 361-368.

Melville, H.W. and A.F. Bickel, (1949). Determination of the velocity coefficients for the polymerization processes. The polymerization of butyl acrylate. Trans. Farad. Soc., 45, 1049-1058.

Meyer, V.E. and G.G. Lowry, (1965). Integral and differential binary copolymerization equations. J. Polym. Sci.: Part A, 3, 2813-2851.

Micromath, (1995). Scientist for Windows user handbook. Chapter 10.

Nandi, U.S., M. Singh and P.V.T. Raghuram, (1982). Chain transfer of alcohols in the polymerization of acrylic esters. Makromol. Chem., 183, 1467-1472.

Nishimura, N., (1966). Kinetics of diffusion-controlled free-radical polymerization. II. Bulk polymerizations of styrene and methyl methacrylate. J. Macromol. Sci., 1, 257-289.

North, A.M., (1974) The influence of chain structure on the free radical termination reaction (Chapt. 5) in "Reactivity, Mechanism and Structure in Polymer Chemistry" Jenkins, A.D. and Ledwith, A., Eds., Wiley-Interscience, New York.

O'Driscoll, K.F. and P.M. Reilly, (1987). Determination of reactivity ratios in copolymerization. Makromol. Chem., Makromol. Symp., 10/11, 355-374.

Odian G., (1991). Principles of Polymerization. 3rd Edition, John Wiley and Sons, New York.

Oga, Y. and M. Yokawa, (1977). Effect of pressure on the propagation and termination rate constants of radical polymerization. Makromol. Chem., 178, 453-464.

Patino-Leal, H., P.M. Reilly and K.F. O'Driscoll, (1980). On the estimation of reactivity ratios. J. Polym. Sci. Polym. Lett., 18, 219-227.

Penlidis, A., S.R. Ponnuswamy, C. Kiparissides and K.F. O'Driscoll, (1992). Polymer reaction engineering: Modeling considerations for control studies. Chem. Eng. J., 50, 95-107.

Ponnuswamy, S.R., A. Penlidis and C. Kiparissides, (1988). Batch solution polymerization of methyl methacylate: Parameter estimation. Chem. Eng. J., 39, 175-183.

Pritchard, D.J. and D.W. Bacon, (1975). Statistical assessment of chemical kinetic models. Chemical Engineering Science, 30, 567-574.

Rajatapiti, P., V.L. Dimonie, M.S. El-Aasser, (1996). Bulk and emulsion copolymerizations of n-butyl acrylate and poly(methyl methacrylate) macromonomer. J. Appl. Polym. Sci., 61(6), 891-900.

Ramelow, U.S., and Q.H. Qiu, (1995). Monomer reactivity ratios in UV-initiated free-radical copolymerization reactions. J. Appl. Polym. Sci. 57(8), 911-920.

Rossignoli, P.J., and Deuver, T.A., (1988). The estimation of copolymer reactivity ratios: A review and case studies using the error-in-variables model and nonlinear least squares. J. Appl. Polym. Sci. 40(1), 35-47.

Russell, G.T., D.H. Napper and R.G. Gilbert, (1988). Termination in free-radical polymerization systems at high conversion. Macromolecules, 21, 2133-2140.

Russell, G.T.; Napper, D.H.; Gilbert, R.G., (1988). Initiator efficiencies in high conversion bulk polymerizations. Macromolecules, (21) 2133, 2141.

Rätzsch, M. and I. Zschach, (1968). Plaste Kautch., 15, 792.

Sack, R.G.; Schulz, G.V.; Meyerhoff, G., (1988). Free-radical polymerization of methyl methacrylate up to the glassy state. Rates of propagation and termination. Macromolecules (21) 3345.

Schmidt, A.D., A.B. clinch and W.H. Ray, (1984). The dynamic behaviour of continuous polymerization reactors - III. An experimental study of multiple steady states in solution polymerization. Chem. Eng. Sci., 39, 419-432.

Scott, G.E. and E. Senogles, (1970). Polymerization kinetics of n-lauryl acrylate. J. Macromol. Sci.-Chem., A4, 1105-1117.

Scott, G.E. and E. Senogles, (1974). Polymerization kinetics of n-alkyl acrylates. J. Macromol. Sci. chem., A8, 753-773.

Shen, J., Y. Tian, G. Wang and M. Yang, (1991). Modeling and kinetic study on radical polymerization of methyl methacrylate in bulk, 1. Propagation and termination rate coefficients and initiation efficiency. Makromol. Chem., 192, 2669-2685.

Shen, J., Y. Tian, G. Wang and M. Yang and Y.-G. Zheng, (1992). A kinetic study on MMA bulk radical polymerization. Polym. Intl., 28, 75-79.

Small, P.A., (1975). Adv. Polym. Sci. (18) 1.

Soh, S.K. and D.C. Sundberg, (1982a). Diffusion-controlled vinyl polymerization. III. Free volume parameters and diffusion-controlled propagation. J. Polym. Sci. Polym. Chem. Ed., 20, 1331-1344.

Soh, S.K. and D.C. Sundberg, (1982b). Diffusion-controlled vinyl polymerization. IV. Comparison of theory and experiment. J. Polym. Sci. Polym. Chem. Ed., 20, 1345-1371.

Stickler, M., (1987). Experimental techniques in free radical polymerization kinetics. Makromol. Chem., Macromol. Symp., 10/11, 17-69.

Styring, M.G. and A.E. Hamielec, (1989). Determination of molecular weight distribution by gel permeation chromatography. In "Determination of Molecular Weight", A.R. Cooper (Ed.), Wiley, 263-300.

Subrahmanyam, B., S.D. Baruah, M. Rahman, J.N. Baruah, and N.N. Dass, (1992). Kinetic studies on the n-alkyl acrylate polymerization. J. Polym. Sci.; Part A: Polym. Chem., 30, 2531-2549.

Sundberg, D.C., J.Y. Hsieh, S.K. Soh and R.F. Baldus, (1981). Diffusion-controlled kinetics in the emulsion polymerization of styrene and methyl methacrylate. In "Emulsion Polymers and Emulsion Polymerization", ACS Symp. Ser. 165, D.R. Bassett and A.E. Hamielec, (Eds.), 327-343.

Tidwell, P.W. and G.A. Mortimer, (1965). An improved method of calculating copolymerization reactivity ratios. J. Polym. Sci. A, 3, 369-387.

Turner, D.T., (1977). Autoacceleration of free-radical polymerization I. The critical concentrations. Macromolecules (10) 221.

Vollmert, B., (1962). Grundriss der Makromolekularen chemie. Berlin-G`ttingen-Heidelberg, 271.

Wang, X., and E. Ruckenstein, (1993). On the gel effect in the presence of a chain transfer agent in methyl methacrylate polymerization and its copolymerization with various acrylates. J. Appl. Polym. Sci., 49, 2179-2188.

Wittmer, P., (1971). Copolymerization in the presence of depolymerization reactions. multi-component Polymer Systems, 140-174.

Wunderlich, W., (1976). Kinetische Untersuchungen der radikalischen Polymerisation von Butylacrylate. Makromol. Chem., 177, 973-989.

Yamamaoto, K. and M. Sugimoto, (1979). Rate constant for long chain branch formation in free-radical polymerization of ethylene. J. Macromol. Sci. Chem., A13, 1067.

Yokawa, M., Y. Ogo and T. Imoto, (1974). Photosensitized polymerization of butyl acrylate under high pressure. Makro. Chem., 175, 2913.

Zhu, S. and A.E. Hamielec, (1991). Heat effects for free-radical polymerization in glass ampoule reactors. Polymer, 32, 3021-3025.

Zhu, S., Y. Tian, A.E. Hamielec and D.R. Eaton, (1990). Radical trapping and termination in free-radical polymerization of MMA. Macromolecules, 23, 1144-1150.

Appendix A

Reactivity Ratio Estimation Experimental Figures

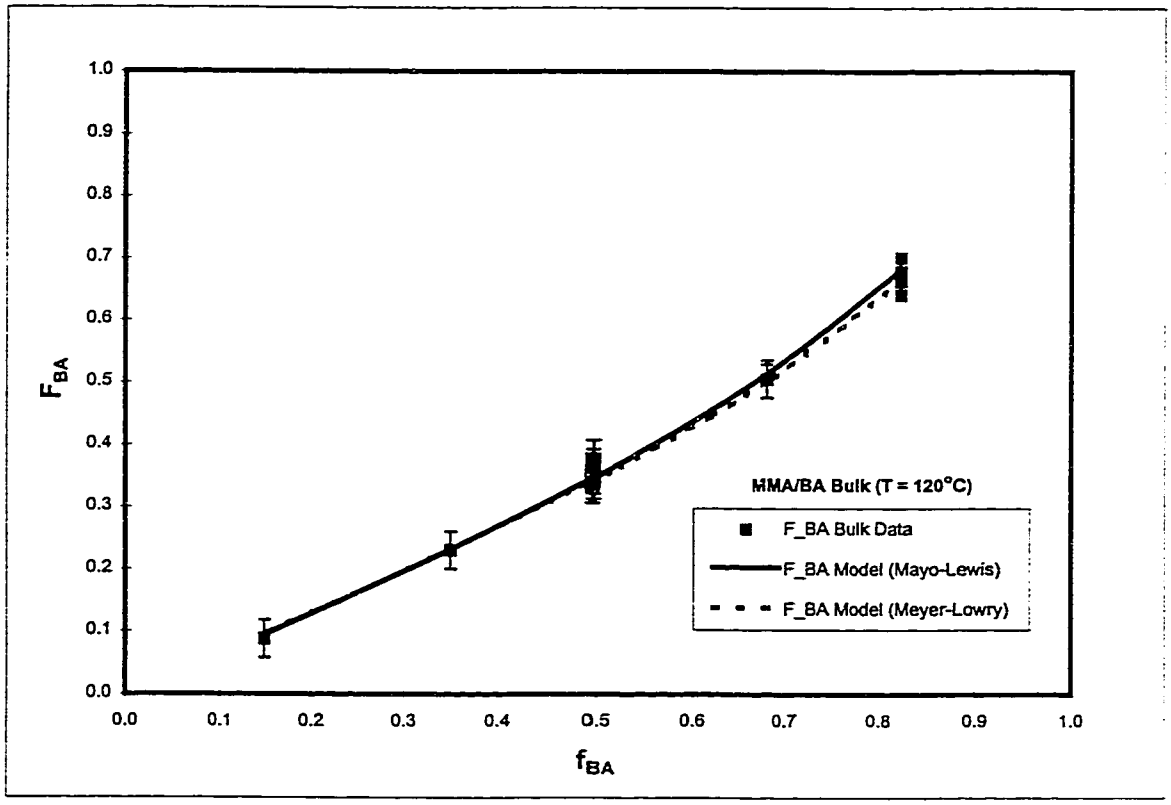

Figure A-1 BA-MMA Reactivity Ratio Bulk Composition Profile at 120 °C

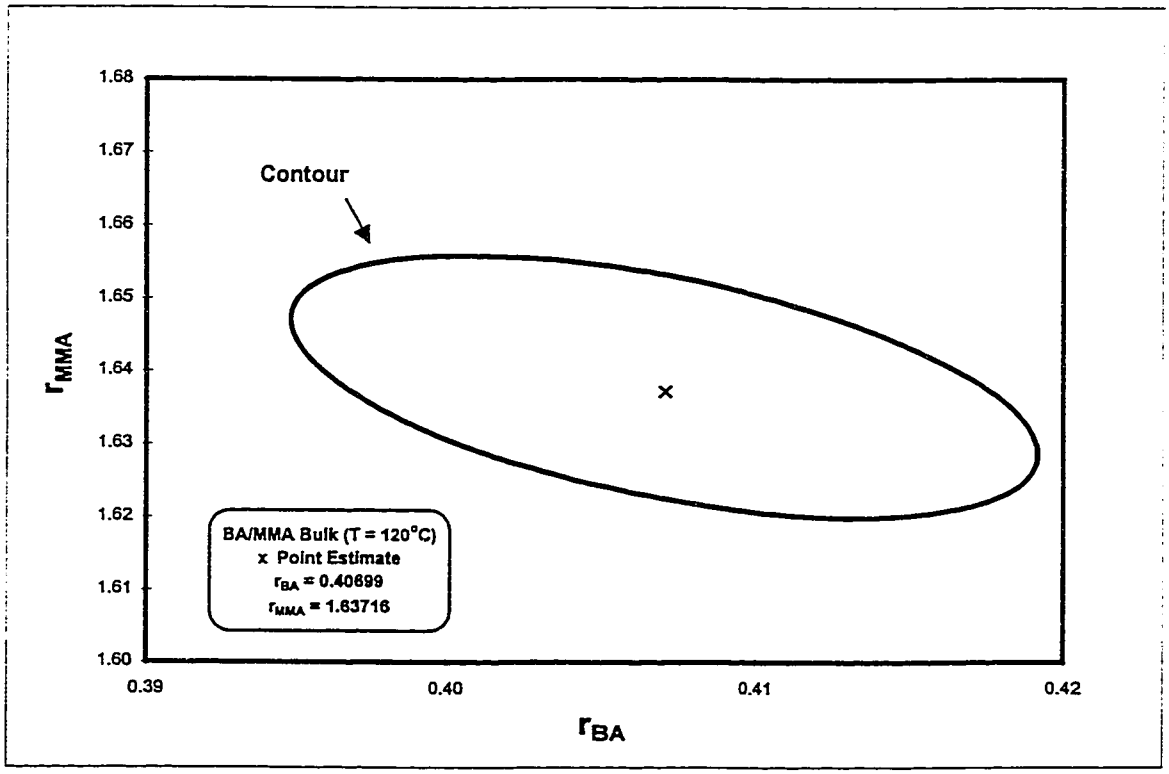

Figure A-2 BA-MMA Reactivity Ratio Bulk Run 95% Posterior Probability Contour

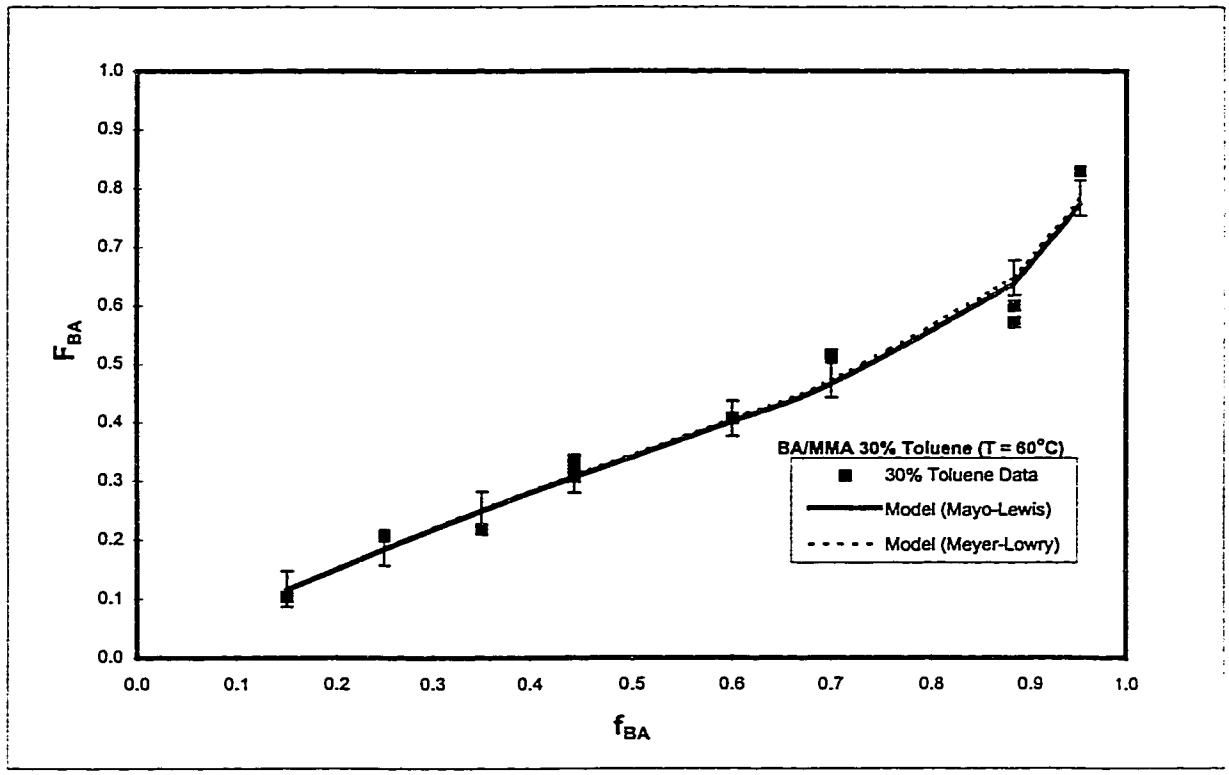

Figure A-3 BA-MMA Reactivity Ratio 30% Toluene Composition Profile at 60 °C

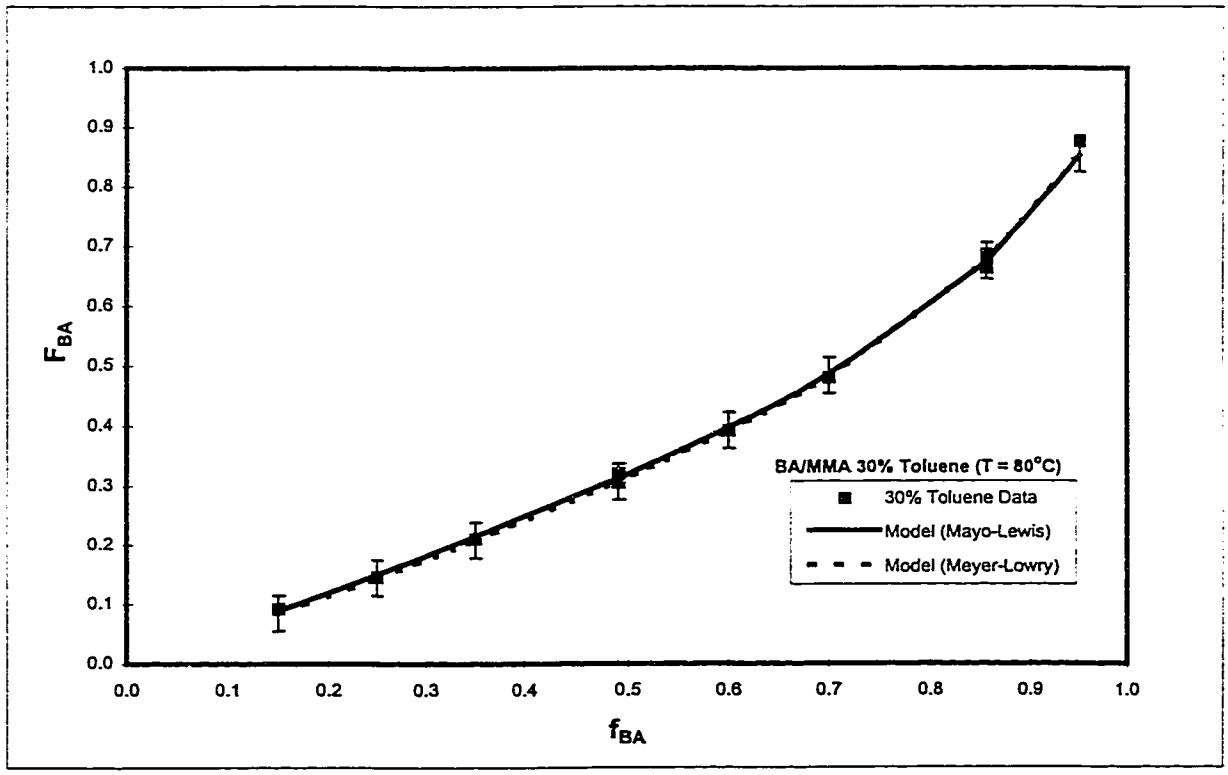

Figure A-4 BA-MMA Reactivity Ratio 30% Toluene Composition Profile at 80 °C

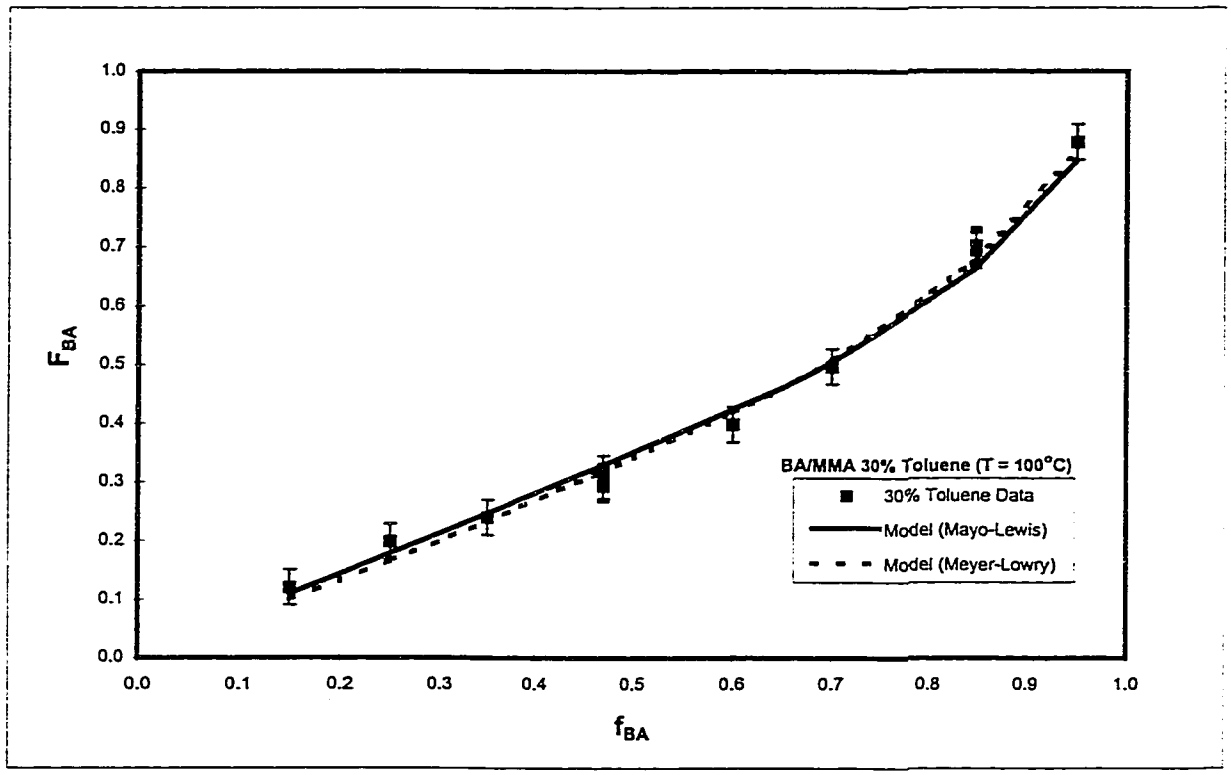

Figure A-5 BA-MMA Reactivity Ratio 30% Toluene Composition Profile at 100 °C

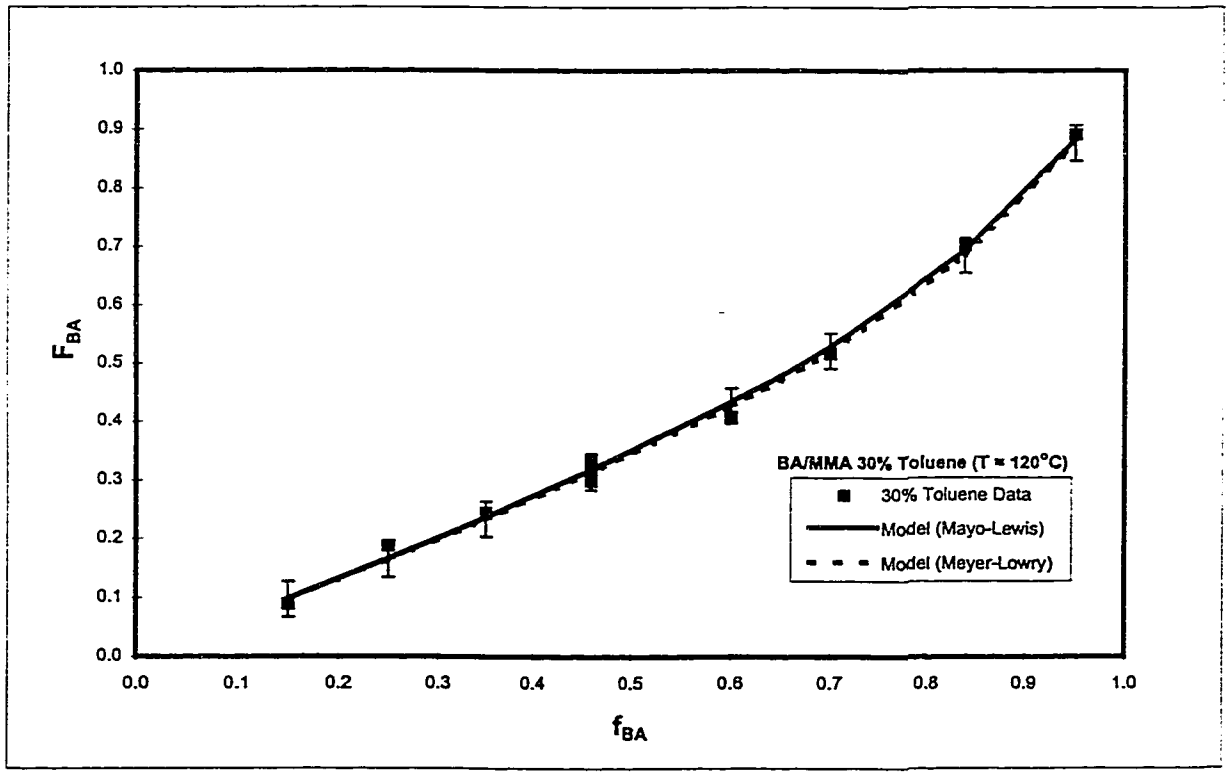

Figure A-6 BA-MMA Reactivity Ratio 30% Toluene Composition Profile at 120 °C

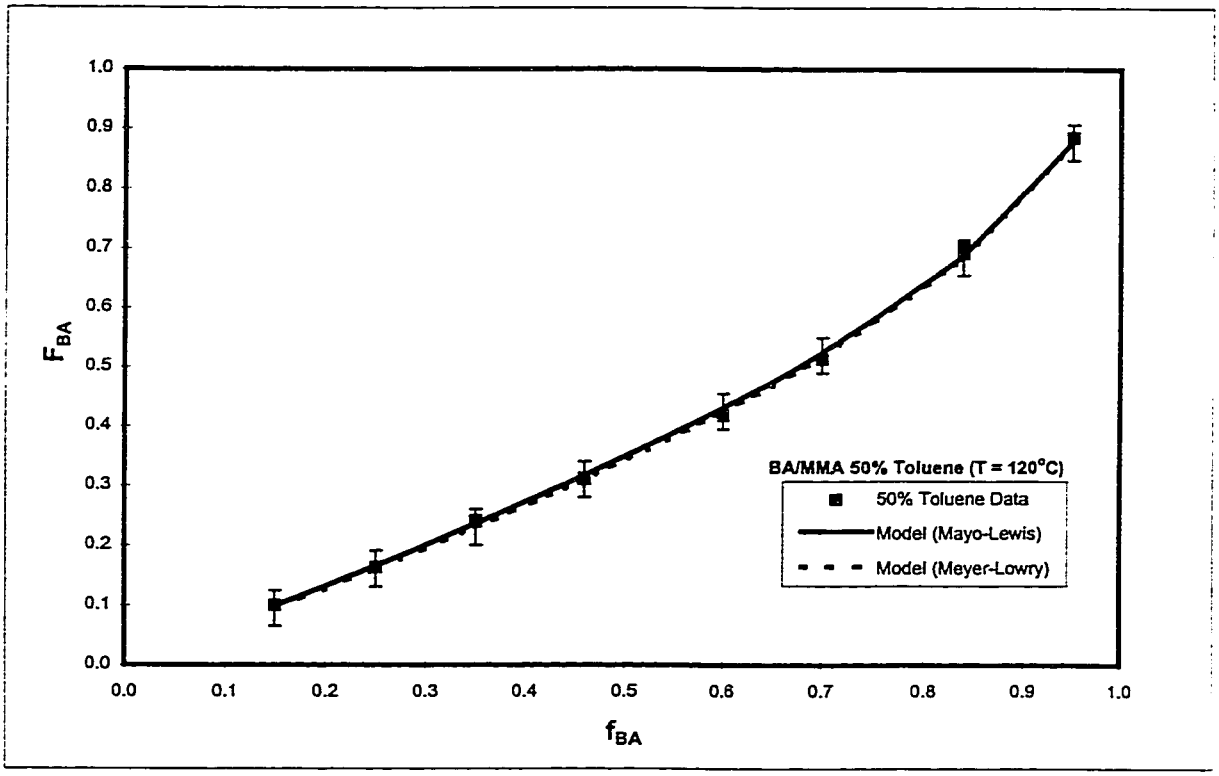

Figure A-7 BA-MMA Reactivity Ratio 50% Toluene Composition Profile at 120 °C

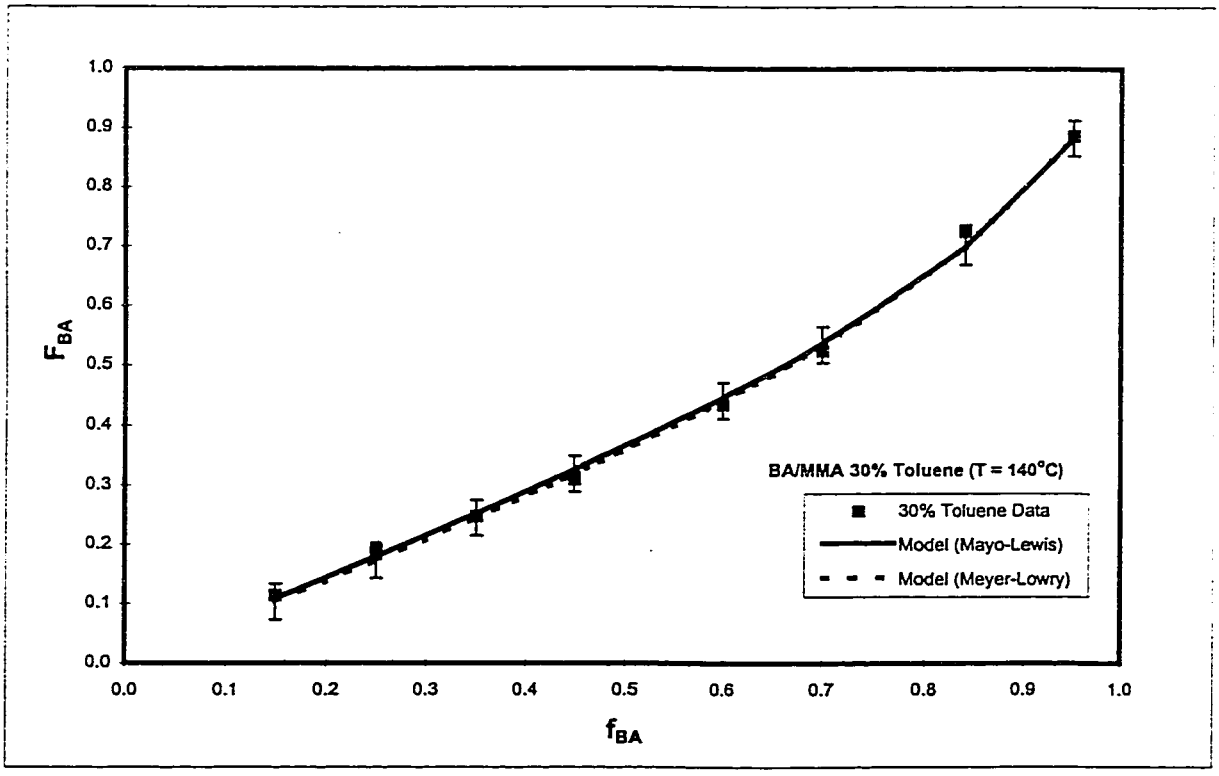

Figure A-8 BA-MMA Reactivity Ratio 30% Toluene Composition Profile at 140 °C

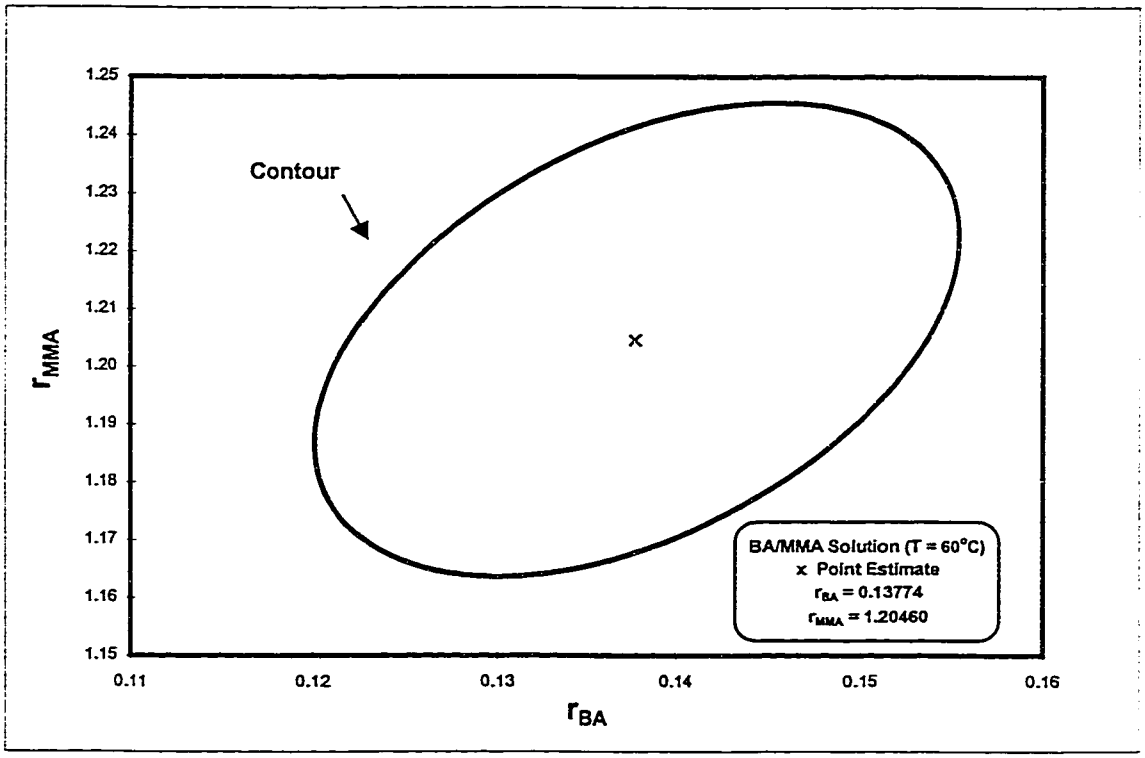

Figure A-9 BA-MMA Reactivity Ratio Solution (30 wt% Toleune) Run 95% Posterior Probability Contour at 60°C

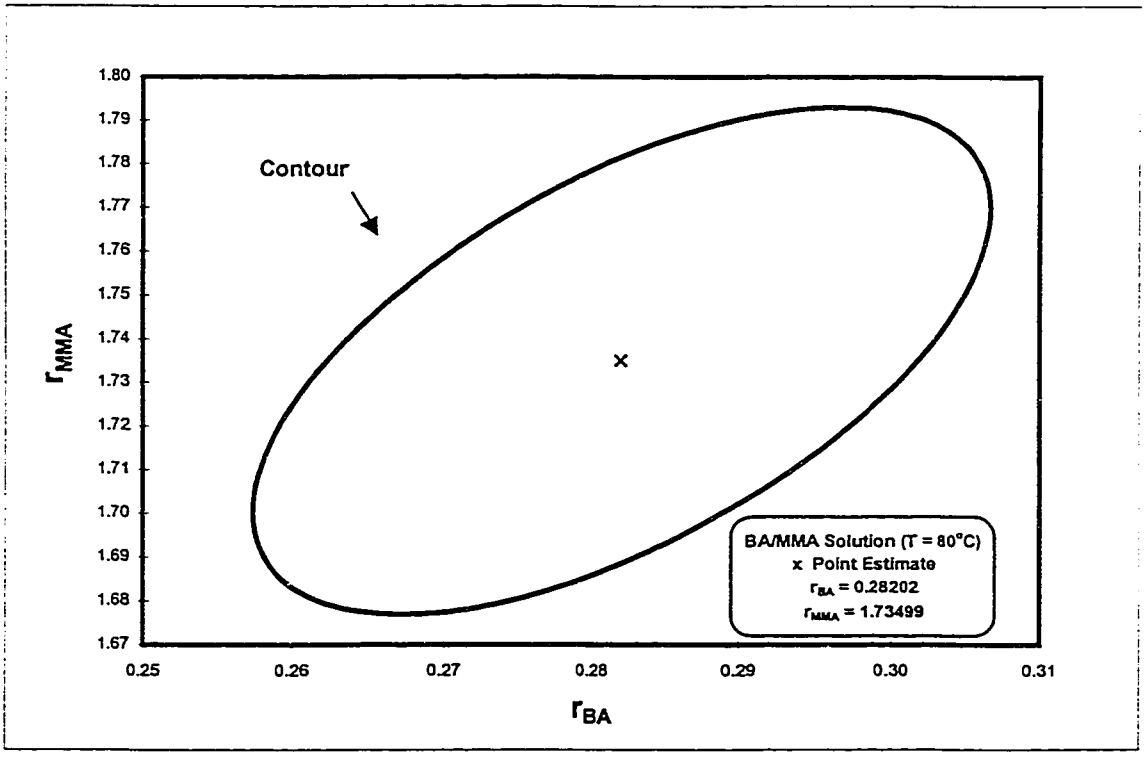

Figure A-10 BA-MMA Reactivity Ratio Solution (30 wt% Toleune) Run 95% Posterior Probability Contour at 80°C

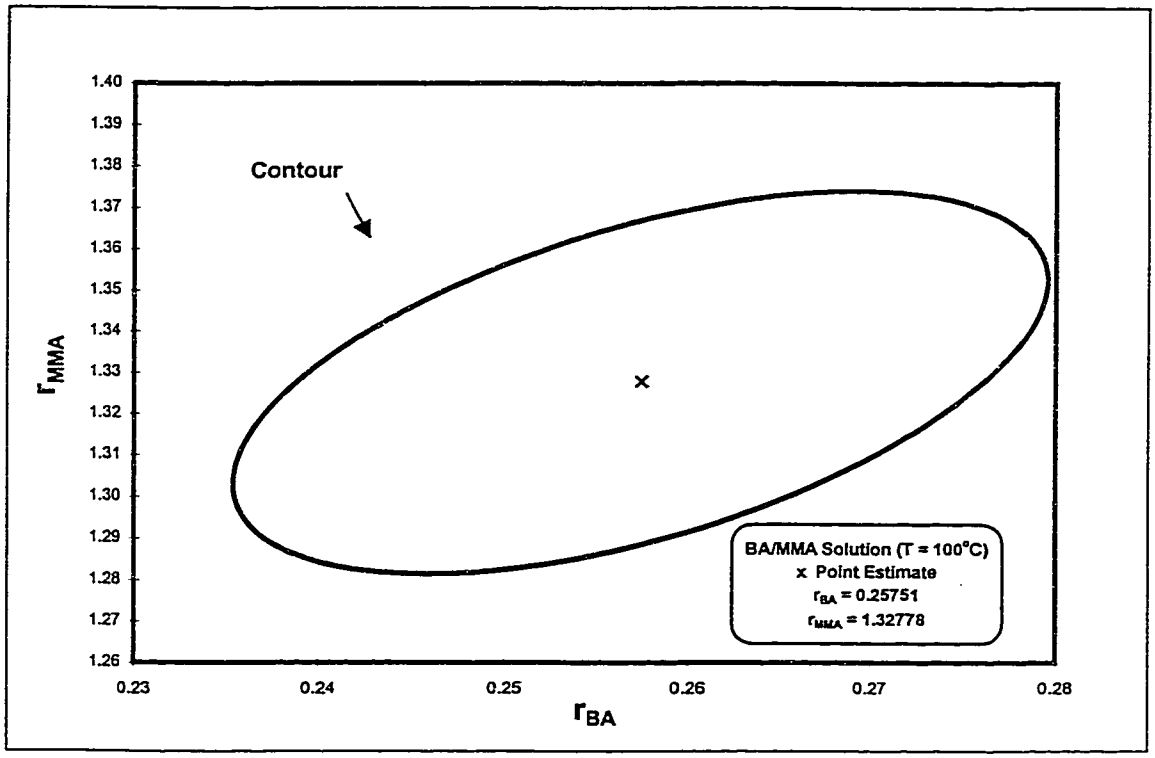

Figure A-11 BA-MMA Reactivity Ratio Solution (30 wt% Toleune) Run 95% Posterior Probability Contour at 100°C

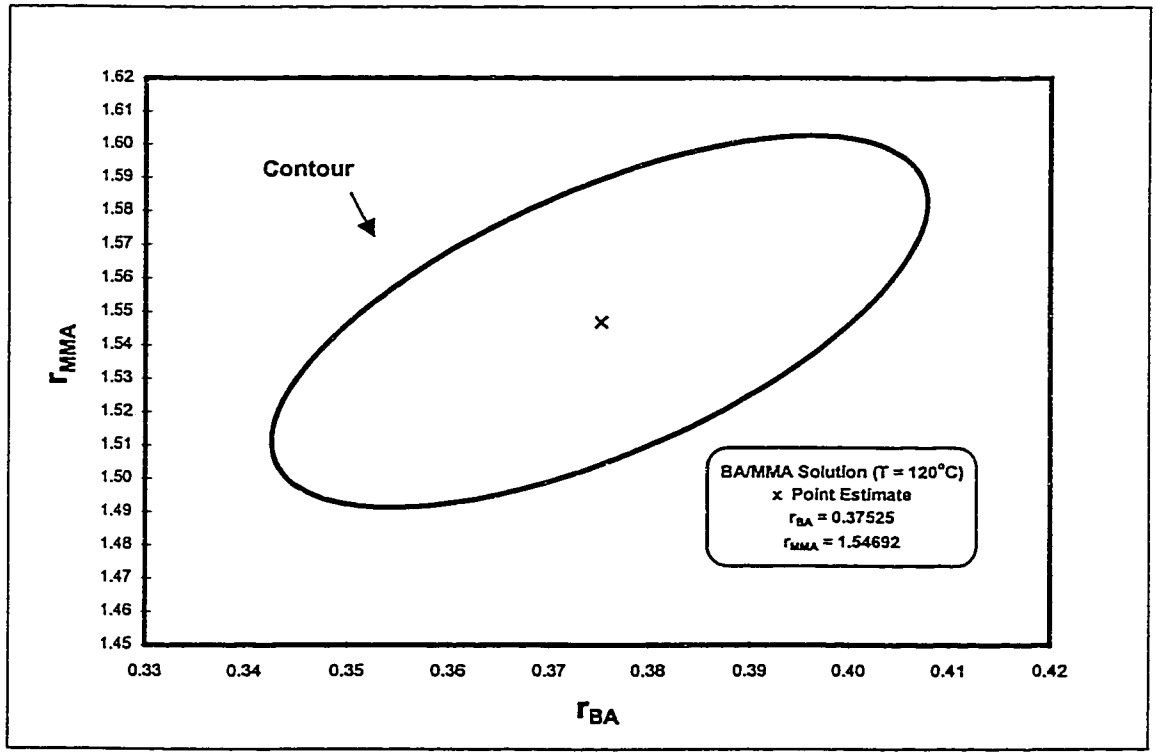

Figure A-12 BA-MMA Reactivity Ratio Solution (30 wt% Toleune) Run 95% Posterior Probability Contour at 120°C

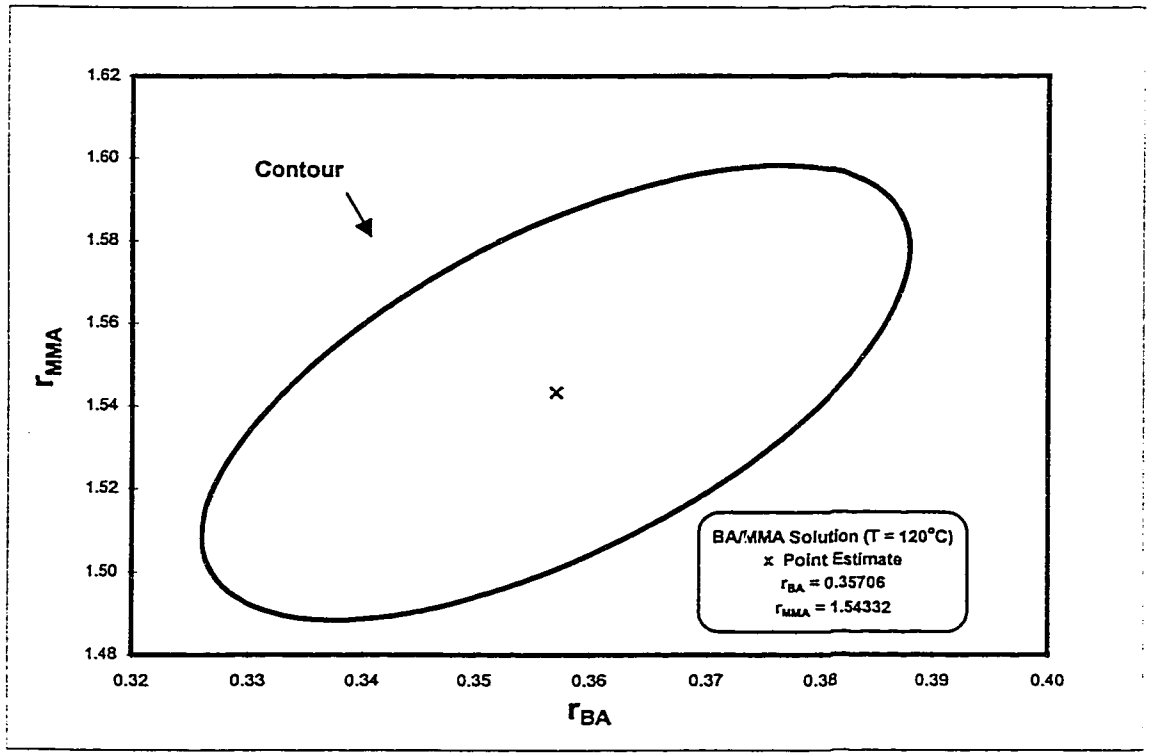

Figure A-13 BA-MMA Reactivity Ratio Solution (50 wt% Toleune) Run 95% Posterior Probability Contour at 120°C

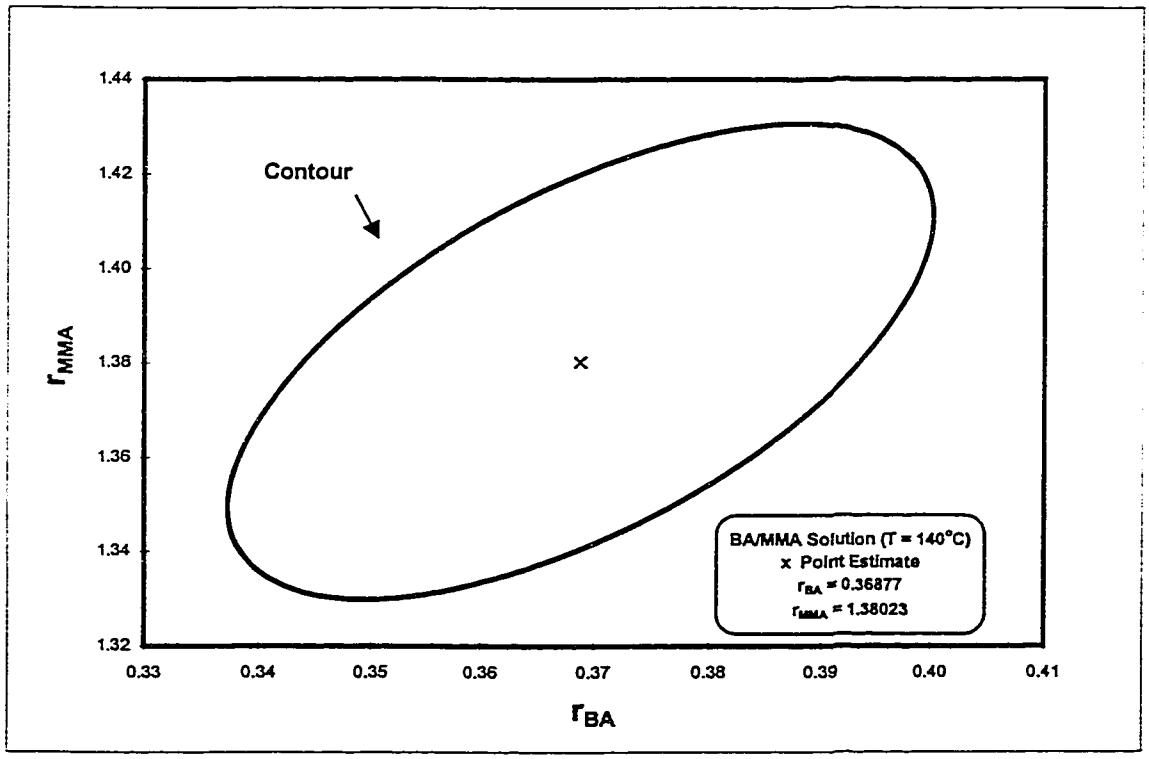

Figure A-14 BA-MMA Reactivity Ratio Solution (30 wt% Toleune) Run 95% Posterior Probability Contour at 140°C

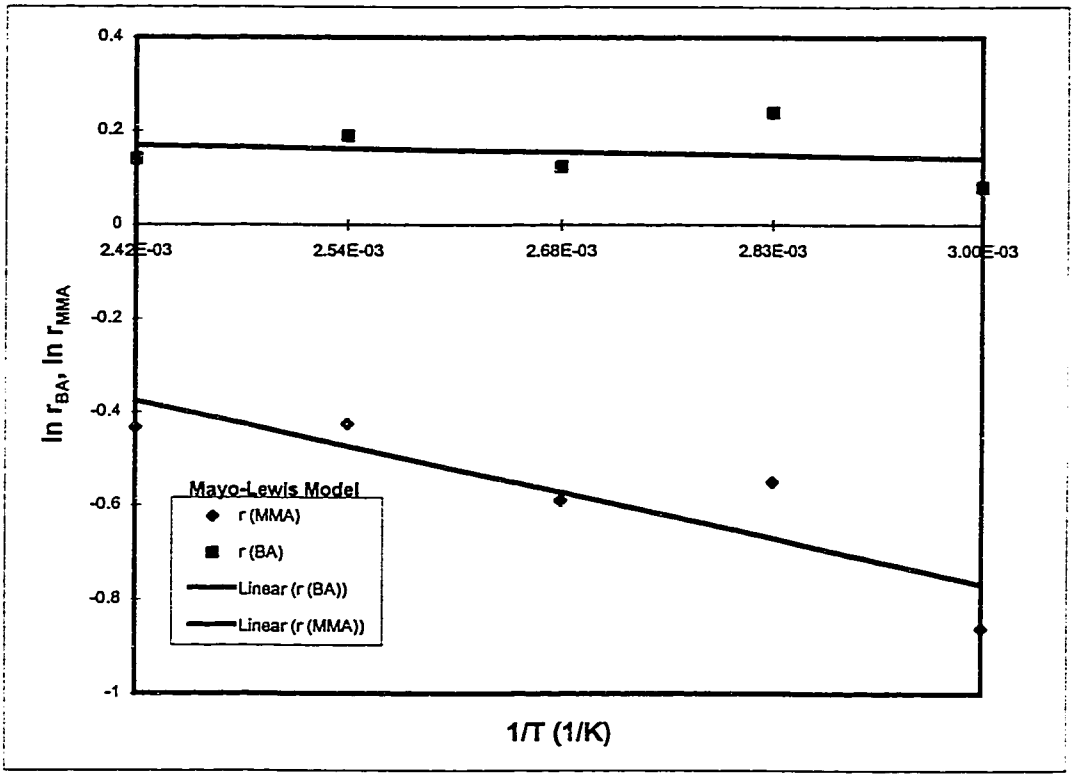

Figure A-15 BA-MMA 30 wt% Toluene Mayo-Lewis Model Arrhenius Test Plot

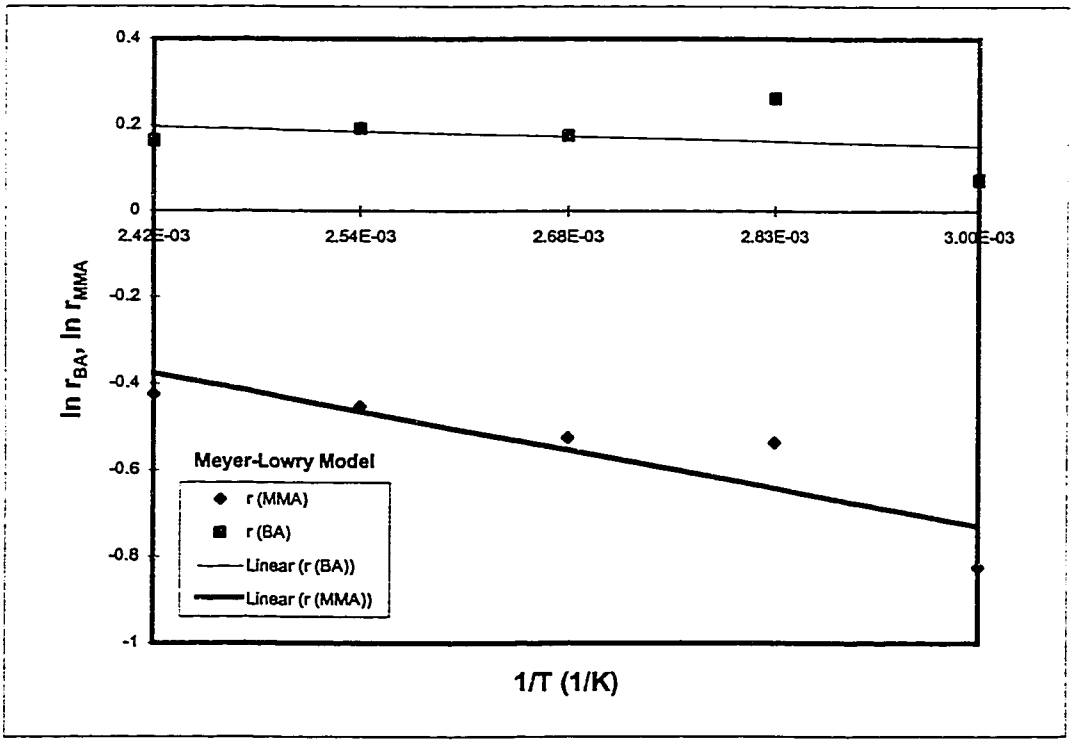

Figure A-16 BA-MMA 30 wt% Toluene Meyer-Lowry Model Arrhenius Test Plot

Appendix B

Reactivity Ratio Estimation Experimental Data

Table B-1 BA-MMA Reactivity Ratio Bulk Runs at 120 °C

New Results

Feed Mole Frac. BA 120 New Res	[Trig. B] (mol/L)	Time (min)	Conversion (wt. %)	F_BA 120 New Res
0.823300	0.0008	10	10.02	0.678935
0.823300	0.0008	10	3.57	0.674232
0.823195	0.0008	10	6.47	0.665188
0.823195	0.0008	10	8.15	0.667260
0.823195	0.0008	10	4.16	0.663130
0.823195	0.0008	10	3.75	0.672043
0.681000	0.0010	15	11.01	0.505954
0.497016	0.0013	15	8.67	0.343249
0.497016	0.0013	15	7.63	0.362319
0.497016	0.0013	15	6.55	0.377834
0.497016	0.0013	15	6.55	0.351288
0.495938	0.0013	15	5.78	0.336676
0.495938	0.0013	15	6.00	0.355056
0.350000	0.0011	15	4.87	0.230875
0.149000	0.0013	15	4.95	0.088254

Table B-2 BA-MMA Reactivity Ratio Solution Runs at 60 °C

New Results

Feed Mole Frac. BA New Res	[Trig. B] (mol/L)	Time (min)	Conversion (wt. %)	F_BA New Res
0.150000	0.0010	20	1.63	0.104384
0.250000	0.0010	20	2.30	0.207699
0.350000	0.0012	20	1.67	0.218978
0.442809	0.0014	20	2.03	0.307479
0.442809	0.0014	20	3.38	NA
0.442809	0.0014	20	2.18	0.335769
0.442809	0.0014	20	2.21	0.318104
0.600000	0.0015	10	0.75	0.406945
0.700000	0.0013	10	0.88	0.515818
0.882668	0.0012	10	1.17	NA
0.882668	0.0012	10	2.79	0.571734
0.882668	0.0012	10	3.08	NA
0.882668	0.0012	10	0.31	0.600000
0.950000	0.0014	10	1.42	0.829187

Notes: NA ^{1}H-NMR data not available due to insufficient amount of polymer product for analysis.

Table B-3 BA-MMA Reactivity Ratio Solution Runs at 80 °C

New Results

Feed Mole Frac. BA New Res	[Trig. B] (mol/L)	Time (min)	Conversion (wt. %)	F_BA New Res
0.149945	0.0005	195	2.45	0.092559
0.249978	0.0005	195	3.49	0.146029
0.349919	0.0004	195	3.25	0.210734
0.490964	0.0185	25	1.37	0.321062
0.490964	0.0185	25	2.17	0.314729
0.490964	0.0185	25	2.14	0.305002
0.490964	0.0185	25	3.53	0.305499
0.599977	0.0006	99	2.32	0.392651
0.699952	0.0006	99	3.59	0.481059
0.856129	0.0185	15	0.79	0.664894
0.856129	0.0185	15	0.89	0.687443
0.856129	0.0185	15	1.14	0.679656
0.856129	0.0185	15	1.40	0.682749
0.950003	0.0004	99	11.43	0.878004

Table B-4 BA-MMA Reactivity Ratio Solution Runs at 100 °C

New Results

Feed Mole Frac. BA New Res	[Trig. B] (mol/L)	Time (min)	Conversion (wt. %)	F_BA New Res
0.149945	0.0005	60	6.83	0.121265
0.249978	0.0005	60	4.44	0.199359
0.349919	0.0004	60	3.76	0.240410
0.469701	0.0064	15	3.14	0.315060
0.469701	0.0064	15	4.19	0.297619
0.469701	0.0064	15	3.92	0.302176
0.469701	0.0064	15	3.32	0.299043
0.599977	0.0006	20	2.01	0.398677
0.699952	0.0006	20	1.84	0.497487
0.848347	0.0065	10	4.01	0.702905
0.848347	0.0065	10	4.06	0.696379
0.848347	0.0065	10	4.11	0.698324
0.848347	0.0065	10	4.52	0.695088
0.950003	0.0004	20	3.93	0.878626

Table B-5 BA-MMA Reactivity Ratio Solution Runs at 120 °C

New Results

Feed Mole Frac. BA New Res	[Trig. B] (mol/L)	Time (min)	Conversion (wt. %)	F_BA New Res
0.149945	0.0005	25	6.51	0.090082
0.249978	0.0005	25	6.01	0.188641
0.349919	0.0004	25	6.13	0.245568
0.459168	0.0017	10	3.44	0.303398
0.459168	0.0017	10	3.38	0.320581
0.459168	0.0017	10	3.14	0.337914
0.459168	0.0017	10	3.30	0.300000
0.599977	0.0006	13	3.88	0.409681
0.699952	0.0006	14	5.16	0.518420
0.838468	0.0017	5	5.37	0.702905
0.838468	0.0017	5	5.25	0.705219
0.838468	0.0017	5	4.69	0.703565
0.838468	0.0017	5	6.44	0.704887
0.950003	0.0004	11	9.69	0.892009

Table B-6 BA-MMA Reactivity Ratio Solution Runs at 120 °C

50% Toluene

New Results

Feed Mole Frac. BA New Res	[Trig. B] (mol/L)	Time (min)	Conversion (wt. %)	F_BA New Res
0.149945	0.0004	19	3.85	0.101124
0.249978	0.0004	20	5.58	0.164229
0.349919	0.0004	21	4.43	0.241850
0.459081	0.0017	10	3.21	0.312826
0.459081	0.0017	10	3.85	0.311139
0.459081	0.0017	10	4.01	0.312435
0.459081	0.0017	10	3.27	0.311139
0.599977	0.0004	12	3.64	0.418774
0.700000	0.0004	10	4.95	0.514091
0.838692	0.0017	5	3.15	0.692521
0.838692	0.0017	5	3.87	0.699301
0.838692	0.0017	5	3.72	0.706215
0.838692	0.0017	5	3.65	0.700280
0.950000	0.0002	11	6.81	0.885910

Table B-7 BA-MMA Reactivity Ratio Solution Runs at 140 °C

New Results

Feed Mole Frac. BA New Res	[Trig. B] (mol/L)	Time (min)	Conversion (wt. %)	F_BA New Res
0.149945	0.0005	5	3.14	0.113868
0.249978	0.0005	5	4.55	0.191266
0.349919	0.0004	5	4.51	0.247555
0.448857	0.0005	10	9.27	0.309789
0.448857	0.0005	10	9.23	0.310881
0.448857	0.0005	10	8.61	0.313480
0.448857	0.0005	10	9.80	0.309981
0.599977	0.0006	2	1.58	0.435825
0.699952	0.0006	2	2.00	0.526179
0.840145	0.0005	5	11.91	0.727449
0.840145	0.0005	5	10.16	0.727096
0.840145	0.0005	5	10.40	0.728155
0.840145	0.0005	5	11.20	0.726392
0.950003	0.0004	2	4.34	0.887514

Appendix C

Full Conversion Experimental Figures

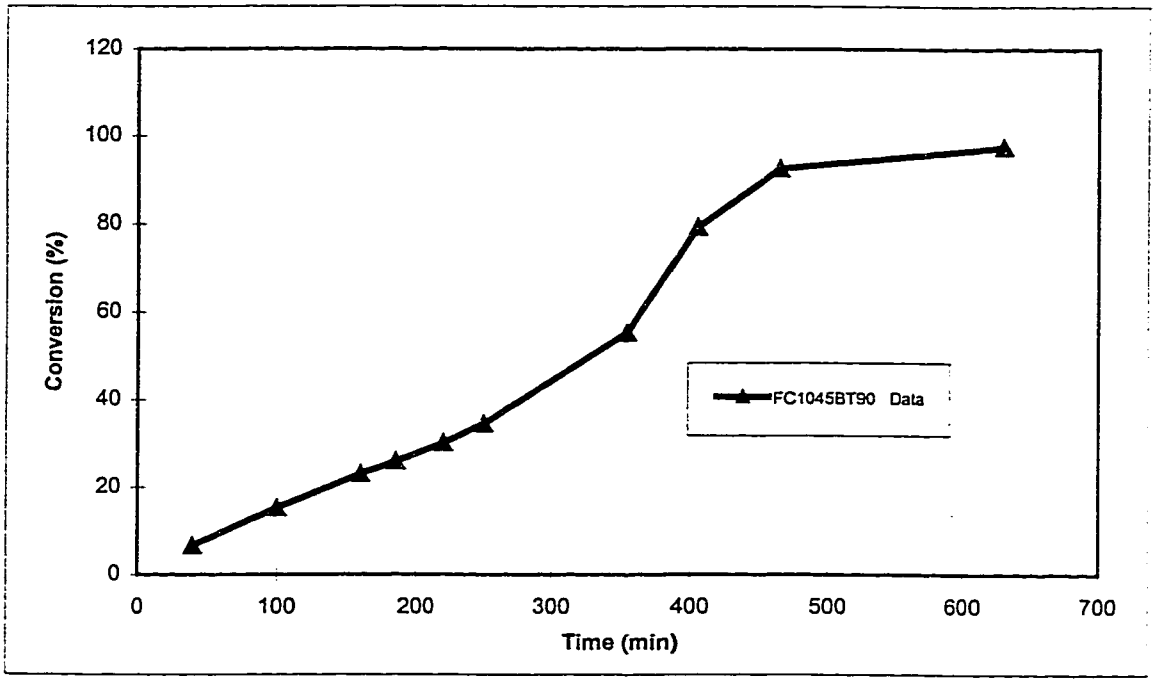

Figure C-1 **Full Conversion 10/45 BA-MMA Bulk Profile At 90 °C**

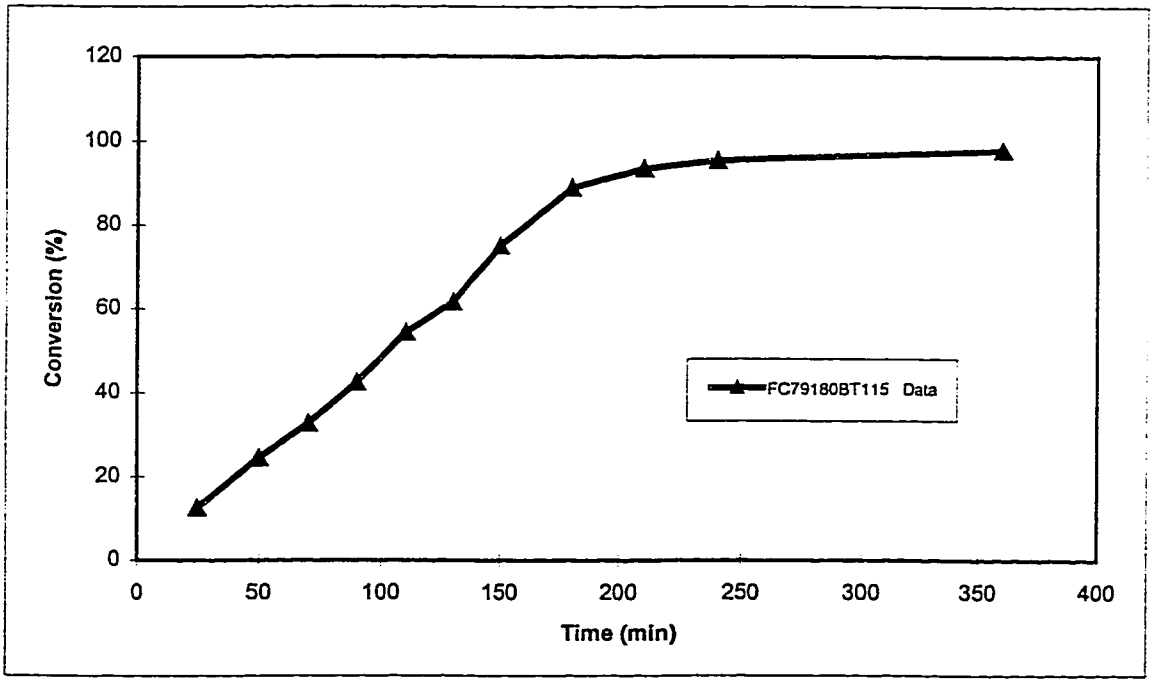

Figure C-2 **Full Conversion 79/180 BA-MMA Bulk Profile At 115 °C**

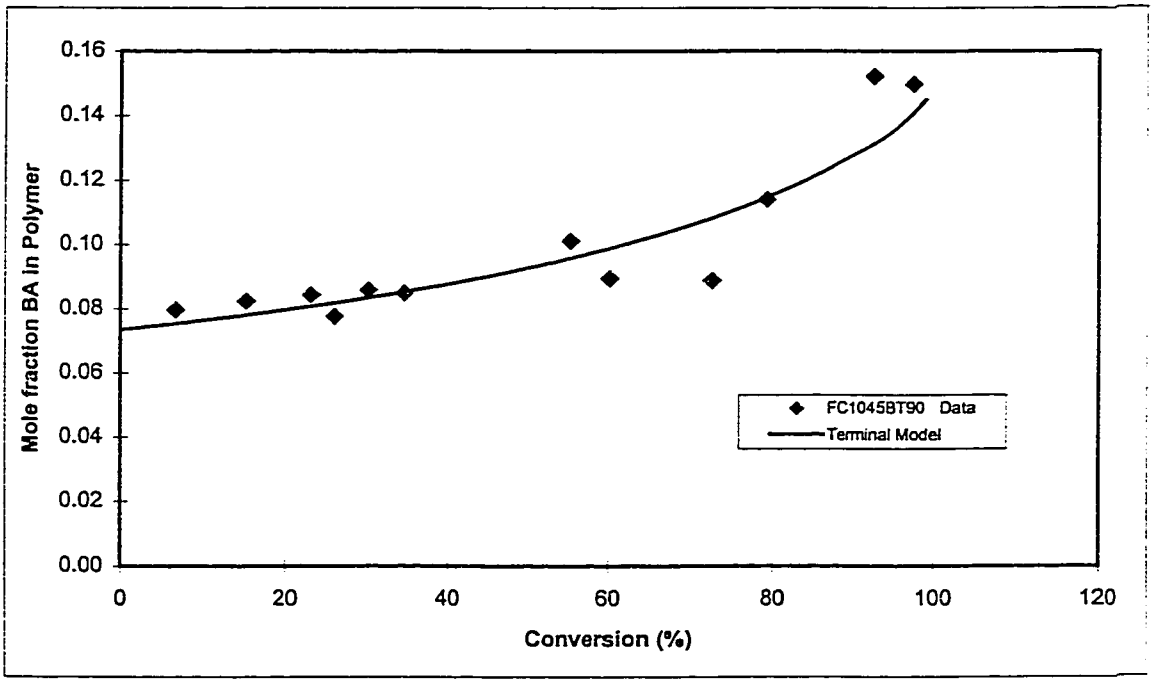

Figure C-3 BA-MMA 10/45 Bulk Composition Profile At 90 °C

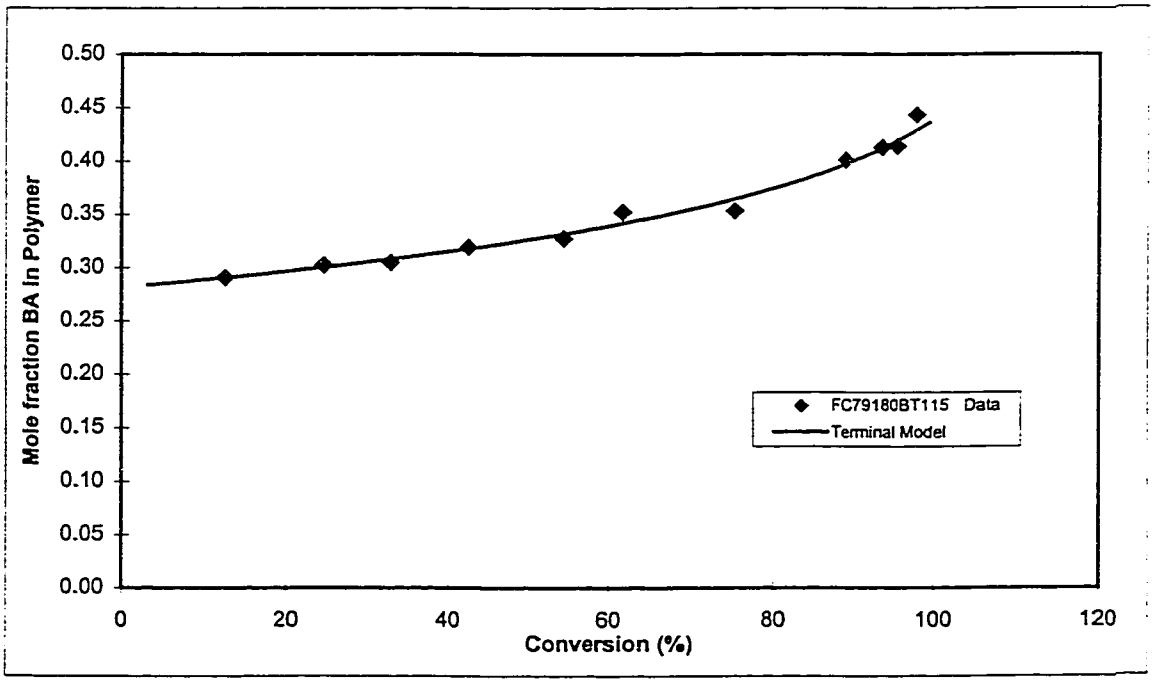

Figure C-4 BA-MMA 79/180 Bulk Composition Profile At 115 °C

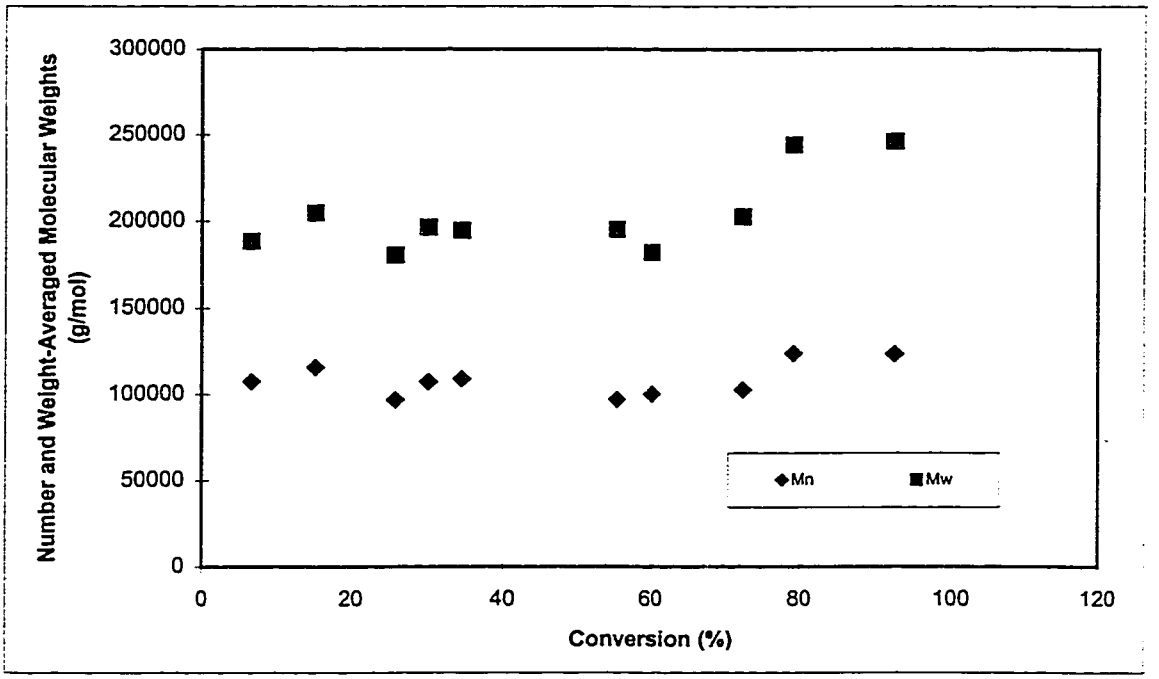

Figure C-5 BA-MMA 10/45 Bulk Molecular Weight Profile At 90 °C

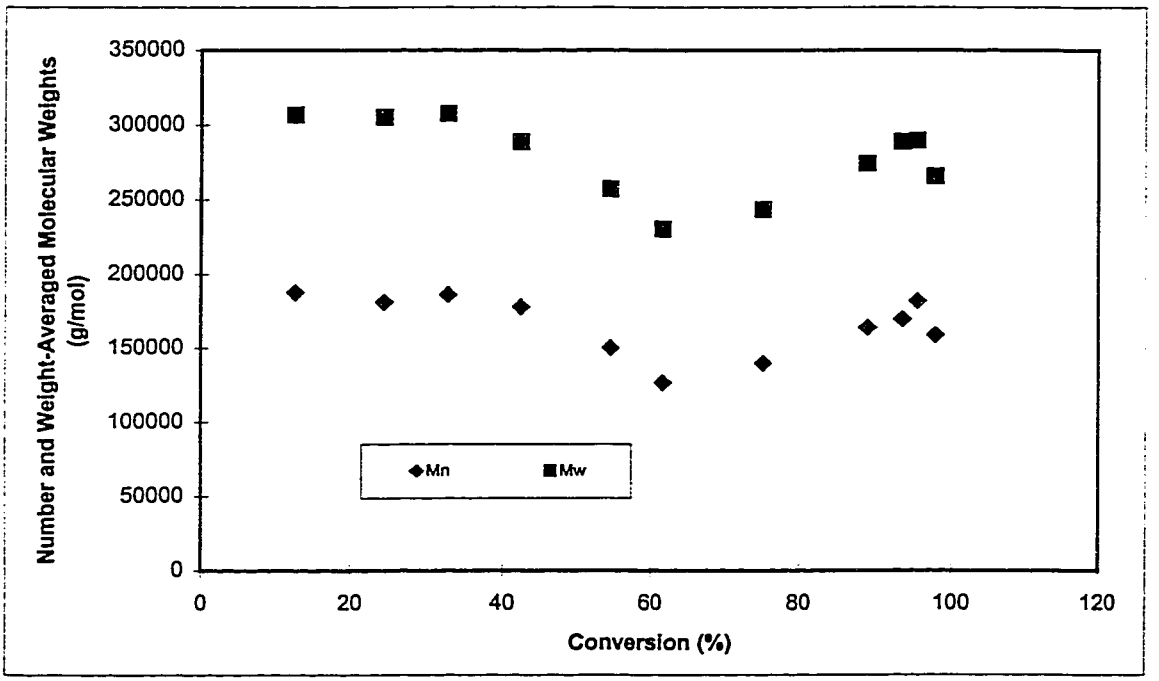

Figure C-6 BA-MMA 79/180 Bulk Molecular Weight Profile At 115 °C

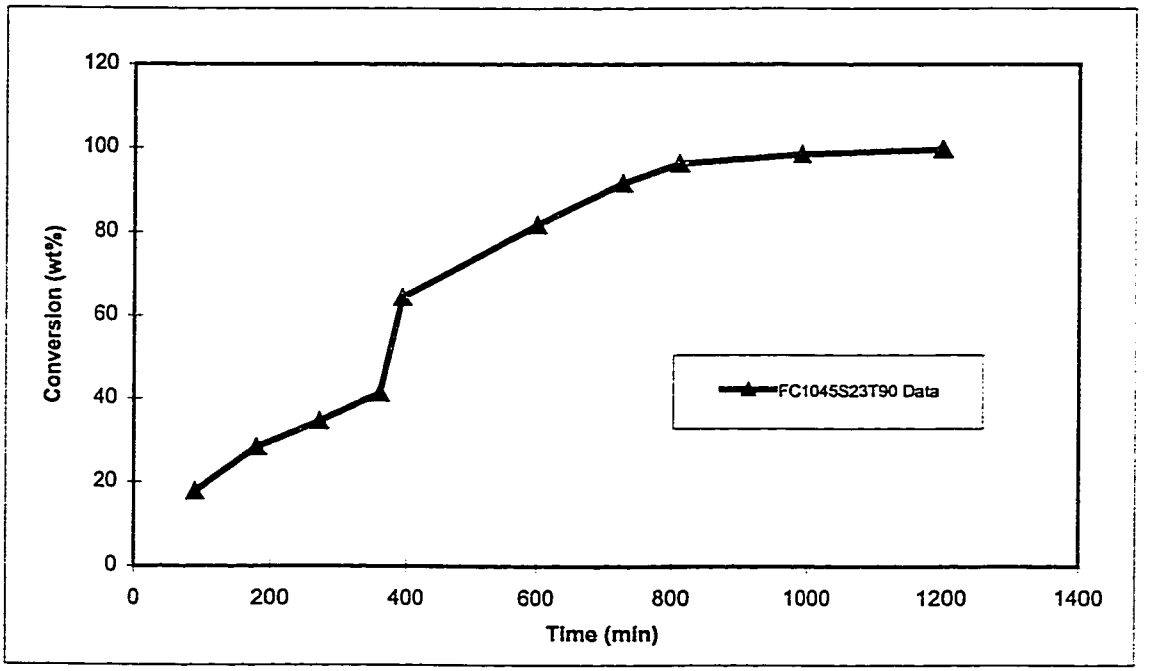

Figure C-7 BA-MMA 10/45 23% Toluene Conversion Profile At 90 °C

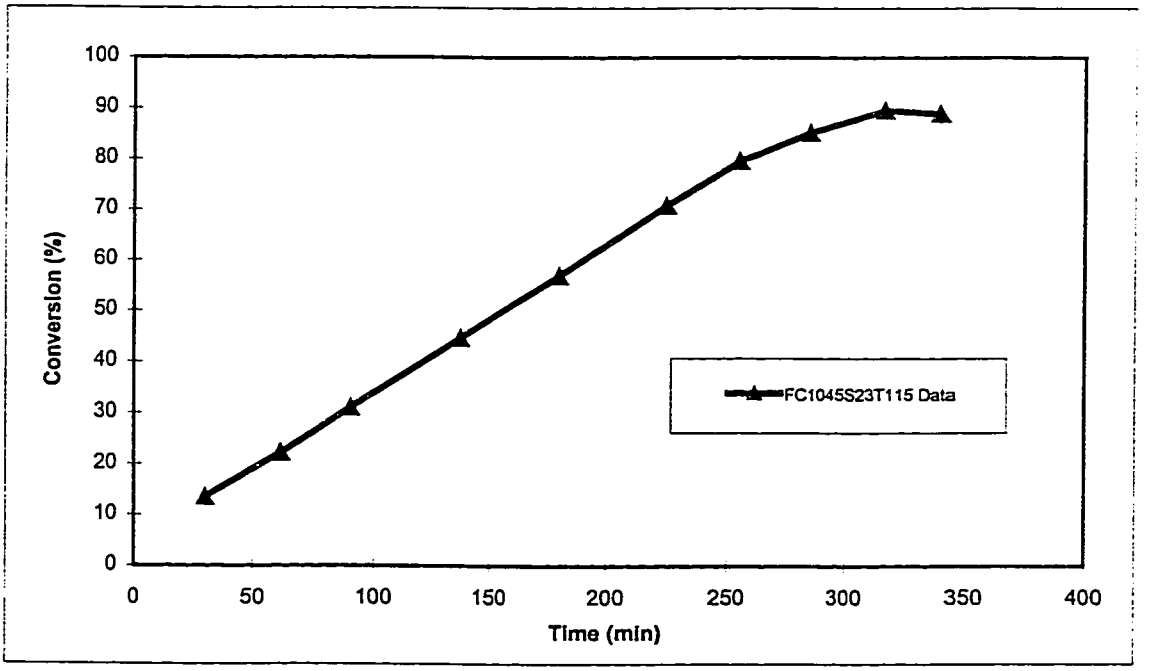

Figure C-8 BA-MMA 10/45 23% Toluene Conversion Profile At 115 °C

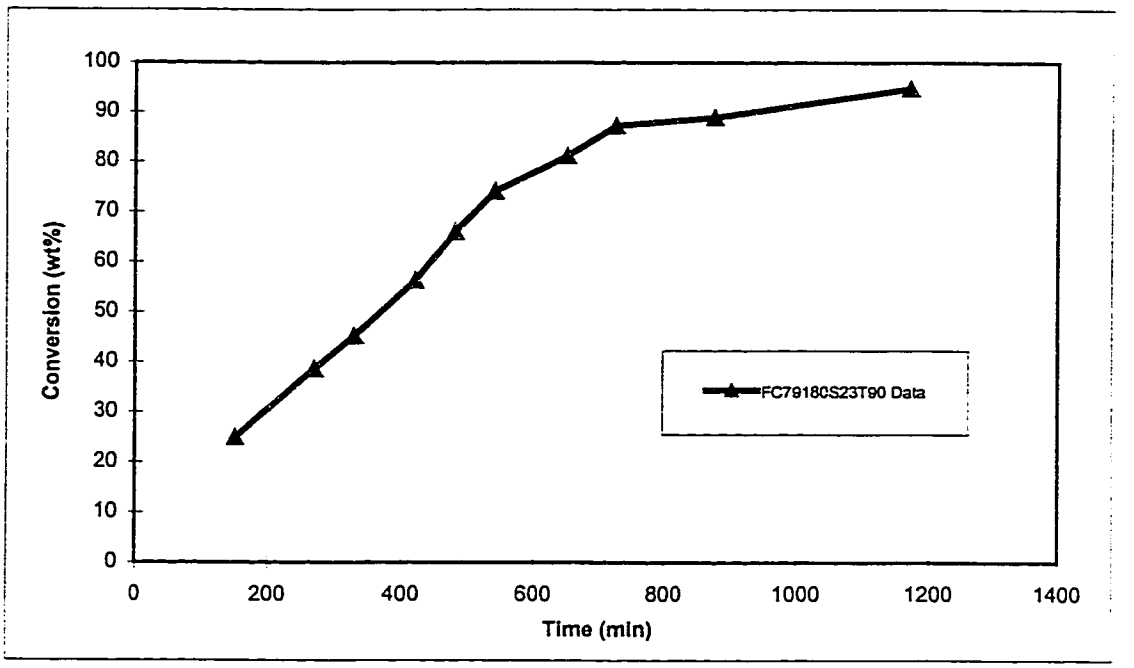

Figure C-9 **BA-MMA 79/180 23% Toluene Conversion Profile At 90 °C**

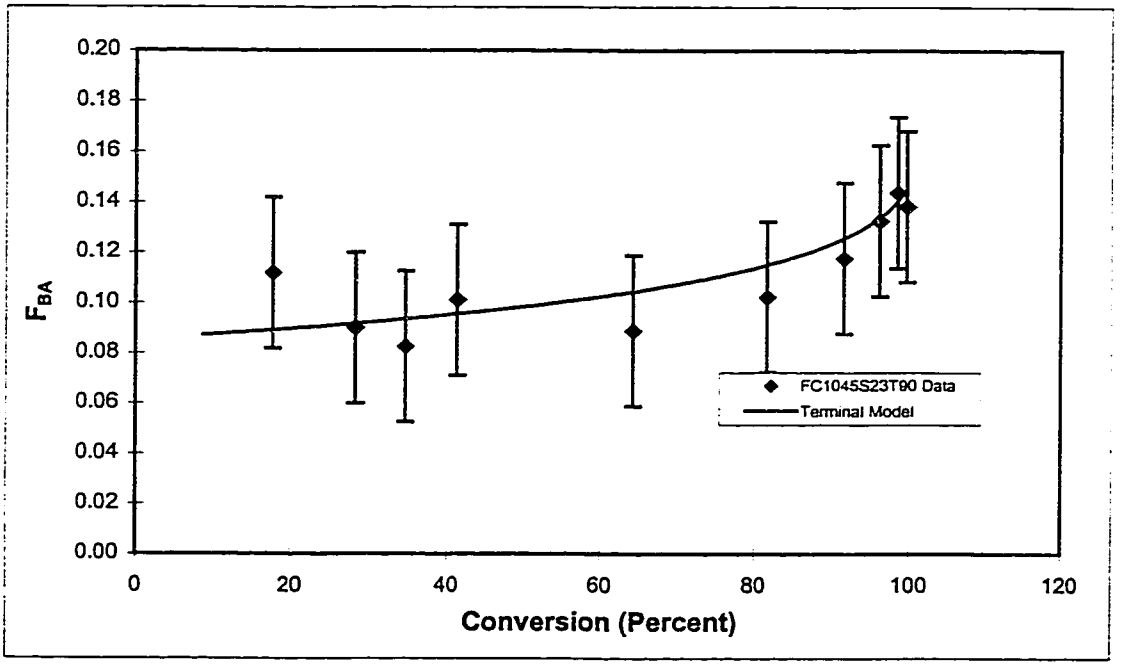

Figure C-10 **BA-MMA 10/45 23% Toluene Composition Profile At 90 °C**

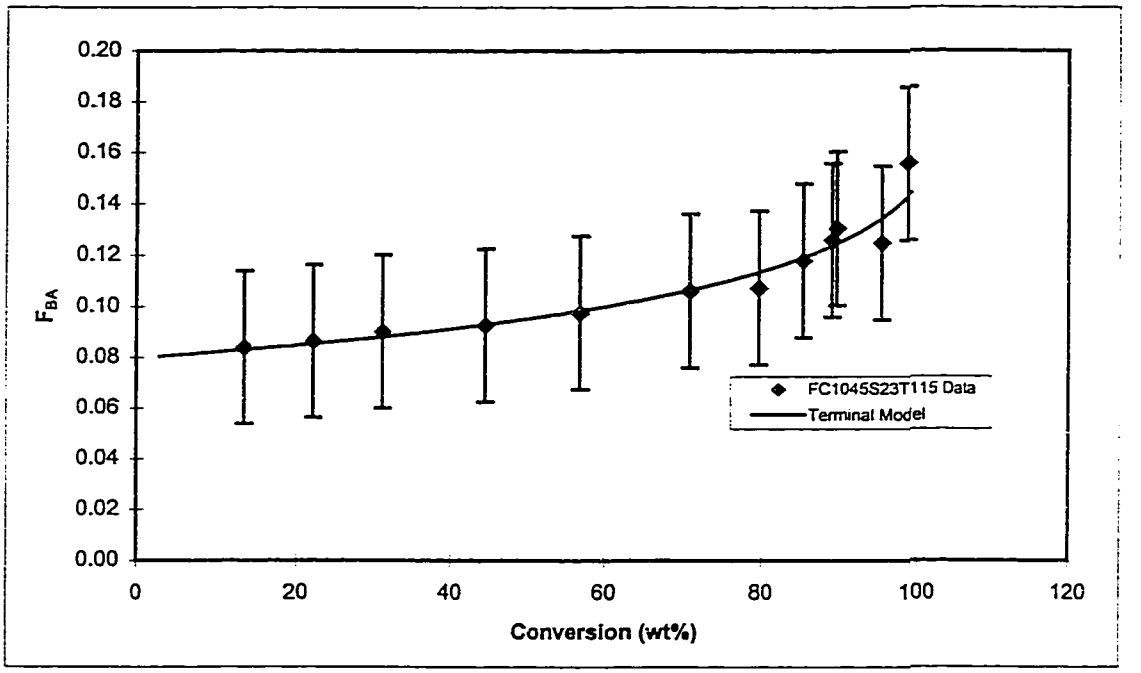

Figure C-11 BA-MMA 10/45 23% Toluene Composition Profile At 115 °C

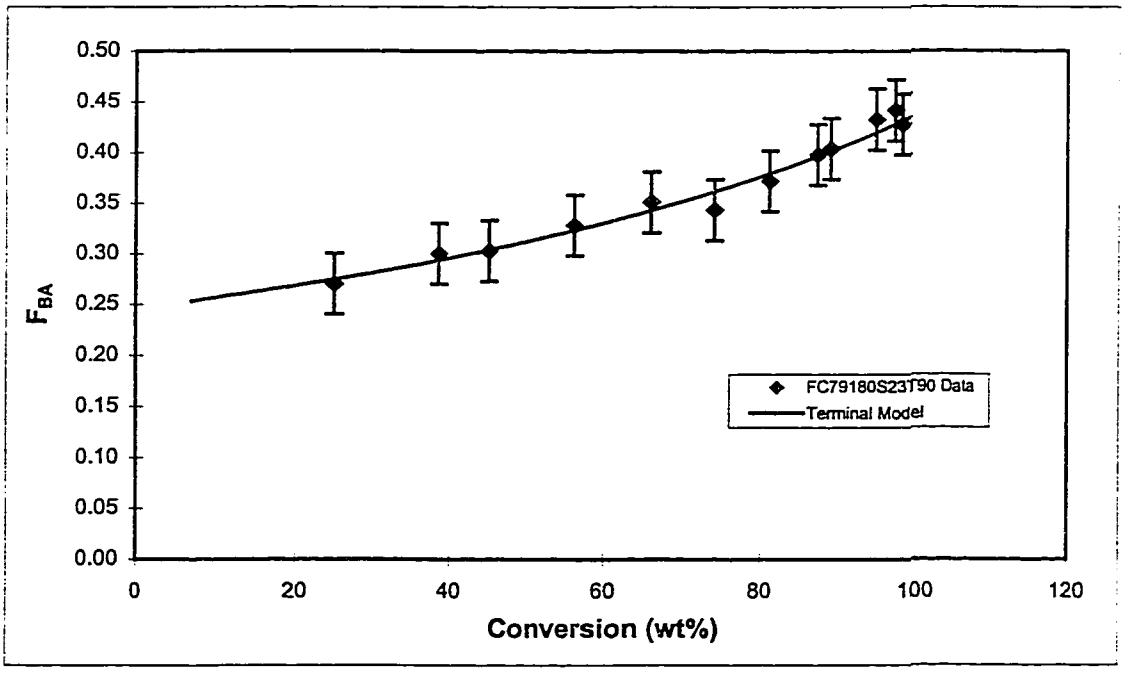

Figure C-12 BA-MMA 79/180 23% Toluene Composition Profile At 90 °C

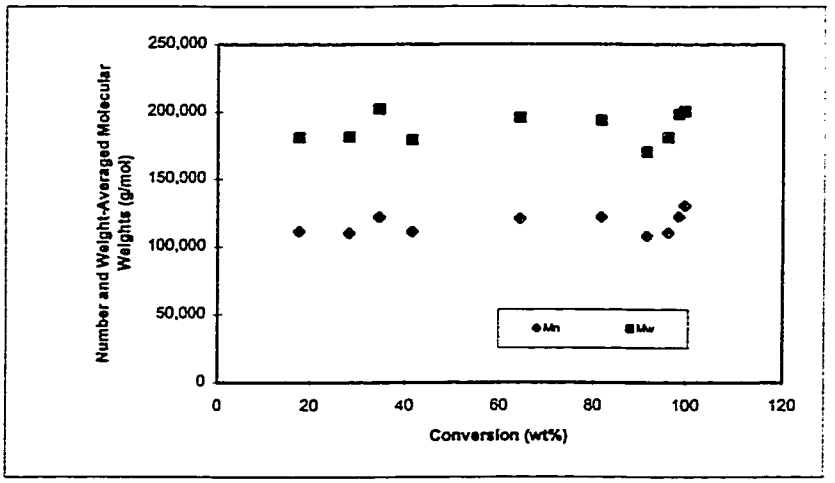

Figure C-13 BA-MMA 10/45 23% Toluene Molecular Weight Profile At 90 °C

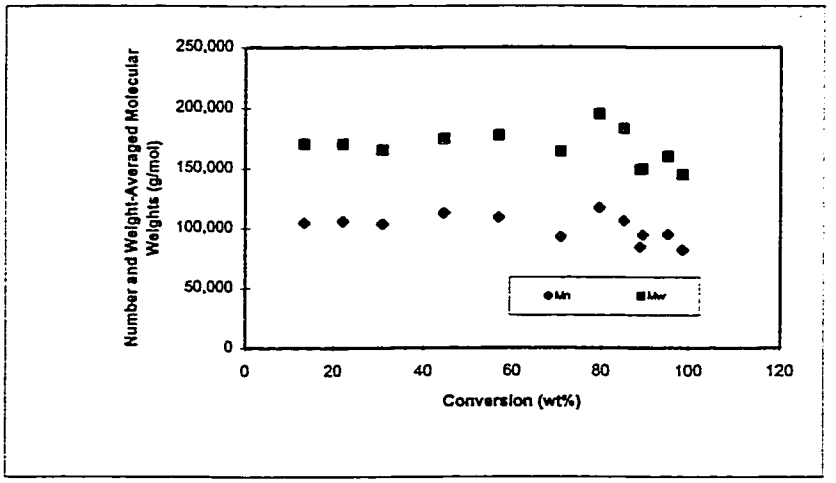

Figure C-14 BA-MMA 10/45 23% Toluene Molecular Weight Profile At 115 °C

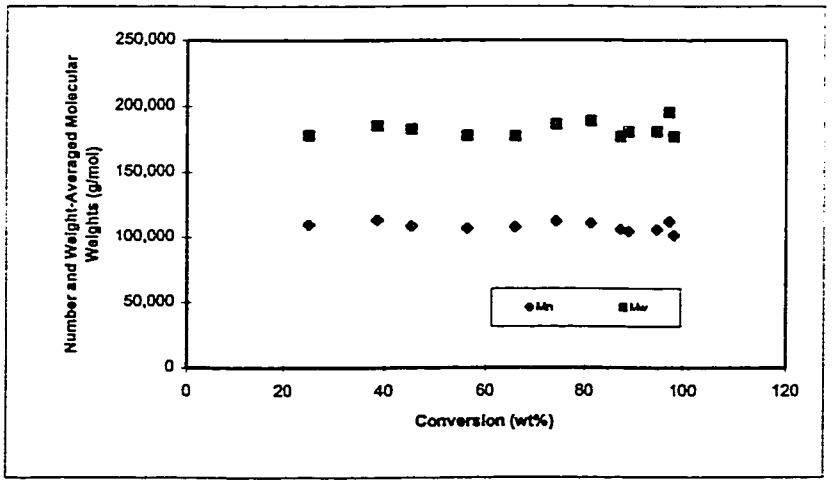

Figure C-15 BA-MMA 79/180 23% Toluene Molecular Weight Profile At 90 °C

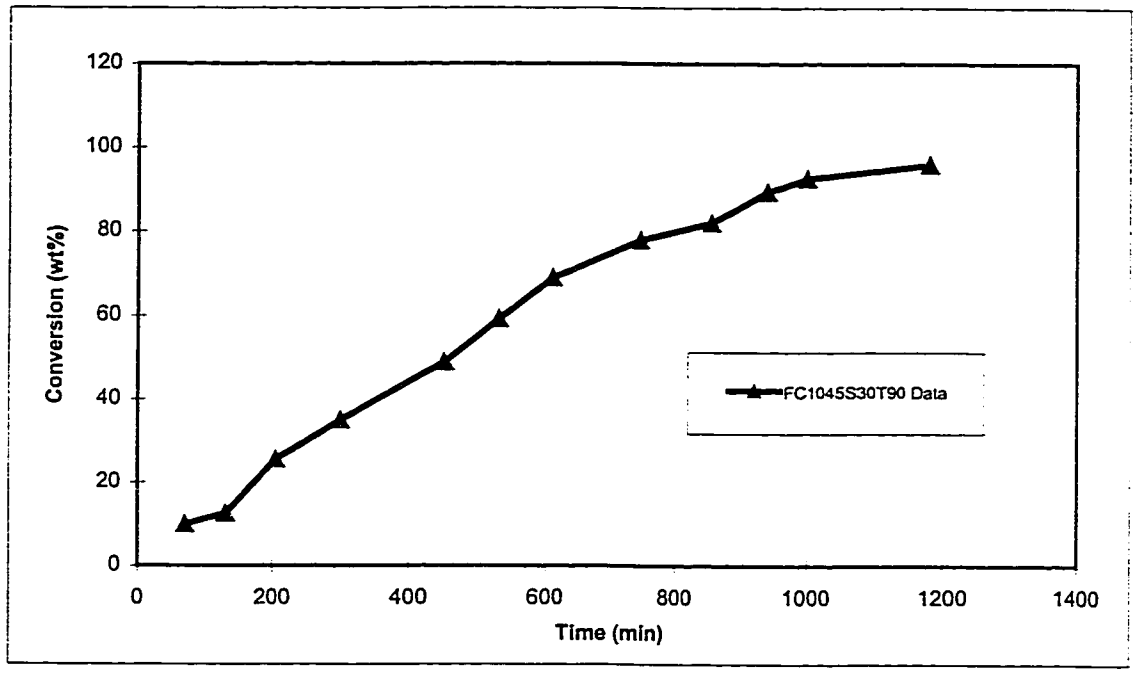

Figure C-16 BA-MMA 10/45 30% Toluene Conversion Profile At 90 °C

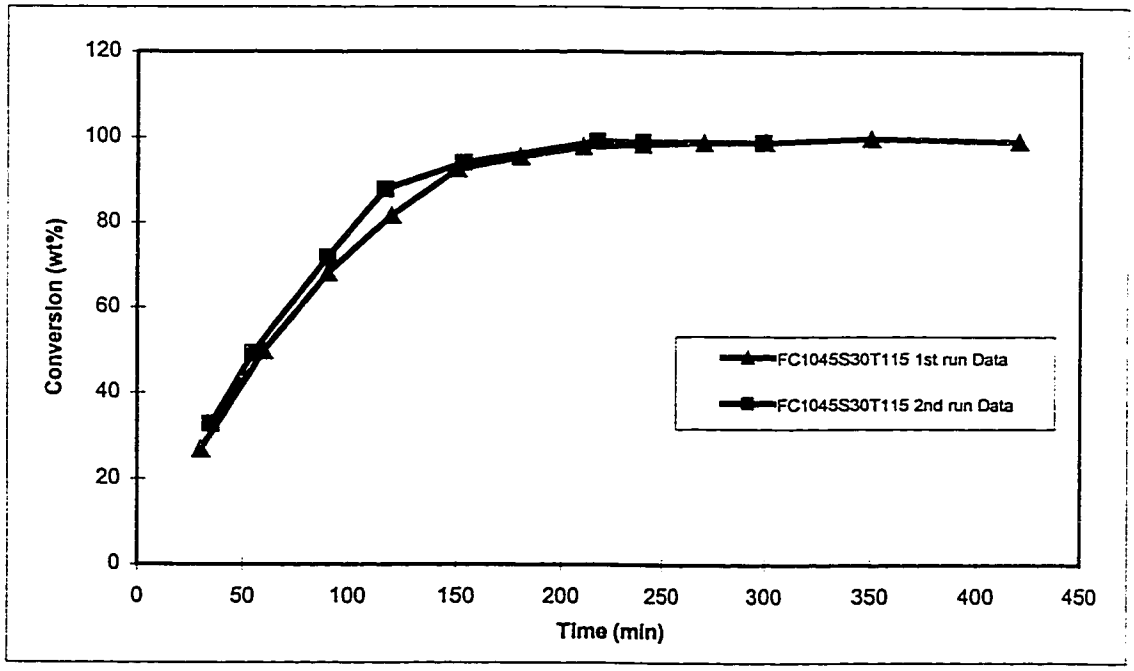

Figure C-17 BA-MMA 10/45 30% Toluene Conversion Profile At 115 °C

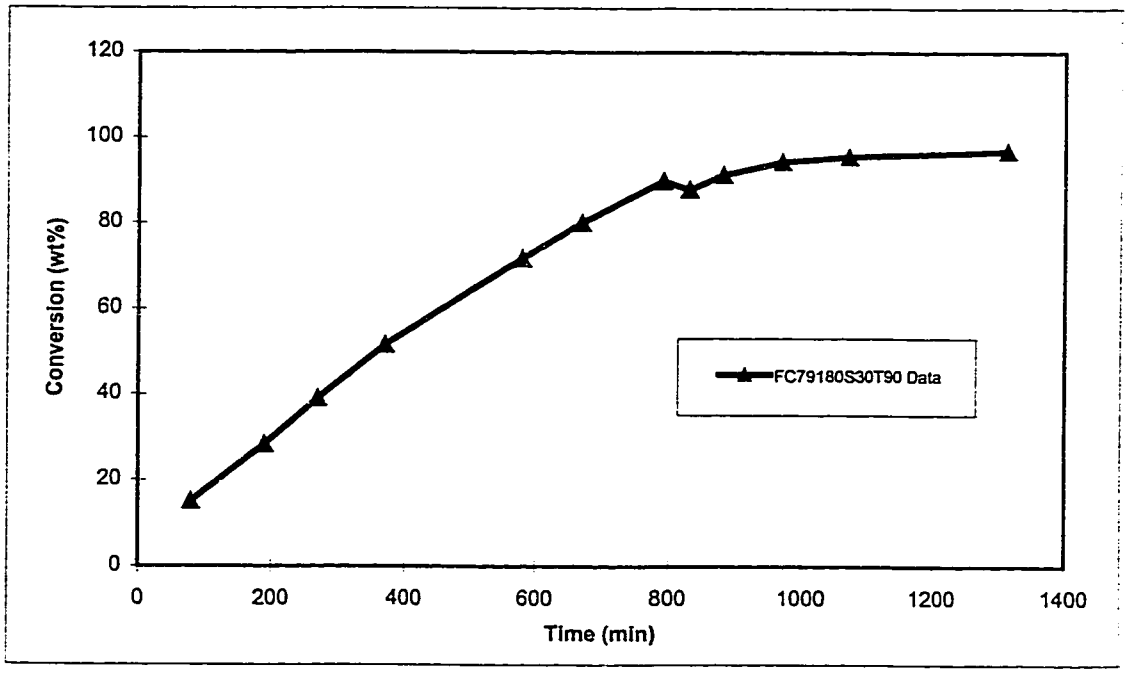

Figure C-18 BA-MMA 79/180 30% Toluene Conversion Profile At 90 °C

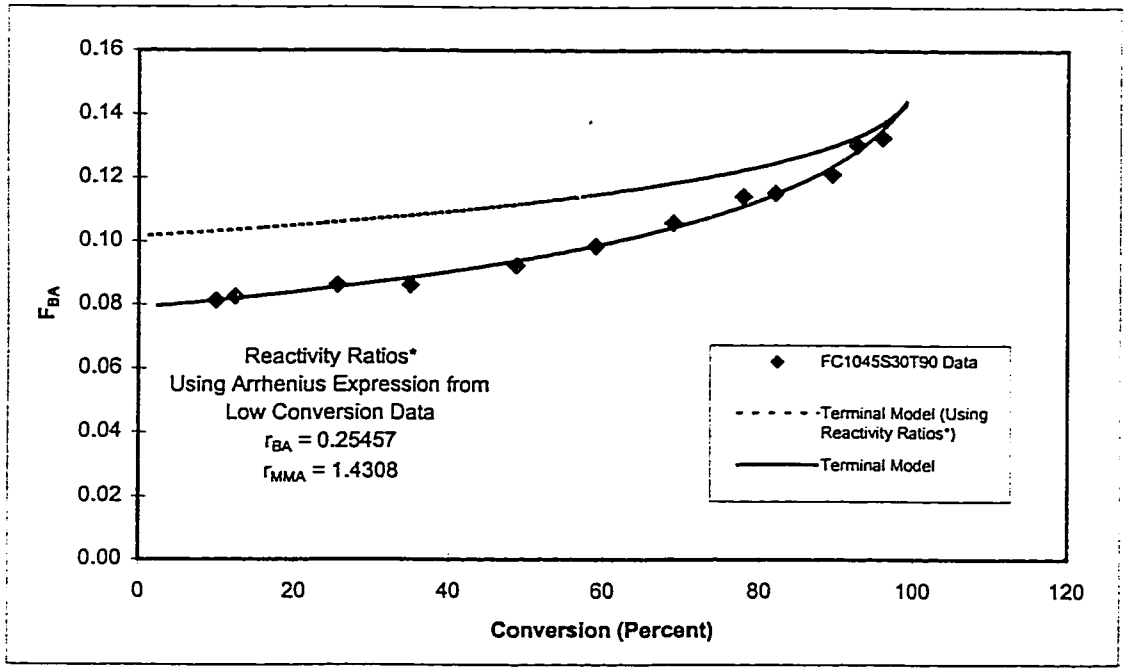

Figure C-19 BA-MMA 10/45 30% Toluene Composition Profile At 90 °C

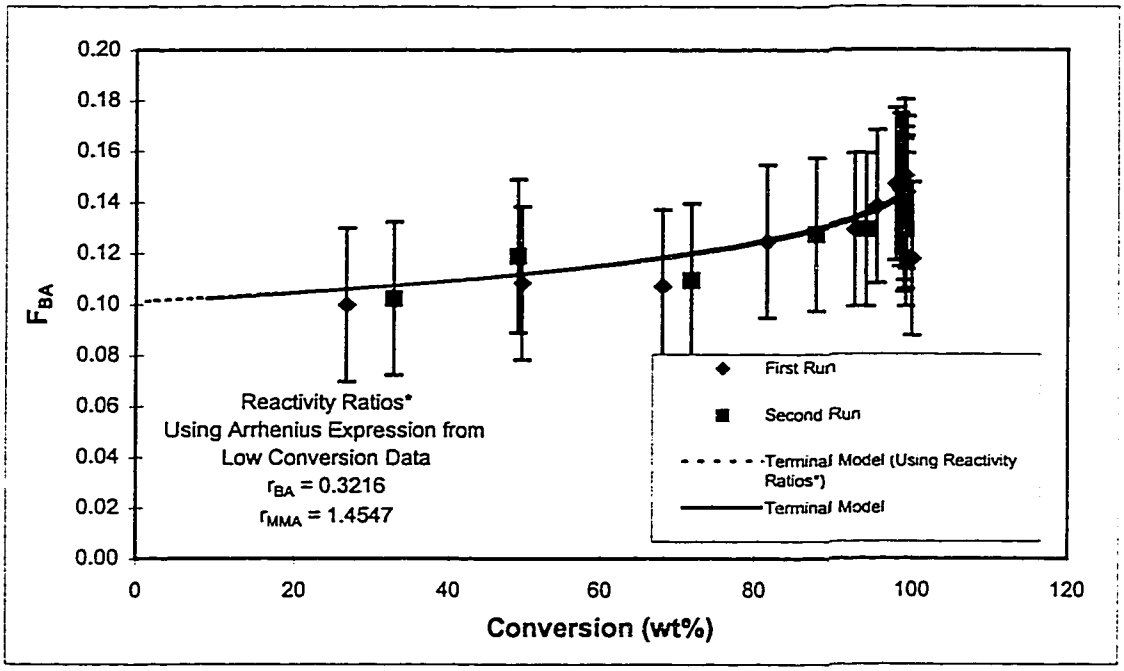

Figure C-20 **BA-MMA 10/45 30% Toluene Composition Profile At 115 °C**

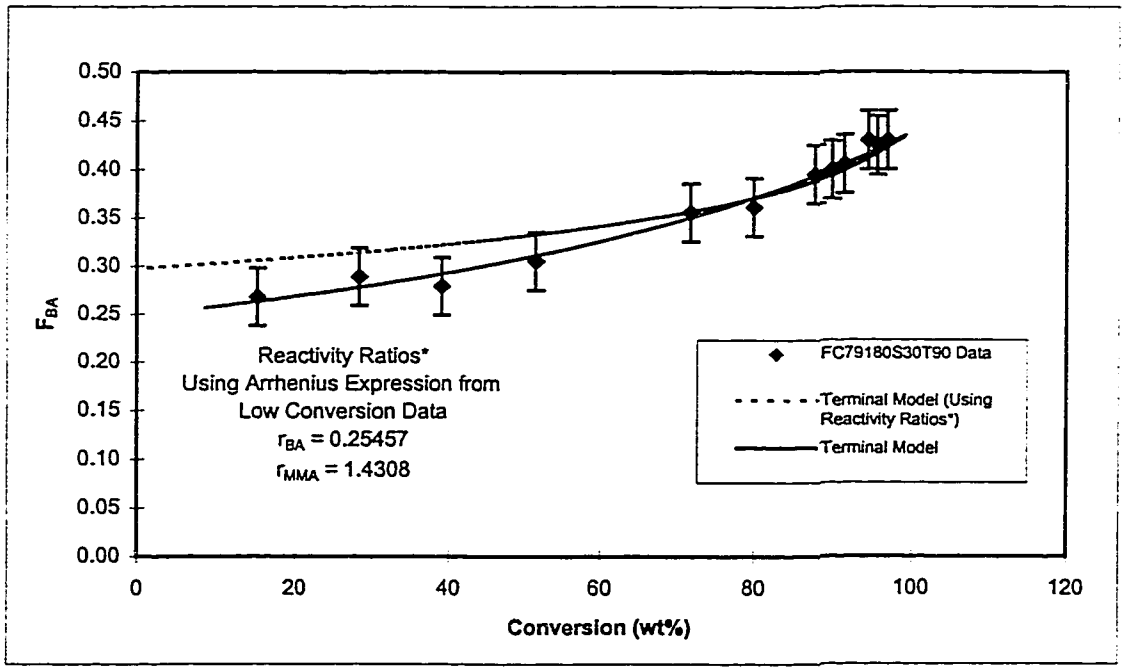

Figure C-21 **BA-MMA 79/180 30% Toluene Composition Profile At 90 °C**

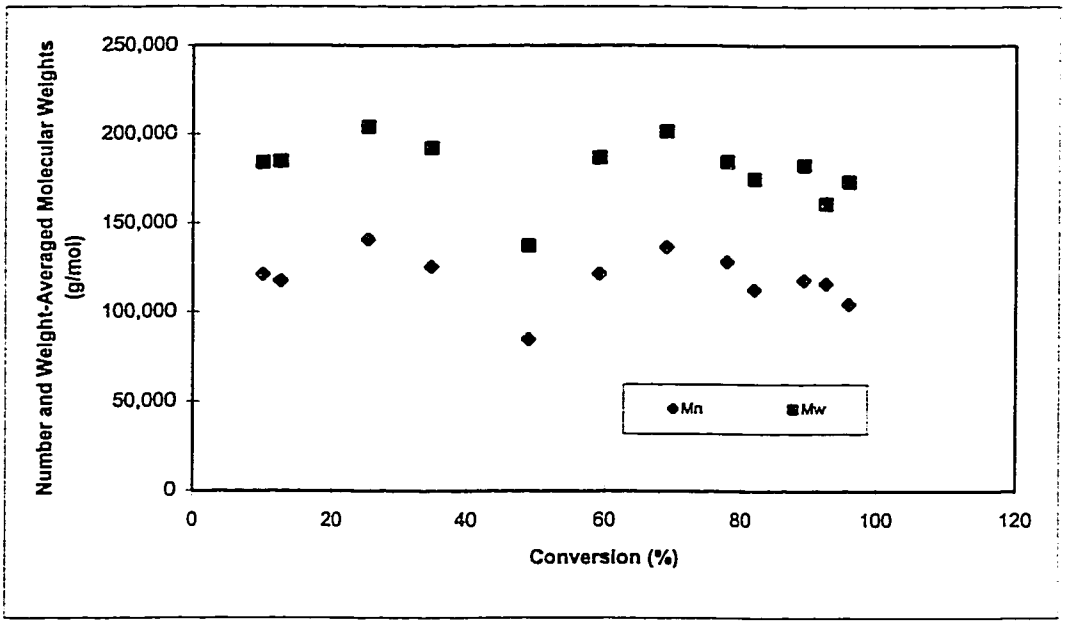

Figure C-22 BA-MMA 10/45 23% Toluene Molecular Weight Profile At 90 °C

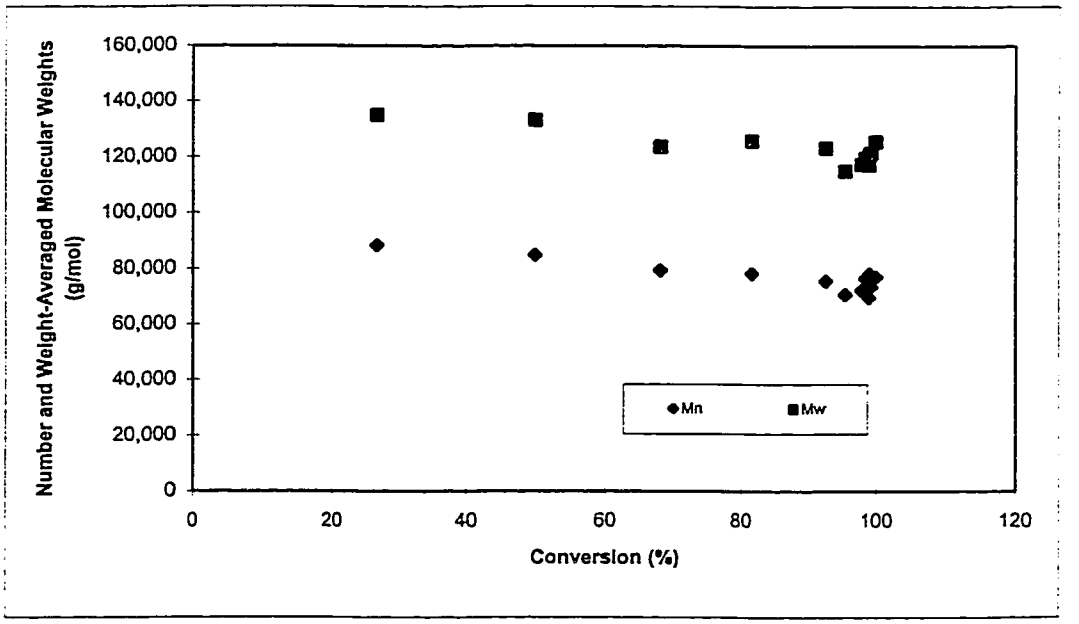

Figure C-23 BA-MMA 10/45 23% Toluene Molecular Weight Profile At 115 °C (1st Run)

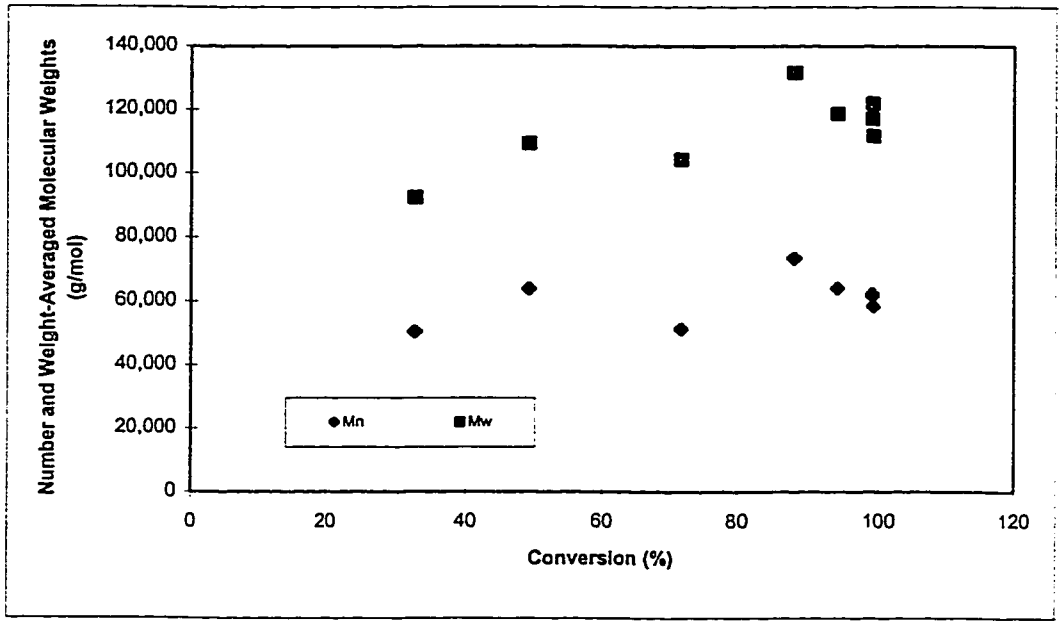

Figure C-24 BA-MMA 10/45 23% Toluene Molecular Weight Profile At 115 °C (2^{nd} Run)

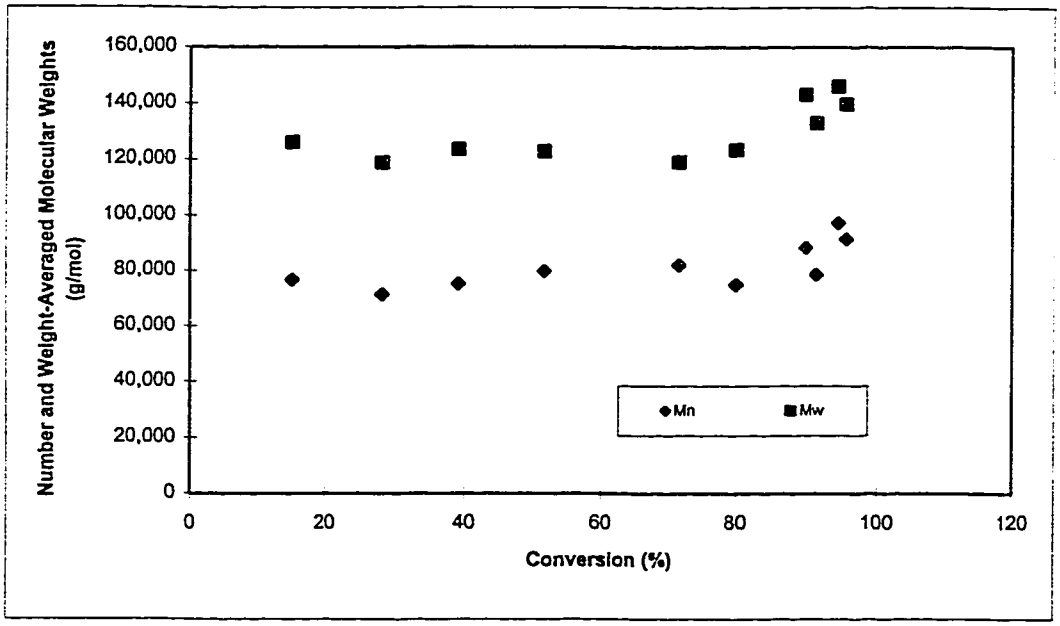

Figure C-25 BA-MMA 79/180 23% Toluene Molecular Weight Profile At 90 °C

Appendix D

Full Conversion Experimental Data

Table D-1 BA-MMA Full Conversion 10/45 Bulk Runs at 90 °C

New Results

Feed Mole Frac. BA 90 New Res	[Trig. B] (mol/L)	[CTA] (NDM) (mol/L)	Time (min)	Conversion (wt. %)	F_BA	M_n (g/mol)	M_w (g/mol)
0.147818	0.0453	0.0058	40	6.67	0.079689	107,491	188,502
0.147818	0.0453	0.0058	100	15.26	0.082431	115,735	204,749
0.147818	0.0453	0.0058	160	23.03	0.084318		
0.147818	0.0453	0.0058	185	25.88	0.077694	96,787	180,397
0.147818	0.0453	0.0058	220	30.08	0.085852	107,211	196,415
0.147818	0.0453	0.0058	250	34.47	0.084883	108,909	194,562
0.147818	0.0453	0.0058	280	60.14	0.089606	100,118	181,935
0.147818	0.0453	0.0058	325	72.43	0.088844	102,497	202,650
0.147818	0.0453	0.0058	355	55.28	0.101176	97,003	195,134
0.147818	0.0453	0.0058	405	79.22	0.114012	123,793	244,362
0.147818	0.0453	0.0058	465	92.56	0.152182	123,436	246,368
0.147818	0.0453	0.0058	630	97.52	0.149731		

Table D-2 BA-MMA Full Conversion 79/180 Bulk Runs at 115 °C

New Results

Feed Mole Frac. BA 115 New Res	[Trig. B] (mol/L)	[CTA] (NDM) (mol/L)	Time (min)	Conversion (wt. %)	F_BA	M_n (g/mol)	M_w (g/mol)
0.439037	0.0061	0.0058	25	12.59	0.290816	187,765	306,687
0.439037	0.0061	0.0058	50	24.46	0.302452	181,107	305,209
0.439037	0.0061	0.0058	70	32.70	0.304611	186,106	307,543
0.439037	0.0061	0.0058	90	42.43	0.319087	177,987	288,727
0.439037	0.0061	0.0058	110	54.38	0.327586	150,228	257,160
0.439037	0.0061	0.0058	130	61.65	0.352477	126,824	230,307
0.439037	0.0061	0.0058	150	75.13	0.353448	139,829	243,323
0.439037	0.0061	0.0058	180	88.95	0.401282	164,047	274,289
0.439037	0.0061	0.0058	210	93.49	0.413115	169,592	288,834
0.439037	0.0061	0.0058	240	95.47	0.414330	182,141	289,754
0.439037	0.0061	0.0058	360	97.84	0.443419	127,540	236,641

Table D-3 BA-MMA Full Conversion 10/45 23% Tol Runs at 90 °C

New Results

Feed Mole Frac. BA	[Trig. B] (mol/L)	[CTA] (NDM) (mol/L)	Time (min)	Conversion (wt. %)	F_BA	Mw (g/mol)	Mn (g/mol)
0.148794	0.0450	0.0060	90	17.70	0.111901	111,107	180,992
0.148794	0.0450	0.0060	180	28.31	0.090082	110,007	181,458
0.148794	0.0450	0.0060	270	34.63	0.082569	121,675	202,161
0.148794	0.0450	0.0060	360	41.33	0.101124	110,879	179,111
0.148794	0.0450	0.0060	393	64.30	0.088838	120,558	195,604
0.148794	0.0450	0.0060	600	81.65	0.102334	121,536	193,528
0.148794	0.0450	0.0060	727	91.62	0.117777	107,893	170,172
0.148794	0.0450	0.0060	810	96.20	0.132697	110,204	180,847
0.148794	0.0450	0.0060	990	98.47	0.143836	122,014	198,263
0.148794	0.0450	0.0060	1200	99.66	0.138302	130,361	200,490

Table D-4 BA-MMA Full Conversion 10/45 23% Tol Runs at 115 °C

New Results

Feed Mole Frac. BA 90 New Res	[Trig. B] (mol/L)	[CTA] (NDM) (mol/L)	Time (min)	Conversion (wt. %)	F_BA	Mw (g/mol)	Mn (g/mol)
0.147872	0.0058	0.0060	30	13.51	0.083830	104,656	170,408
0.147872	0.0058	0.0060	61	22.16	0.086341	105,968	170,408
0.147872	0.0058	0.0060	90	31.01	0.090082	103,530	165,357
0.147872	0.0058	0.0060	137	44.60	0.092559	112,611	174,753
0.147872	0.0058	0.0060	180	56.89	0.097473	109,014	177,415
0.147872	0.0058	0.0060	225	70.76	0.105945	92,787	163,933
0.147872	0.0058	0.0060	255	79.60	0.107143	116,995	194,977
0.147872	0.0058	0.0060	285	85.24	0.117777	105,936	182,852
0.147872	0.0058	0.0060	317	89.61	0.130435	94,148	149,411
0.147872	0.0058	0.0060	340	88.98	0.125874	84,191	148,929
0.147872	0.0058	0.0060	360	95.34	0.124726	94,582	159,856
0.147872.	0.0058	0.0060	1445	98.70	0.155762	81,856	144,893

Table D-5 BA-MMA Full Conversion 79/180 23% Tol Runs at 90 °C

New Results

Feed Mole Frac. BA 115 New Res	[Trig. B] (mol/L)	[CTA] (NDM) (mol/L)	Time (min)	Conversion (wt. %)	F_BA	Mw (g/mol)	Mn (g/mol)
0.438924	0.0450	0.0060	150	24.92	0.270339	109,600	177,712
0.438924	0.0450	0.0060	270	38.58	0.300210	113,238	185,154
0.438924	0.0450	0.0060	330	45.21	0.303136	108,429	182,469
0.438924	0.0450	0.0060	420	56.26	0.328408	106,761	177,624
0.438924	0.0450	0.0060	480	65.95	0.351281	107,746	176,940
0.438924	0.0450	0.0060	540	74.06	0.343617	112,196	186,172
0.438924	0.0450	0.0060	650	81.13	0.372057	110,807	188,679
0.438924	0.0450	0.0060	725	87.24	0.398134	105,701	176,603
0.438924	0.0450	0.0060	875	88.94	0.404052	104,269	180,253
0.438924	0.0450	0.0060	1170	94.75	0.432946	105,751	180,557
0.438924	0.0450	0.0060	1500	97.21	0.441964	111,929	194,957
0.438924	0.0450	0.0060	1785	98.11	0.428081	101,216	176,587

Table D-6 BA-MMA Full Conversion 10/45 30% Tol Runs at 90 °C

New Results

Feed Mole Frac. BA New Res	[Trig. B] (mol/L)	[CTA] (NDM) (mol/L)	Time (min)	Conversion (wt. %)	F_BA	Mw (g/mol)	Mn (g/mol)
0.147932	0.0451	0.0060	70	9.91	0.081305	121,029	184,015
0.147932	0.0451	0.0060	130	12.45	0.082569	117,517	184,751
0.147932	0.0451	0.0060	205	25.47	0.086341	140,667	204,249
0.147932	0.0451	0.0060	300	34.86	0.086341	125,529	192,254
0.147932	0.0451	0.0060	450	48.80	0.092559	84,642	137,317
0.147932	0.0451	0.0060	530	59.08	0.098693	121,450	186,843
0.147932	0.0451	0.0060	610	68.89	0.105945	136,380	201,603
0.147932	0.0451	0.0060	745	77.84	0.114260	128,142	184,406
0.147932	0.0451	0.0060	855	81.97	0.115436	112,620	174,789
0.147932	0.0451	0.0060	940	89.31	0.121265	117,971	182,636
0.147932	0.0451	0.0060	1000	92.55	0.130435	116,073	160,989
0.147932	0.0451	0.0060	1180	95.90	0.132697	104,579	173,359

Table D-7 BA-MMA Full Conversion 79/180 30% Tol Runs at 90 °C

New Results

Feed Mole Frac. BA 115 New Res	[Trig. B] (mol/L)	[CTA] (NDM) (mol/L)	Time (min)	Conversion (wt. %)	F_BA 115 New Res	Mw (g/mol)	Mn (g/mol)
0.438902	0.0450	0.0060	80	15.10	0.267936	76,556	126,039
0.438902	0.0450	0.0060	190	28.30	0.289015	71,158	118,699
0.438902	0.0450	0.0060	270	39.05	0.279019	75,069	123,447
0.438902	0.0450	0.0060	370	51.55	0.305314	79,674	122,791
0.438902	0.0450	0.0060	580	71.69	0.355670	81,929	119,125
0.438902	0.0450	0.0060	670	79.95	0.361226	74,943	123,488
0.438902	0.0450	0.0060	791	89.74	0.399760	88,211	143,081
0.438902	0.0450	0.0060	830	87.75	0.395405	38,188	87,622
0.438902	0.0450	0.0060	880	91.26	0.405646	78,455	133,022
0.438902	0.0450	0.0060	970	94.33	0.430037	97,204	145,991
0.438902	0.0450	0.0060	1070	95.53	0.424626	91,355	139,766
0.438902	0.0450	0.0060	1313	96.82	0.430037	57,960	115,272

Table D-8 BA-MMA Full Conversion 10/45 30% Tol Runs at 115 °C (First Run)

New Results

Feed Mole Frac. BA 90 New Res	[Trig. B] (mol/L)	[CTA] (NDM) (mol/L)	Time (min)	Conversion (wt. %)	F_BA (mole Fraction)	Mw (g/mol)	Mn (g/mol)
0.148776	0.0451	0.0060	30	26.76	0.099910	88,246	134,878
0.148776	0.0451	0.0060	60	49.74	0.108337	84,740	133,157
0.148776	0.0451	0.0060	90	68.03	0.107143	79,284	123,660
0.148776	0.0451	0.0060	120	81.60	0.124726	78,150	125,893
0.148776	0.0451	0.0060	150	92.56	0.129299	75,496	123,315
0.148776	0.0451	0.0060	180	95.40	0.138302	70,622	115,040
0.148776	0.0451	0.0060	210	97.87	0.147122	72,232	117,448
0.148776	0.0451	0.0060	240	98.42	0.144934	76,410	119,712
0.148776	0.0451	0.0060	270	98.91	0.134948	69,559	117,271
0.148776	0.0451	0.0060	300	98.98	0.150382	78,052	121,102
0.148776	0.0451	0.0060	350	99.90	0.117777	76,895	125,491
0.148776	0.0451	0.0060	420	99.21	0.143836	73,293	121,404

Table D-9 BA-MMA Full Conversion 10/45 30% Tol Runs at 115 °C (Second Run)

New Results

Feed Mole Frac. BA 90 New Res	[Trig. B] (mol/L)	[CTA] (NDM) (mol/L)	Time (min)	Conversion (wt. %)	F_BA (mole Fraction)	Mw (g/mol)	Mn (g/mol)
0.147932	0.0451	0.0060	35	32.77	0.102334	50,465	92,369
0.147932	0.0451	0.0060	55	49.22	0.118943	63,892	109,338
0.147932	0.0451	0.0060	90	71.80	0.109528	51,357	104,266
0.147932	0.0451	0.0060	117	87.85	0.127500	73,446	131,536
0.147932	0.0451	0.0060	153	94.02	0.129299	64,074	118,685
0.147932	0.0451	0.0060	217	99.14	0.129299	58,434	111,762
0.147932	0.0451	0.0060	240	99.07	0.136069	62,277	121,943
0.147932	0.0451	0.0060	299	98.99	0.139415	61,720	117,121

Appendix E

Depropagation Kinetics Modeling Figures

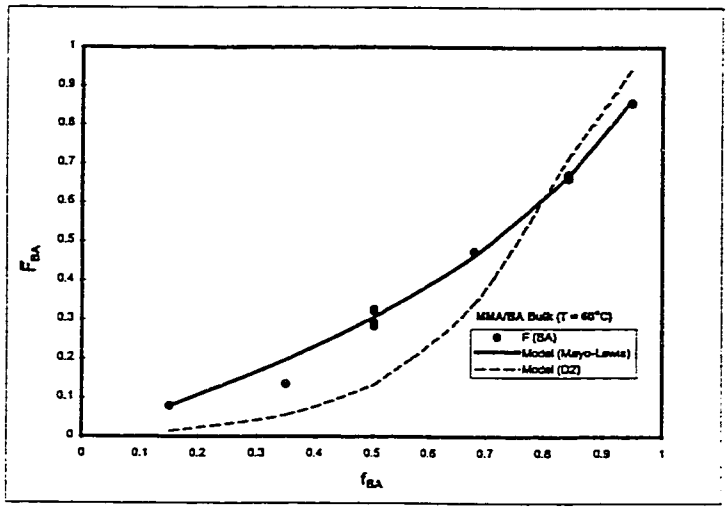

Figure E-1 BA-MMA Bulk Model Composition Profiles at 60 °C

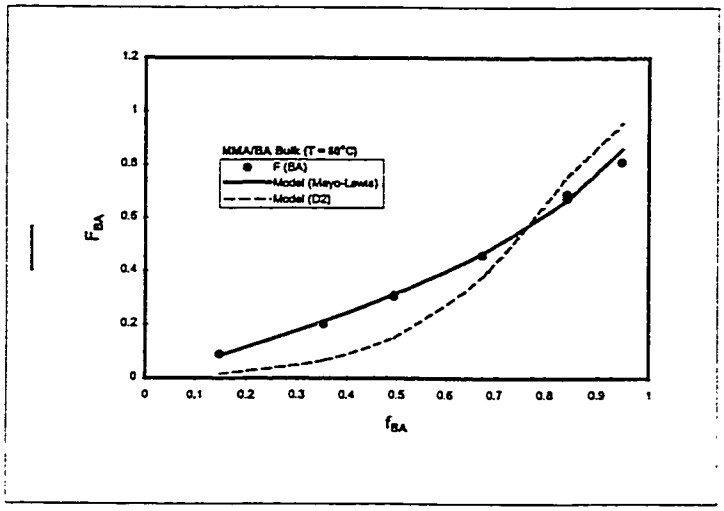

Figure E-2 BA-MMA Bulk Model Composition Profiles at 80 °C

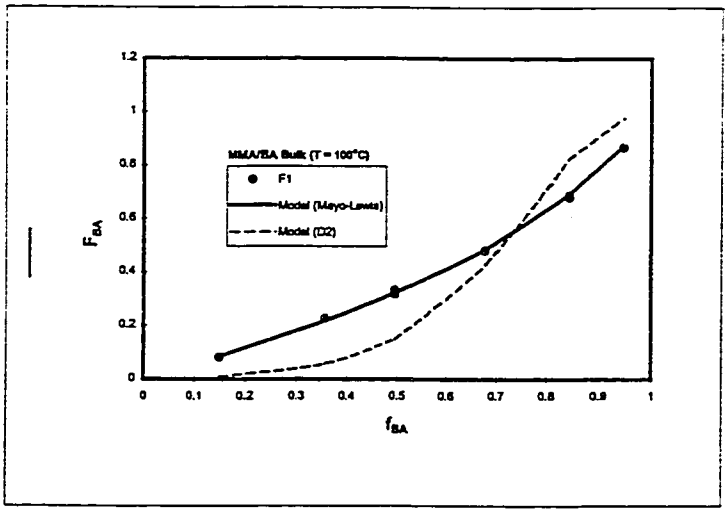

Figure E-3 BA-MMA Bulk Model Composition Profiles at 100 °C

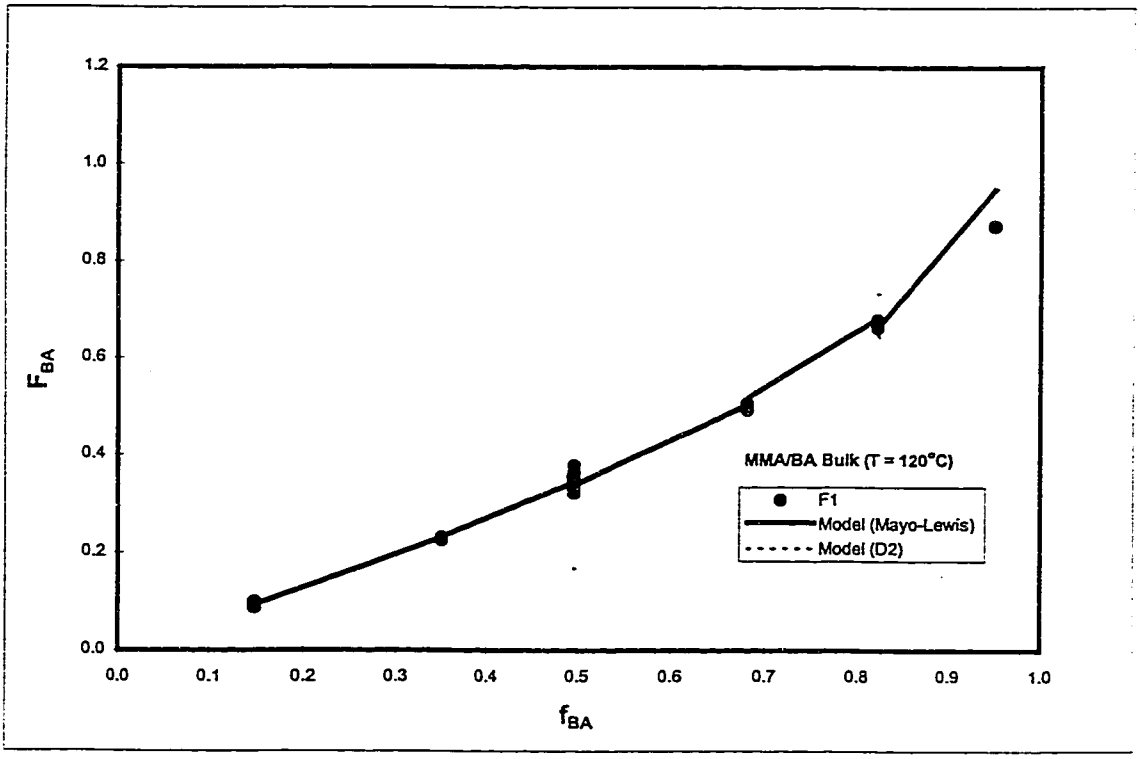

Figure E-4 BA-MMA Bulk Model Composition Profiles at 120 °C

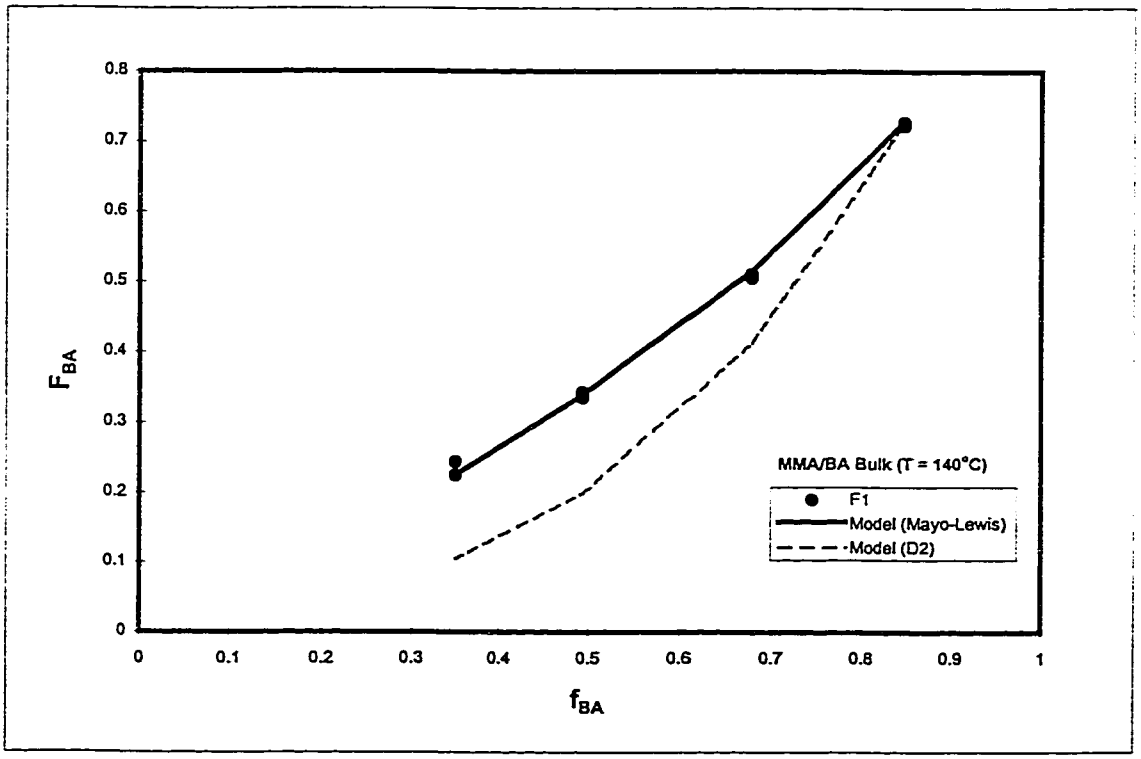

Figure E-5 BA-MMA Bulk Model Composition Profiles at 140 °C

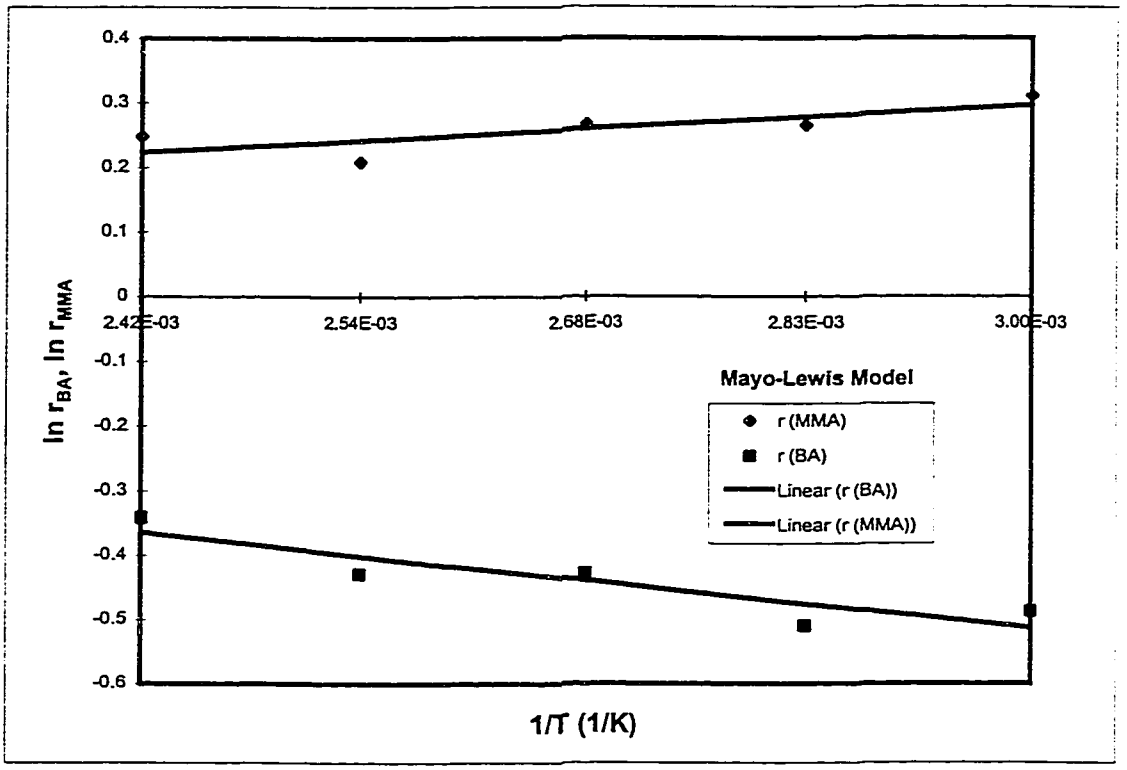

Figure E-6 BA-MMA Bulk Mayo-Lewis Model Arrhenius Test Plot

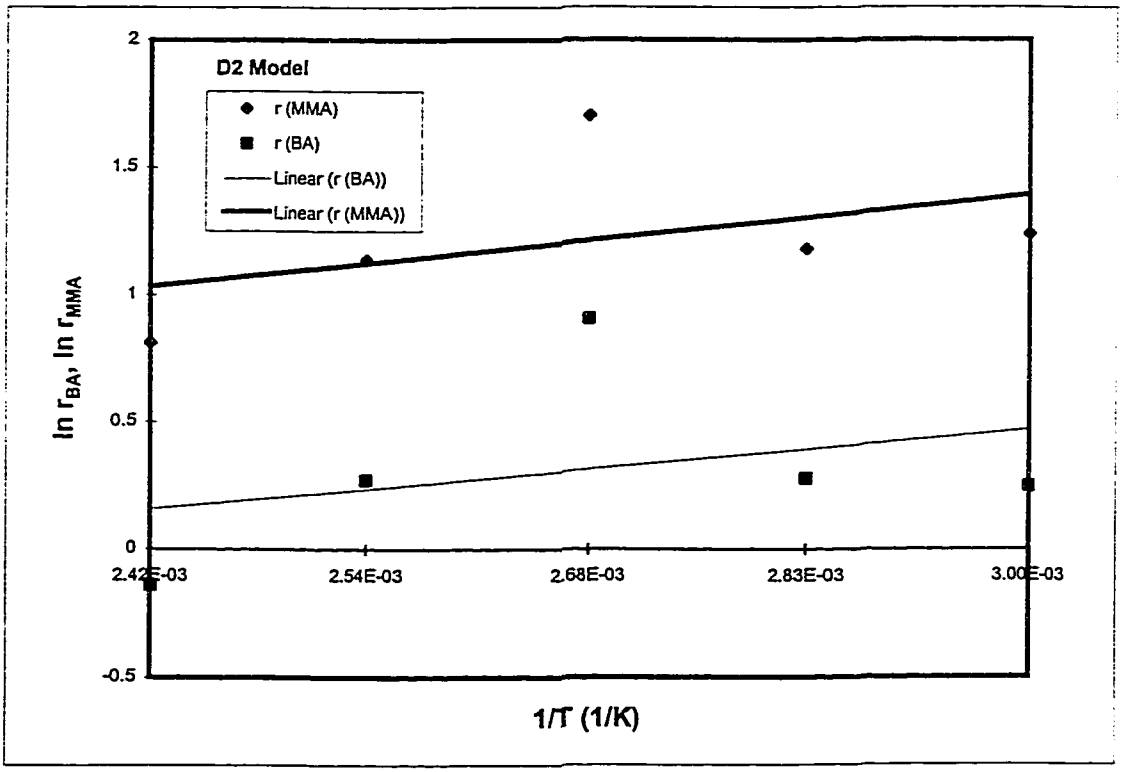

Figure E-7 BA-MMA Bulk D2 Model Arrhenius Test Plot

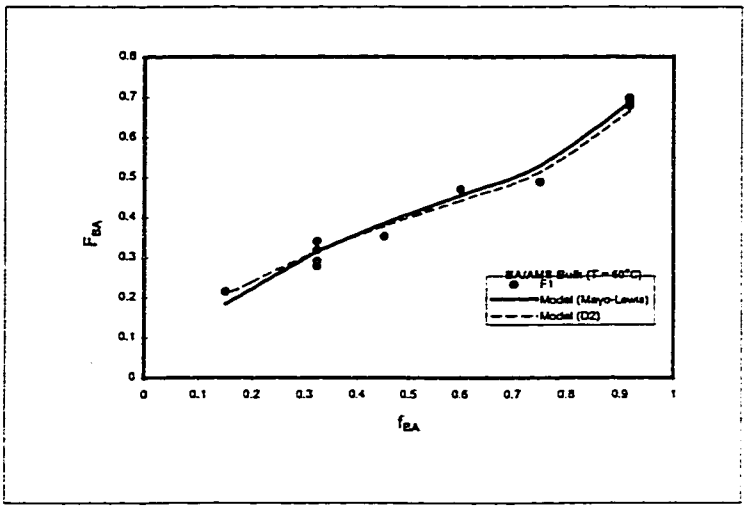

Figure E-8 BA-AMS Bulk Model Composition Profiles at 60 °C

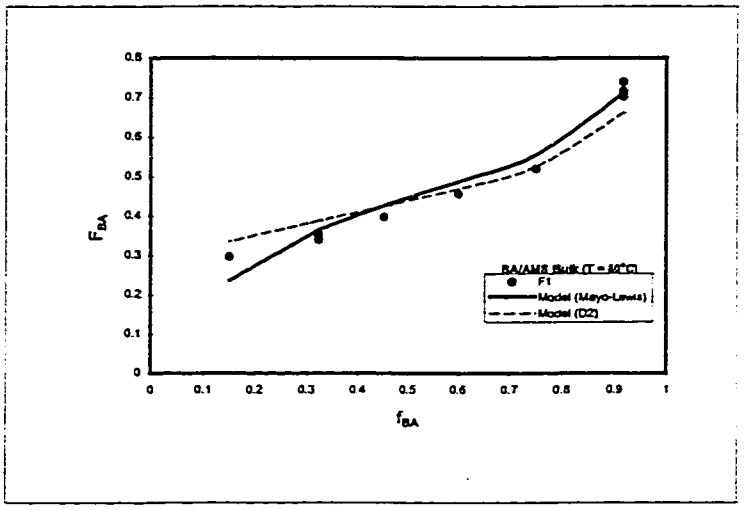

Figure E-9 BA-AMS Bulk Model Composition Profiles at 80 °C

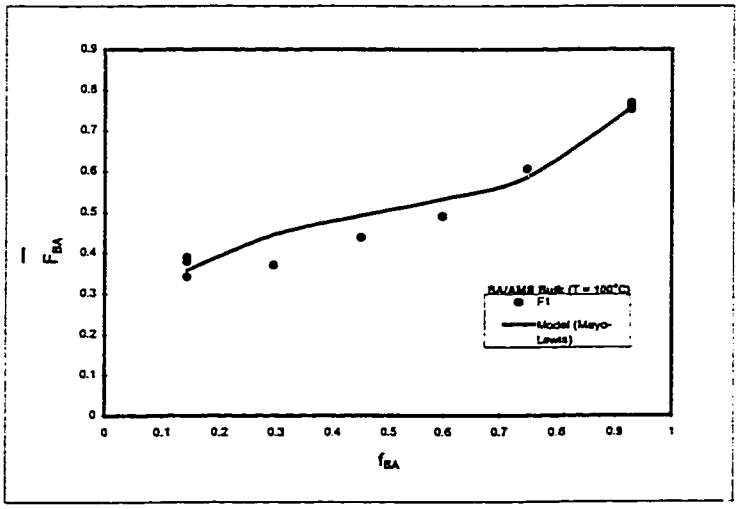

Figure E-10 BA-AMS Bulk Model Composition Profiles at 100 °C

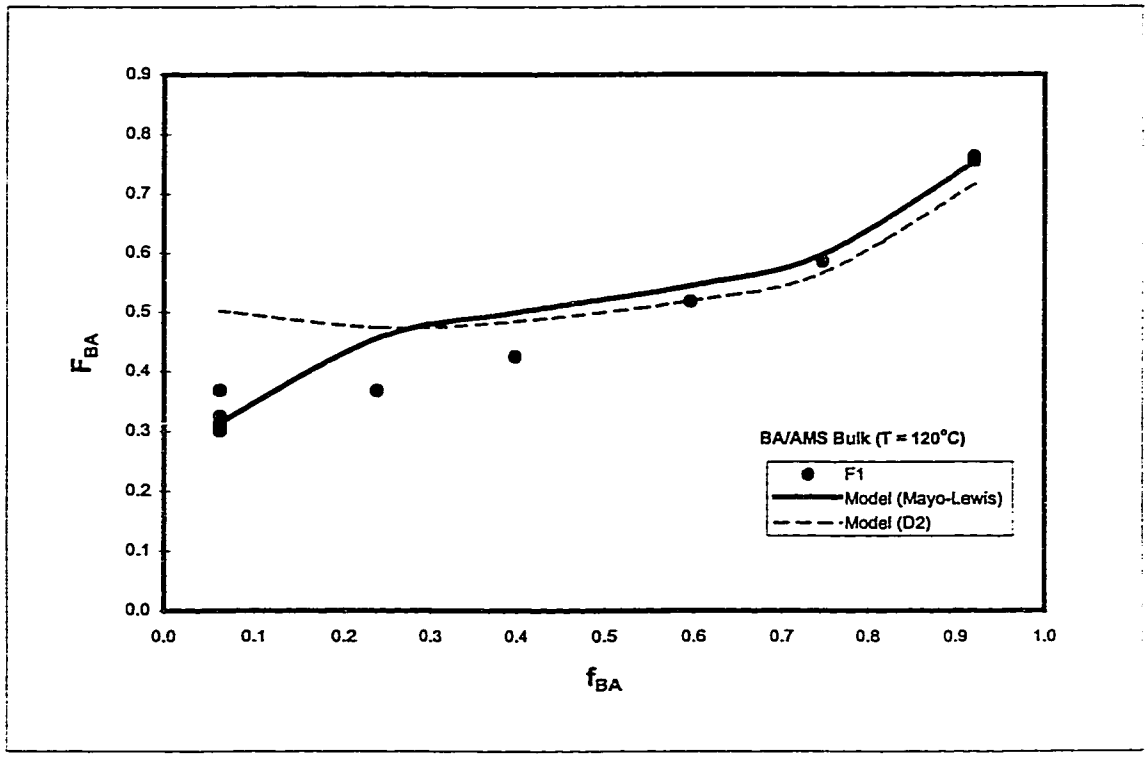

Figure E-11 BA-AMS Bulk Model Composition Profiles at 120 °C

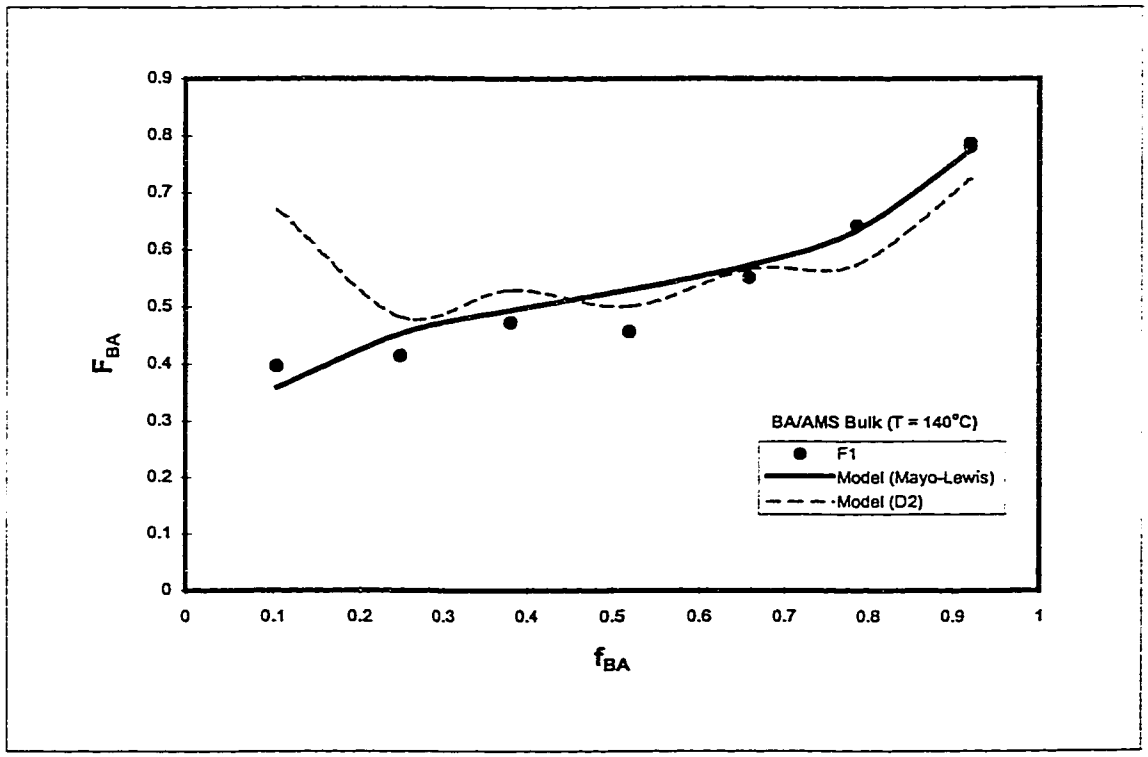

Figure E-12 BA-AMS Bulk Model Composition Profiles at 140 °C

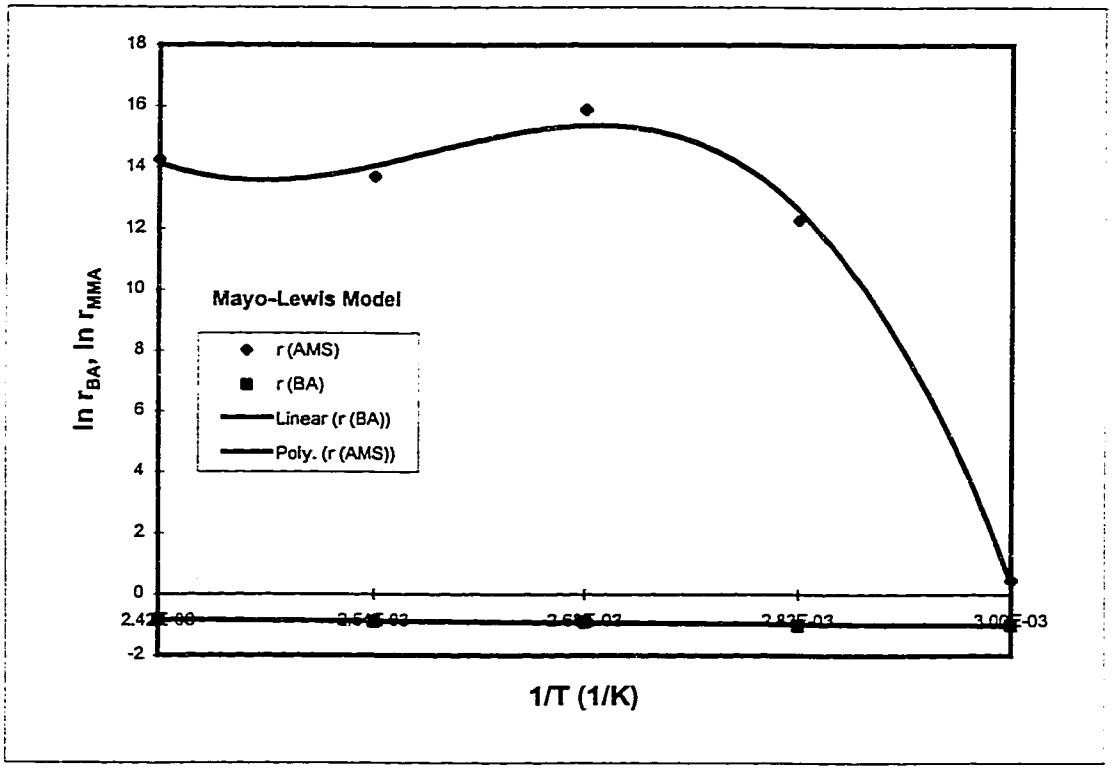

Figure E-13 BA-AMS Bulk Mayo-Lewis Model Arrhenius Test Plot

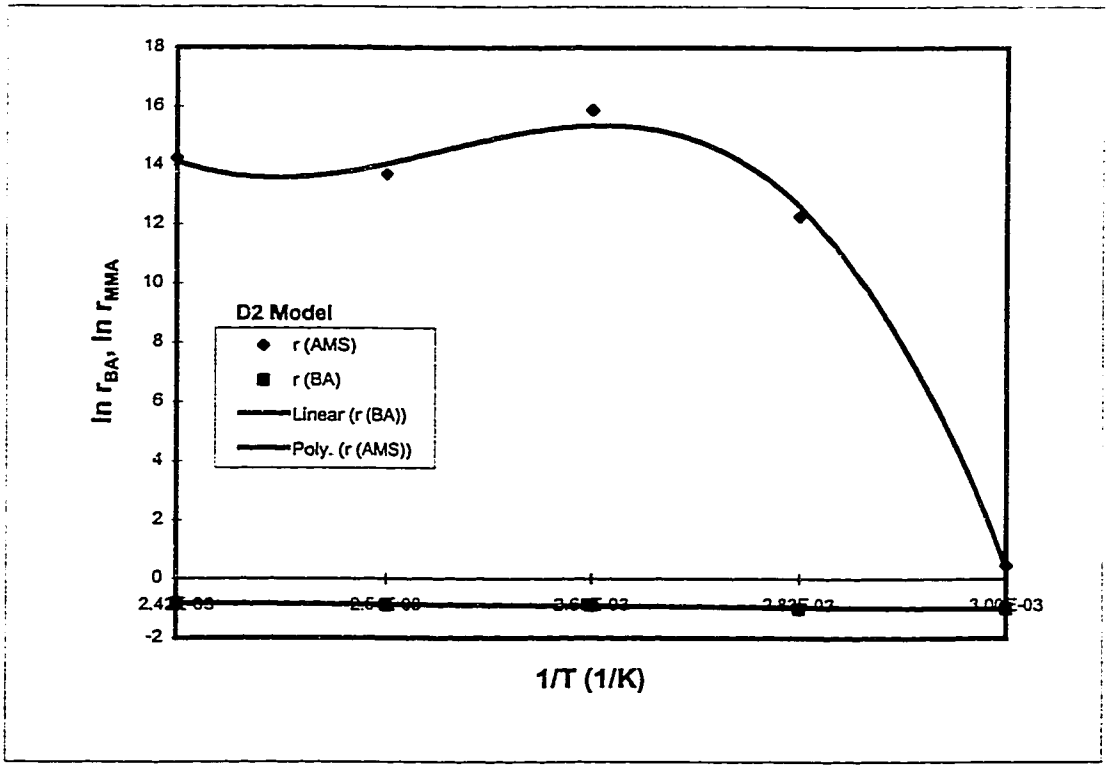

Figure E-14 BA-AMS Bulk D2 Model Arrhenius Test Plot

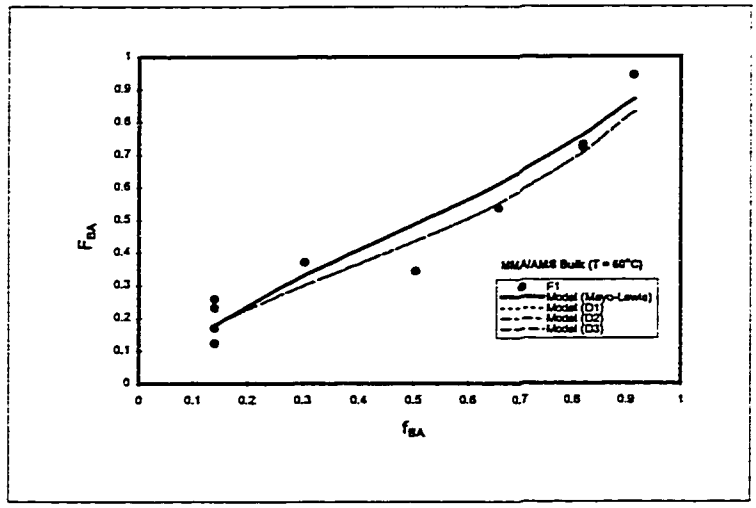

Figure E-15 MMA-AMS Bulk Model Composition Profiles at 60 °C

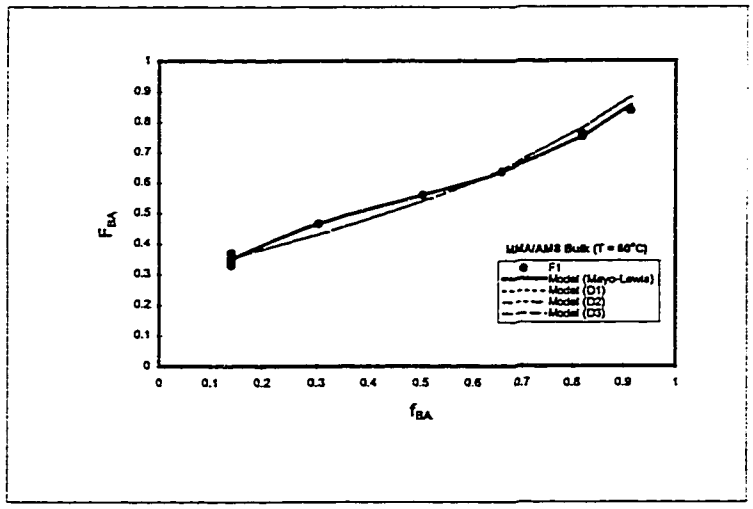

Figure E-16 MMA-AMS Bulk Model Composition Profiles at 80 °C

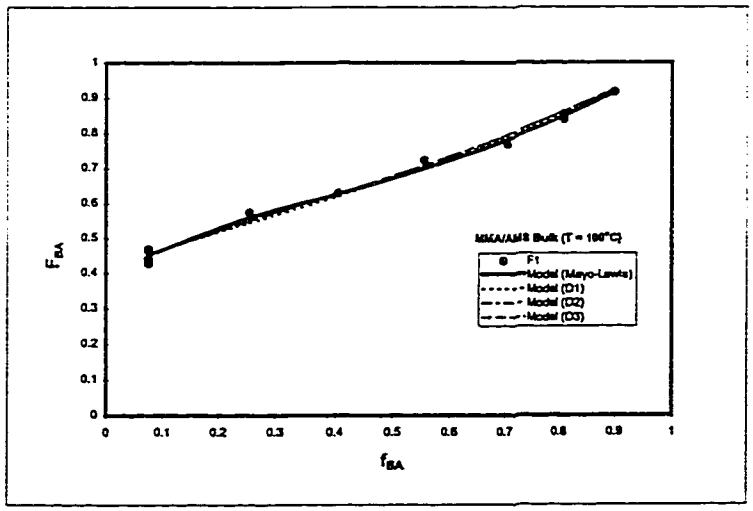

Figure E-17 MMA-AMS Bulk Model Composition Profiles at 100 °C

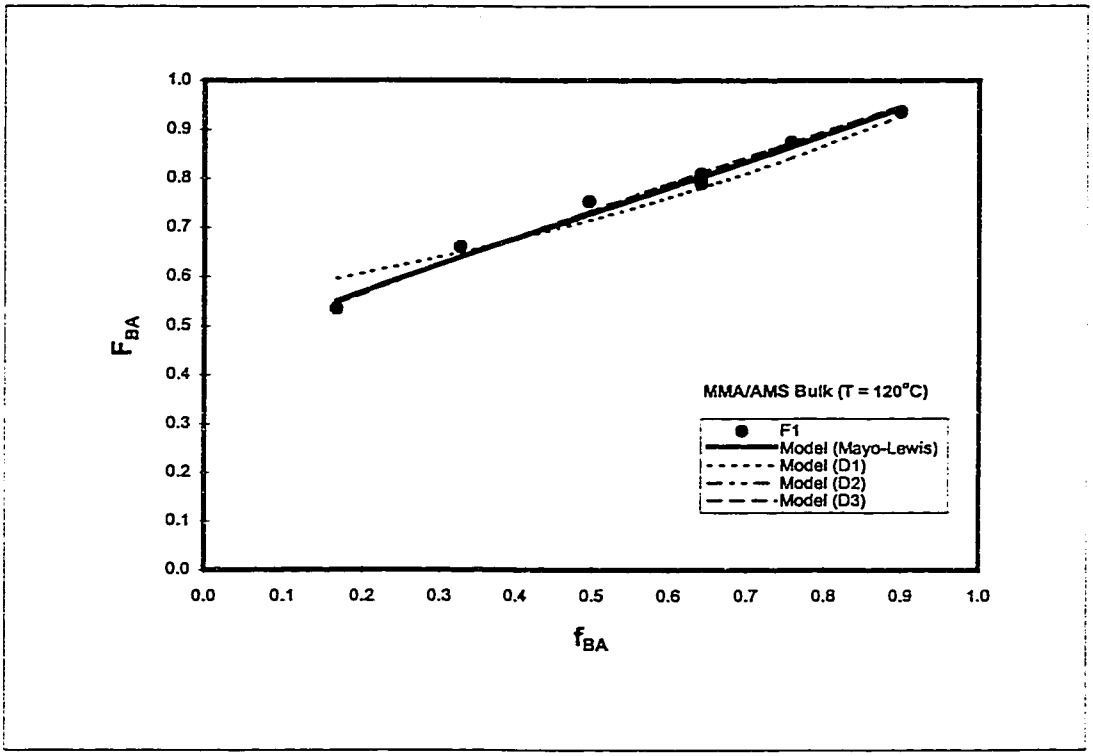

Figure E-18 **MMA-AMS Bulk Model Composition Profiles at 120 °C**

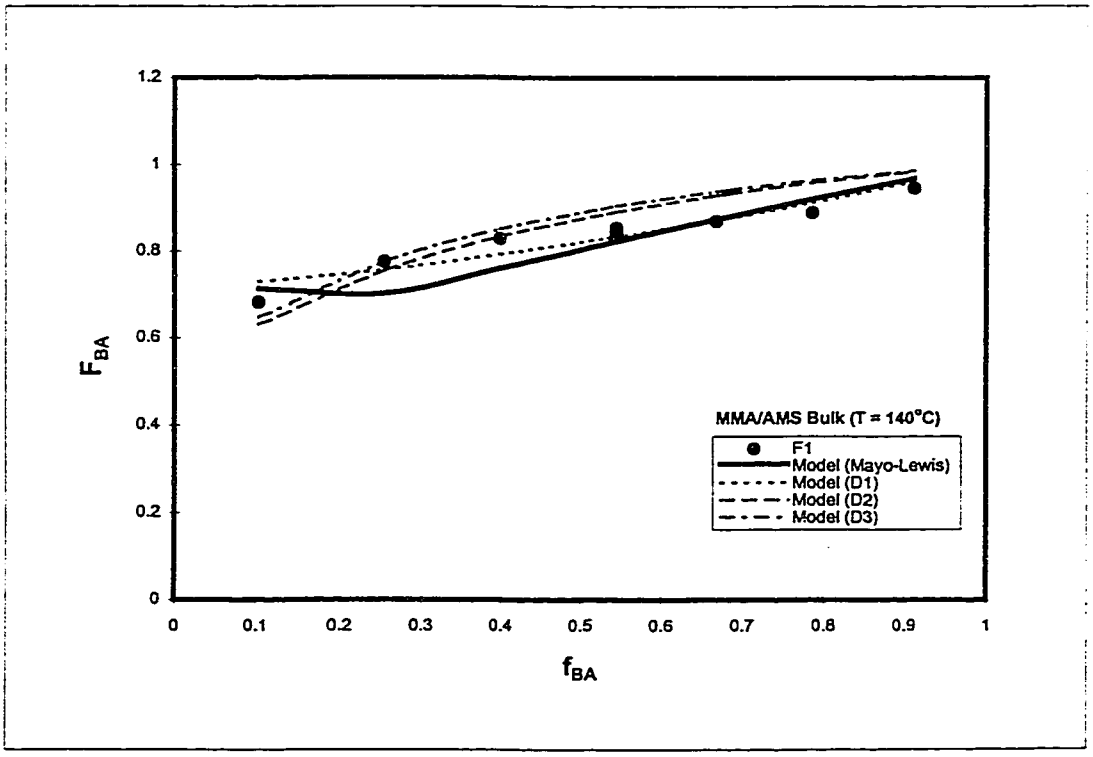

Figure E-19 **MMA-AMS Bulk Model Composition Profiles at 140 °C**

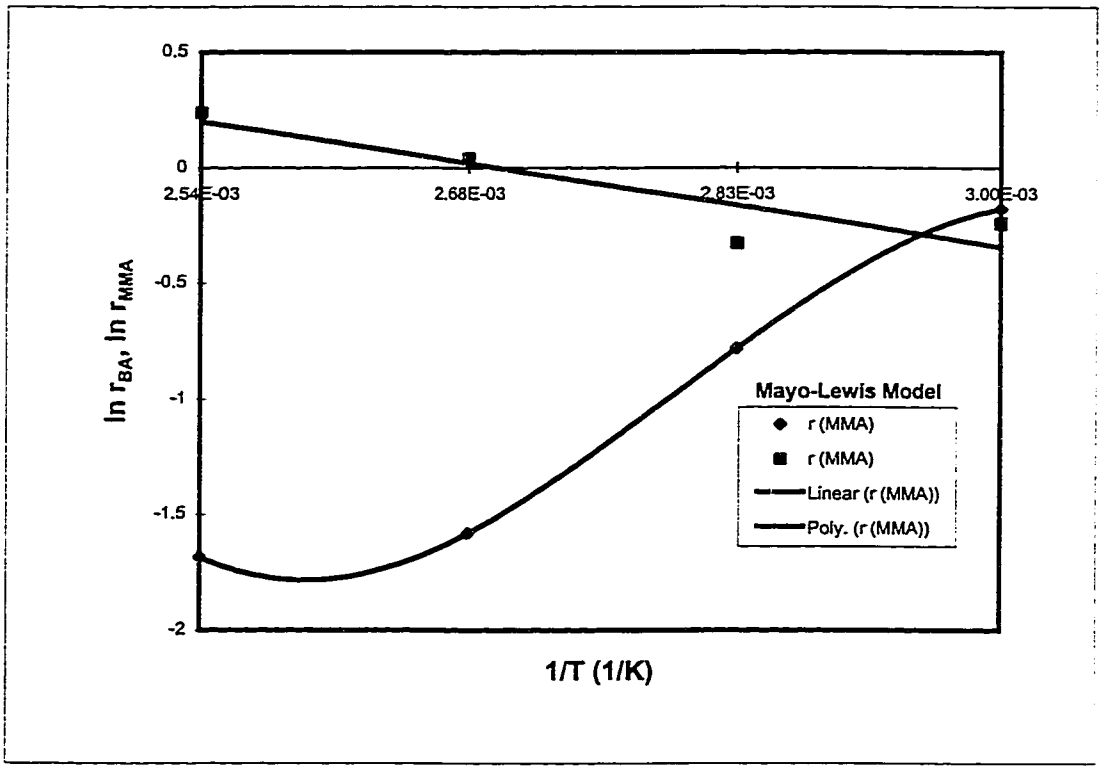

Figure E-20 MMA-AMS Bulk Mayo-Lewis Model Arrhenius Test Plot

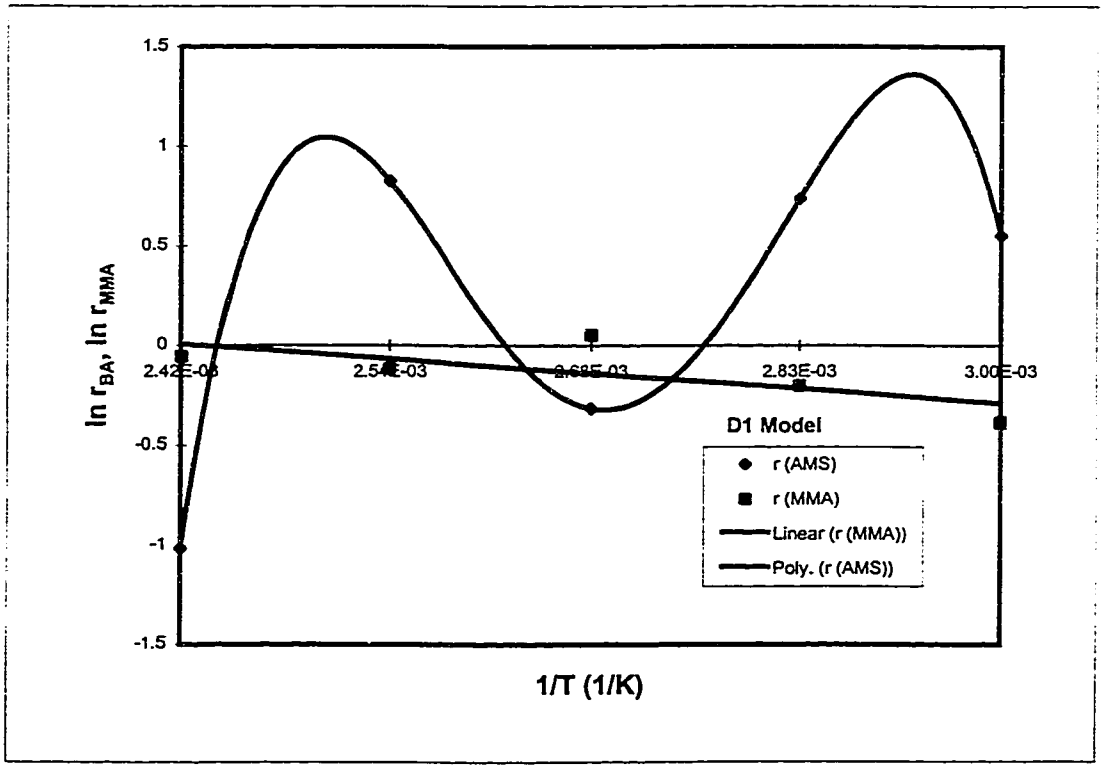

Figure E-21 MMA-AMS Bulk D1 Model Arrhenius Test Plot

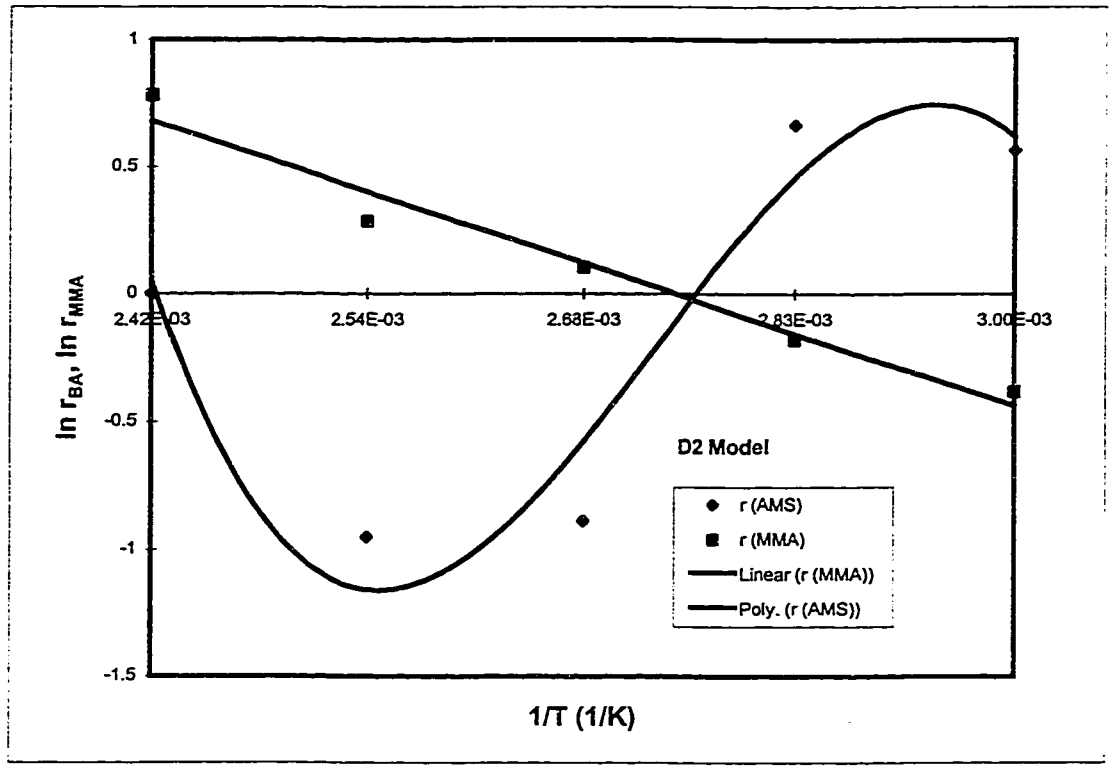

Figure E-22 MMA-AMS Bulk D2 Model Arrhenius Test Plot

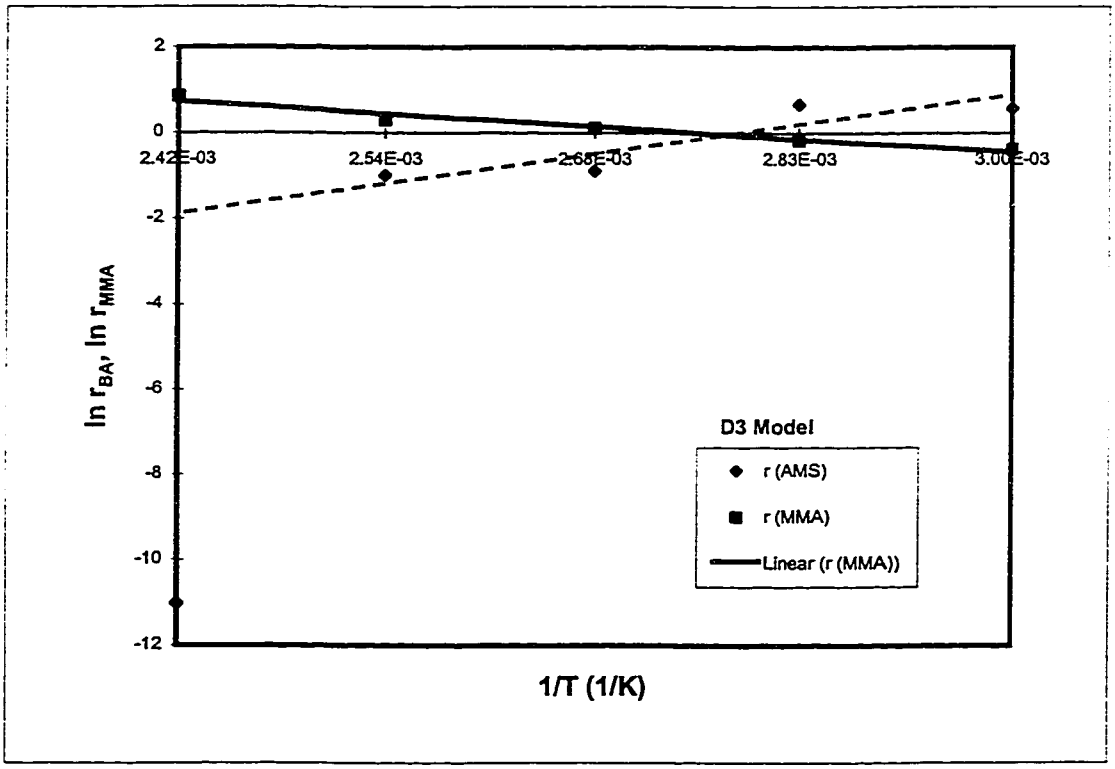

Figure E-23 MMA-AMS Bulk D3 Model Arrhenius Test Plot

IMAGE EVALUATION TEST TARGET (QA-3)

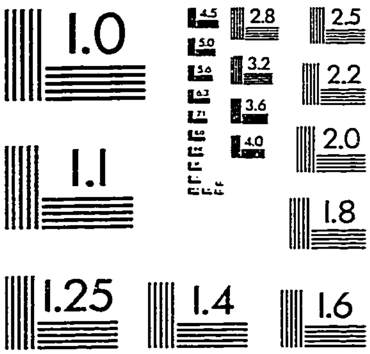

150mm

6″

APPLIED IMAGE, Inc
1653 East Main Street
Rochester, NY 14609 USA
Phone: 716/482-0300
Fax: 716/288-5989